JOURNAL OF CONDENSED MATTER NUCLEAR SCIENCE

Experiments and Methods in Cold Fusion

VOLUME 18, February 2016

JOURNAL OF CONDENSED MATTER NUCLEAR SCIENCE

Experiments and Methods in Cold Fusion

JOURNAL OF CONDENSED MATTER NUCLEAR SCIENCE

Volume 18, February 2016

ISSN 2227-3123

Orders, claims, author inquiries and journal inquiries

Please contact the Editor-in-Chief, CMNSEditor@iscmns.org or webmaster@iscmns.org

J. Condensed Matter Nucl. Sci. 18 (2016) 1–75
 ISSN 2227-3123

JOURNAL OF CONDENSED MATTER NUCLEAR SCIENCE

Volume 18 2016

CONTENTS

Editorial

Volume 18 of the *Journal of Condensed Matter Nuclear Science* includes only four papers that I believe are important. In particular, the theoretical paper by Frederic Henry-Couannier shines a new light on Low Energy Nuclear Reactions (LENR) theories. So far, most of the well-known theories are based on quantum mechanics, classical physics or the introduction of new particles. For the first time, Henry-Couannier has developed a theory of Cold Fusion based on an extension of General Relativity. This is an interesting approach, since it is hard to believe that what aims at explaining the Universe can also explain what is happening at the nuclear level. The future will confirm or not the validity of such an approach.

Sincerely,

Jean-Paul Biberian
(*Editor-in-Chief*)
February 2016

J. Condensed Matter Nucl. Sci. 18 (2016) 1–23

Research Article

From Dark Gravity to LENR

Frederic Henry-Couannier*

Université d'Aix-Marseille,163 Avenue De Luminy, 13009 Marseille, France

Abstract

Dark Gravity (DG) theories are extensions of General Relativity having a stable anti-gravitational sector. From the beginning, the motivation for such an extended framework was not only phenomenological, trying to address several well-known enigmatic cosmological discoveries in an alternative way: missing mass effects, universe acceleration, ... but also theoretical, and the main achievement is that indeed, it is possible to avoid most if not all generic instability issues which are well known to prevent the introduction of negative masses in General Relativity. Moreover it was also shown that such constructions are not arbitrary but can be entirely derived following the alternative mathematical choice for understanding the Time Reversal Symmetry, that of a Unitary T operator in QFT, needing a complete rehabilitation of negative energies in theoretical physics. All versions of DG theories studied so far unsurprisingly share many phenomenological outcomes, but here we shall focus on one which, for the first time, very naturally leads us to investigate the likely existence of genuine field discontinuities. The resulting phenomenology started to be explored. The first part of the article is a reminder of the main steps that led us to Dark Gravity. The second part focuses on discontinuities to show that these are all we need to explain in an unifying and very simple way many if not all of the well known so called "LENR miracles": Large eXcess Power (XP) not possibly of chemical origin with extremely low levels of nuclear radiations (alpha, beta, gamma, neutrons) as compared to what would be expected from nuclear processes producing the same amount of energy, Transmutations and isotopic anomalies in cold conditions, Incredible properties such as huge inertia anomalies and temperature discontinuities of a new category of objects produced in association with LENR and behaving as extremely magnetic micro ball lightnings.
 ISSN 2227-3123

Keywords: Anti-gravity, Field discontinuities, Janus field, LENR, Negative energies, Time reversal

1. Introduction

So far, most popular attempts to explain the cold fusion "miracles" have been based on a bet which also corresponds to a widely accepted view among LENR leader theorists: standard physics alone must be able to explain them. Those scientists generally agree that it is only the extreme complexity of how the accepted fundamental laws apply to a variety of condensed matter non trivial structures subjected to unusual treatments that had prevented for decades the identification of those peculiar configurations and involved combinations of processes allowing these unexpected phenomena to occur.

*E-mail: fhenryco@yahoo.fr

 ISSN 2227-3123

Given how challenging indeed is a priori the identification of processes based on standard physics alone that would allow to overcome the Coulomb barrier in usual temperature and pressure conditions (this is the first LENR miracle), what appeared to me so paradoxical was this extremely conservative principled stand among the same adventurers who often had sacrificed their own careers relentlessly continuing their efforts down this direction of research. The more and more absurd this sounded to me when after studying some of the more popular candidates, I realised that the more involved were the models and complicated the equations, the more incredibly unphysical the hypothesis these too often tried to hide or minimize. The miracle that needed to be explained was just repeatedly, more or less explicitly, translated into another hidden miracle which was sooner or later identified by the other LENR theorists and skeptics. Eventually each such new cross in the cemetery of LENR theories apparently added ever growing confirmation to the common skeptical view that the effort was doomed to failure. Even worse, many models focusing on the first "miracle", were neglecting the growing accumulation of new evidence showing even more challenging other related "miracles". These are for instance the transmutations always favouring final stable nuclei in the absence of high energy particles radiation that were considered to be the unavoidable nuclear products underscoring the occurrence of any kind of nuclear processes according to the laws of nuclear physics. Last but not least, even the models meeting the challenge of the first two miracles almost always completely missed another category of observations, pointing the "miracles" of the third kind that I will try to address in more details in the second part of this article: the existence of extremely enigmatic objects, genuine micro ball lightnings produced in association with the LENR type of transmutations thus undoubtedly linked to the first two "miracles". This convinced me that for a theory to have any chance of successfully addressing the two other so called LENR miracles, the theory should first take seriously and address in detail not just some selected properties of these objects but all of them, starting from the most incredible and challenging ones: temperature discontinuities, huge inertia anomalies, ability to propagate through matter and so on.

This surely would not have been possible if a theoretical framework did not already exist providing the right cards in hand, my own version [1,2,7] of a Dark Gravity [1–5] theory which I had initially (knowing nothing about LENR) developed to deal with well known theoretical instability issues of General Relativity in the presence of negative energy objects. One of the right cards was the new physics of field discontinuities which occurrence is made natural by the new dynamical status of discrete symmetries in this version of Dark Gravity theory the genesis of which I will outline the main steps in the first part of the article. As I will try to convince the reader in the second part, these are so perfectly suited to describe the very peculiar properties of the micro ball lightnings, that these properties can even certainly be considered to be as many signatures of the physics of field discontinuities.

2. Negative Energies, the Forgotten Solutions; a Scandal at the Root of All Modern Quantum Field Theories

Just because of the famous formula

$$E = \pm\sqrt{p^2 + m^2} \tag{1}$$

negative energy field solutions were expected in any relativistic classical field theory for both massive and massless ($m = 0$) particles. For instance the free scalar negative energy field just requires negative kinetic energy terms in its action and maximization of this action to get its free motion equations and a negative Hamiltonian through the Noether Theorem [6].

There is however a very widespread belief that eventually, thanks to second quantization, the negative energy states were completely understood and re-interpreted in terms of antiparticles. In many modern QFT academic courses the reader is actually faced with an incredible zoo of wrong demonstrations and arguments starting from the Dirac sea saturated with negative energy states, which holes would have been interpreted as antiparticles (an interpretation given up a long time ago by theorists because the picture does not work for bosons, not affected by the Pauli exclusion principle, and yet also having their antiparticles, see [8] pages 12,13), up to the more stubborn view that in the plane wave

Fourier expansion of a field, terms such as $e^{i(Et-px)}$ and $e^{-i(Et-px)}$ respectively initially stood for the negative and positive energy solutions of (1). Then, given that after second quantization the plane wave $e^{i(Et-px)}$ cannot anymore be interpreted as a negative energy wave but, now being associated with an annihilation operator in $a(p,E)e^{i(Et-px)}$ rather represents the operation of removing E, p from a given state, provided *E* is positive, we avoid the creation of negative energy particles by annihilating instead positive energy particles. Of course in this case the mistake was to consider that $e^{i(Et-px)}$ a priori had to stand for the negative energy solution in (1). Yet it is well known that in any real signal Fourier decomposition one can always artificially generate such negative frequency terms by simply rewriting $\cos x = (e^{ix} + e^{-ix})/2$, a purely mathematical trick which does not at all imply that the negative frequencies or energies that would appear in this way are physically relevant.

It is only after second quantization that one understands the genuine physical meaning now acquired by such terms when, being associated with creation and annihilation operators makes clear that the $\pm i$ alternative has nothing to do with the sign of the particle energies involved but rather with the operation of removing or adding quanta to a given state. Indeed, if a plane wave term is associated to a creator the complex conjugate one must be to an annihilator and vice versa, see [8] formulas 5.1.15 and 5.1.16. Then because a field is required to mix the creation and annihilation operators as in formula 5.1.31 of [8], it will involve the creation and annihilation of particles of only one sign of the energy. Therefore if the positive energy scalar field solution of the Klein–Gordon equation is:

$$\phi(x,t) = \int \frac{d^3p}{(2\pi)^{3/2}(2E)^{1/2}} \left[a(p,E)\, e^{i(Et-px)} + a^\dagger(p,E)\, e^{-i(Et-px)}\right] \tag{2}$$

with $E = \sqrt{p^2+m^2}$, we have no reason at all to discard the negative energy scalar field solution of the same Klein–Gordon equation:

$$\tilde{\phi}(x,t) = \int \frac{d^3p}{(2\pi)^{3/2}(2E)^{1/2}} \left[\tilde{a}^\dagger(-p,-E)\, e^{i(Et-px)} + \tilde{a}(-p,-E)\, e^{-i(Et-px)}\right], \tag{3}$$

where we just required the field here to create and annihilate negative energy quanta, this field having its own negative action and Hamiltonian [6]. In other words there are still two possible ways to add (resp remove) a positive energy *E* from a given state: either one creates (resp annihilates) a particle of energy *E*, or one annihilates (resp creates) a particle of energy $-E$, the second option being mathematically as valid as the first. Neglecting the second possibility just amounts to miss half of the solutions of all our equations! Thus, it is certainly correct to argue that QFT convincingly demonstrated that positive and negative energy states cannot be mixed in a Field, but not to claim that we eventually understood the negative energy sector.

As for the anti-particles their existence is required for a charged field to have definite charge, i.e., we cannot have in the same superposition the creator of a charge *Q* and the annihilator of this charge, rather we need to introduce in place of a the annihilator usually called a_c of the opposite charge. It is this argument, not related at all to the negative energies issue, that actually implies the existence of anti-particles, see [8] page 199.

At last we also all remember the famous Feynman interpretation of these anti-particles as negative energies propagating backward in time. But this still has nothing to do with the badly discarded negative energy solutions of all our fundamental field equations which of course should be propagating forward in time.

It is a pity that so many QFT academic courses use kind of magical tricks to try to convince their reader that we were well in our right to discard the negative energy states from the landscape. Fortunately this is not the case in more serious courses such as the Weinberg QFT where the author admits honestly that the only reason to put aside these solutions is that the corresponding particles were never detected in any experiment and also because of the catastrophic instabilities which are apparently unavoidable whenever we shall let them interact with the positive energy states.

At this stage of our reflexion it remains that, as admitted also by [9,10], one could perfectly imagine a mirror standard model of negative energy particles, perfectly stable and with the same phenomenology as in the positive

energy standard model, provided interactions are strictly forbidden between the two standard models; this is of no physical interest and, as we shall see, this is not the picture required from a deeper investigation.

3. Unitary Time Reversal

Not only are negative energy fields solutions of all our field theory equations but there is a symmetry, time reversal, believed to be a very fundamental one, that applied to any positive energy state is expected to regenerate the corresponding negative energy state. Indeed, according to special relativity alone, *E* should flip to $-E$ as t flips to $-t$ just because these are the fourth component of their respective four vectors. Fortunately for QF theorists this can be avoided if i also flips to $-i$ at the same time thanks to the mathematical choice of an anti-unitary time reversal operator in QFT. Let us cite [8] pages 75,76: "If *P* were anti Unitary ... for any state Ψ of energy *E* there would be another state $P^{-1}\Psi$ of energy $-E$. There are no states of negative energy ... so we are forced to choose the other alternative: *P* Unitary. On the other hand if we supposed that *T* is unitary we could simply cancel the is in $TiHT^{-1} = -iH$ (where *i* is nothing but the familiar complex number satisfying $i^2 = -1$) and find $THT^{-1} = -H$ with the again disastrous conclusion that for any state Ψ of energy *E* there would be another state $T^{-1}\Psi$ of energy $-E$. To avoid this we are forced to conclude that *T* is anti-unitary."

Recalling the story of Dirac equation solutions that were considered unphysical for many years until the discovery of anti-particles, extreme caution should be the rule before discarding solutions of so fundamental equations. Even more, we believe that such attitude was a genuine collective fault given that even after second quantization there is still no convincing theoretical argument to discard them as we explained. Instead, based on the non observation of negative energy states and the related instability issues, a significant effort was required to better understand how the consistent rehabilitation of such states could be carried on assuming Unitary time reversal linking naturally positive to negative energy states is the correct option. The first impediment we encountered on this way and that turned out to be very instructive is that even though

$$T\phi(x,t)T^{-1} = \tilde{\phi}(x,-t) \tag{4}$$

and

$$Ta^{\dagger}(p,E)T^{-1} = \tilde{a}^{\dagger}(p,-E). \tag{5}$$

It seems impossible to transform the "positive" Hamiltonian for our free neutral scalar positive energy field:

$$H = +\frac{1}{2}\int \mathrm{d}^3x \left[\left(\frac{\partial\phi(x,t)}{\partial t}\right)^2 + \left(\frac{\partial\phi(x,t)}{\partial x}\right)^2 + m^2\phi^2(x,t)\right] \tag{6}$$

into the "negative" Hamiltonian for the corresponding negative energy field:

$$\tilde{H} = -\frac{1}{2}\int \mathrm{d}^3x \left[\left(\frac{\partial\tilde{\phi}(x,t)}{\partial t}\right)^2 + \left(\frac{\partial\tilde{\phi}(x,t)}{\partial x}\right)^2 + m^2\tilde{\phi}^2(x,t)\right] \tag{7}$$

through Unitary Time Reversal (see [6]).

The only way out of this dead end was to reconsider the problem in a gravitational context, i.e., after introducing everywhere as they should be, in the actions and Hamiltonians the order two tensor field of GR provided it should also transform in a non trivial way under time reversal, i.e., in another order two tensor field, different in the sense that such a transformation would not merely be a general coordinate transformation but would also involve a non trivial jump from the initial inertial coordinate system to another inertial coordinate system. Only such an approach would still

respect and allow it to remain meaningful, even in a gravitational framework, the discrete character of time reversal, a symmetry linking as we know otherwise disconnected representations of the Lorentz group [2] pages 4,5.

This approach was from the beginning very promising as it would obviously isolate the positive and negative energy sectors from each other, given that propagating on different sets of geodesics these would never meet (interact through EM, weak or strong interactions) each other. This would explain why the negative energy particles escaped observation and at the same time avoid the instability issues at least for all non gravitational interactions.

Before setting out the concrete solution that eventually has emerged, it is worth recalling two other interesting results collected from our investigation of negative energies in a non gravitational framework [6].

- If we actually allow both positive and negative energy boson propagators to propagate an interaction what we actually discovered is that the interaction vanishes. This might be interesting to cancel QFT UV loop divergences by allowing the reconnection between positive and negative energy worlds beyond a given energy threshold.
- Vacuum divergences for positive and negative energy fields being unsurprisingly found to be exactly opposite, it is hoped a cancellation of their gravitational effects, solving thereby a very long lasting issue.

It is also worth recalling that any new ingredient manifesting anti gravitational properties is irresistibly attractive for cosmologists given that the LCDM model of course passes many tests with flying colours but still relies on many enigmatic components: Dark Energy, Dark Matter, Inflation, still badly understood and introducing very serious issues such as fine tuning and coincidence problems. This was actually the motivation for the first Dark Gravity theory ever published by [3] which has been followed by his many other publications detailing the very rich expected new phenomenology and showing for instance how efficiently the negative masses of our twin universe can help our galaxies rotate as observed, see [12,11] and references therein. One can convince oneself of the extreme motivation for anti-gravity among theorists by typing “phantom fields” or “ghost fields” on arXiv: thousand of articles, a huge theoretical effort all over the world to try nevertheless to introduce negative energy fields in such a way that Hawking positive energy conditions would not be violated too seriously. All this waste of time and energies could have been avoided by recognizing the correct way to reintroduce negative energies in GR while avoiding all instability issues as S. Hossenfelder states on her famous blog [13], mentioning her Phys Rev D publication [5], strongly convergent to my previously published works [1,2] (read the next section then look at the Janus relation (47) in her Annex).

It was a pleasant surprise when I learned recently that Milgrom himself, who is very famous for being the father of MOND theories, has refined his modified gravity theories in such a way that this effort eventually has resulted in a genuine Dark Gravity theory [4].

4. The Janus Gravitational Field

The previous section led us to the conclusion that we certainly need to introduce another gravitational field which geodesics the negative energy fields will have to follow. However, this mere idea is strongly conflicting with an almost religious belief shared by almost all gravity experts: a good theory should be background independent. Before studying gravity, we thought that we had the right to build theories with as many fields we wanted and of any kind: scalar, vector, higher order tensors, and Dirac fields upon a flat non dynamical space-time described by the Minkowski metric η. But according GR experts, the order two tensor field of GR has a very special and privileged status: it is the metric that describes the geometry of space-time itself! Of course this belief has been supported by the fact that the tensor of gravity, as any order two tensor field, has the required properties to be a metric and since η is now completely absent from the fundamental general covariant equations of gravity, g could replace completely η in the role of being the genuine metric of space-time itself. Anyway, as a consequence of this a priori, one could not consider anymore the possibility of having two different gravitational fields defining two different incompatible geometries in a theory, given

that we have only one space-time. By the way, another far reaching consequence is that for both string theorists and loop quantum gravity theorists, quantizing gravity means quantizing space-time itself.

For us, who need to introduce two different gravitational fields on a single manifold (x, y, z, ct) such fields obviously cannot describe the geometry of space-time itself. These just describe the two different geometries felt by the matter and radiation fields propagating along their respective geodesics. Eventually just as light is deflected from air to water, in the same way light can be deflected by interacting with a gravitational field even though in this latter case it has been possible to interpret this interaction as mere propagation along deformed geodesics of space-time itself, a view that we have to give up completely.

However, now the Minkowskian background η describing the still flat and non dynamical background geometry of space-time itself certainly cannot be neglected as we did in GR: we are not anymore background independent. More specifically η is now the object we need to rise and lower tensor indices. But then in a theory where we have a priori both η and the usual gravitational field g we also unavoidably have the other tensor field $\tilde{g}$ obtained by lowering the indices of the contravariant g^{-1} with η. This is

$$\tilde{g}_{\mu\nu} = \eta_{\mu\rho}\eta_{\nu\sigma}\left[g^{-1}\right]^{\rho\sigma} = \left[\eta^{\mu\rho}\eta^{\nu\sigma}g_{\rho\sigma}\right]^{-1}. \tag{8}$$

Thus the Janus gravitational field, like the Janus God, has two faces, $g_{\mu\nu}$ and $\tilde{g}_{\mu\nu}$ linked by the above manifestly covariant and background dependent relation. The two forms play perfectly equivalent roles relative to the background metric $\eta_{\mu\nu}$ so should be treated on the same footing in our actions if we do not want to artificially destroy the basic symmetry of the picture under their permutation. Symmetrizing the roles of $g_{\mu\nu}$ and $\tilde{g}_{\mu\nu}$ is performed by simply adding to the usual GR action, the similar action built from $\tilde{g}_{\mu\nu}$ and its inverse.

$$\int \mathrm{d}^4x(\sqrt{g}R + \sqrt{\tilde{g}}\tilde{R}) + \int \mathrm{d}^4x(\sqrt{g}L + \sqrt{\tilde{g}}\tilde{L}), \tag{9}$$

where R and $\tilde{R}$ are the familiar Ricci scalars built from g or $\tilde{g}$ as usual and L and $\tilde{L}$ the Lagrangians for respectively SM F type fields propagating along $g_{\mu\nu}$ geodesics and $\tilde{F}$ fields propagating along $\tilde{g}_{\mu\nu}$ geodesics. The theory that follows from just symmetrizing the roles of $g_{\mu\nu}$ and $\tilde{g}_{\mu\nu}$ is DG which turns out to be essentially the other option of a binary choice that must be done at the level of the conceptual foundations of a covariant theory of a symmetric order two tensor field: either the space-time is curved with metric $g_{\mu\nu}$ and we get GR, or it is flat with background metric $\eta_{\mu\nu}$ and we get DG!

Now remember our initial purpose, which was to identify another field which geodesics would welcome the forgotten negative energy standard model of QFT. We shall show that the "inverse form" $\tilde{g}_{\mu\nu}$ is this field (this is not truly speaking of another field because it is not independent from g) that we get for free from Eq. (8), i.e., just from our understanding that we should not be in a background independent theory anymore. The two faces of the Janus Field will turn out to be conjugate under the time reversal symmetry, and all energies of field propagating on one face will be seen opposite from the point of view of the fields living on the other face and feeling their anti-gravitational effect. So the choice between DG and GR becomes an easy one. The usual extreme action principle must be used by eliminating the $\tilde{g}_{\mu\nu}$ degrees of freedom thanks to the Janus relation Eq. (8) to eventually get a single field equation in place of Einstein equation satisfied by $g_{\mu\nu}$. The solution also allows to get immediately $\tilde{g}_{\mu\nu}$.

5. The Static Isotropic Elementary Solution

In [2], we were led to explore many non standard theoretical possibilities because we did not want to miss any prediction that could allow us to decide between GR and DG, one "problem" being that DG, without any free additional parameter, mimics so perfectly GR. Here we shall take instead the most standard path until we introduce the new phenomenology relevant for LENR.

We found a couple of static isotropic conjugate solutions in vacuum of the form $g_{\mu\nu} = (B, A, A, A)$ and $\tilde{g}_{\mu\nu} = (1/B, 1/A, 1/A, 1/A)$

$$A = \mathrm{e}^{\frac{2MG}{r}} \approx 1 + 2\frac{MG}{r} + 2\frac{M^2G^2}{r^2}, \tag{10}$$

$$B = -\frac{1}{A} = -\mathrm{e}^{\frac{-2MG}{r}} \approx -1 + 2\frac{MG}{r} - 2\frac{M^2G^2}{r^2} + \frac{4}{3}\frac{M^3G^3}{r^3} \tag{11}$$

perfectly suited to represent the field generated outside an elementary source mass *M* (understood to include all contributions to the total gravific mass including the energy of the gravitational field). This is different from the GR one, though in good agreement up to post-Newtonian order. It is straightforward to check that this Schwarzschild new solution involves no horizon: no more black hole! Only future precision experiments able to probe the PPN order terms or strong gravity tests near the Schwarzschild radius will be able to decide between GR and DG.

The solution also confirms that a positive mass *M* in the conjugate metric is seen as negative mass $-M$ from its gravitational effect felt on our side. Masses on the same side attract each other, masses on different sides repel each other. There is no longer the runaway instability that was unavoidable when one naively introduced negative energies on the same side as positive energies. Neither do we find any instability in the gravitational sector.

Indeed, the requirement that the conjugate metrics should satisfy the same isometries is very constraining. This is easily seen by adding an arbitrary Spherical Harmonic perturbation $f(r)Y_{l,m}(\theta, \phi)$ to any element of an isotropic $g_{\mu\nu}$. Then the inverse form $\tilde{g}_{\mu\nu}$ elements will develop an infinite number of other Spherical Harmonics, meaning that obviously the two forms do not share the same isometries anymore. So the only acceptable metrics are a priori in the isotropic form $g_{\mu\nu} = (B, A, A, A)$, and $\tilde{g}_{\mu\nu} = (1/B, 1/A, 1/A, 1/A)$. We also introduced new exchange symmetries constraining the fields even more to either $B = -1/A$ or $B = -A$! As a consequence of these fundamental requirements, our new $B = -1/A$ Schwarzschild solution cannot accept any kind of the non isotropic Spherical Harmonics perturbations as the ones introduced by [14] to test the stability of the Schwarzschild solution. But then, the only isotropic non static perturbation solution in vacuum must be in the sector $B = -A$ which stability is granted (see Section 6).

Moreover the impossibility of any $B = -1/A$ perturbation that would satisfy a wave equation means that there is no wave at all allowed in this sector of the theory and that our gravitostatic field is un-propagated. It is instantaneous but may be no more than the electrostatic field according recent impressive experimental results [15] that seriously call into question the traditional understanding that the static fields in our theories actually result from the exchange of waves at the speed of light. Alternatively it might soon become common knowledge that a non propagated sector have always co-existed with a propagated sector in all our most familiar theories. This will probably require that the EM differential equations no longer be considered valid from $t = -\infty$ to $t = +\infty$ and everywhere but only piecewise over finite time and space intervals where it will be possible to replace them by timeless differential equations in case of a static elementary source.

The most natural interpretation of our isotropic $B = -1/A$ field, is that, as we explained above, this is the elementary field sourced by an elementary mass. Fortunately, it is easy, thanks to the exponential form of the metric [2] Eq. (14) to combine any elementary metrics of this kind for source points even moving with respect to each other, after exporting them to a common coordinate system. From this you can get the total gravitational field produced by any extended distribution of energy and momentum, pressure (from massive relativistic particles only), any potential energies either gravitational (energy of the gravitational field) or non-gravitational being taken into account in the same way as in GR up to post-Newtonian order with the same quantitative predictions. Then we can later require matter and radiation fields to follow, as in GR, the geodesics of the $B = -A$ dynamical field combined with this total $B = -1/A$ field which is not dynamical anymore (the various elementary fields already played their dynamics in their

own individual actions where their point mass source was not dynamical). One of course can derive in this way as usual the covariant conservation equation $T^{\mu\nu}_{;\mu} = 0$ describing energy exchange between matter and gravitation, keeping in mind that as far as the $B = -1/A$ total field is concerned this exchange is not the radiation of gravitational waves. This is just the familiar exchange between kinetic energy and potential energy of a mass throughout its trajectory, the latter being nothing else but the energy of the total non dynamical $B = -1/A$ gravitational field.

6. $B = -A$ Field: The Global Homogeneous Solution + Perturbations

6.1. The $B = -A$ field and perturbations

The theory at this stage will remain globally static. To get both background expansion and gravitational radiation we need the $B = -A$ field but with drastically reduced number of degrees of freedom, a metric defined from a scalar field Φ that we can write $g_{\mu\nu} = (-A, A, A, A) = \Phi\eta_{\mu\nu}$ and $\tilde{g}_{\mu\nu} = (-1/A, 1/A, 1/A, 1/A) = \frac{1}{\Phi}\eta_{\mu\nu}$. Recall that the forms taken both by the elementary static isotropic field of the previous section and by this new global homogeneous field were justified based on discrete space-time symmetry arguments, [2] Section VI.

Reducing the number of degrees of freedom to a single scalar is mandatory to have an energy–momentum tensor for gravity that does not vanish to second order in perturbation to get binary pulsars decays as observed. As for the stability in the $B = -A$ sector, it is granted because a mass always couples to the side of the Janus Field which waves carry the same sign of the energy as itself.

6.2. Cosmology

We immediately noticed that the two conjugate metrics cannot be both homogeneous and isotropic unless the spatial curvature is zero. Thus the conjugate universe solutions are necessarily flat in DG without needing inflation! Perturbations about Minkowski can account for the radiative decay of pulsars as in GR, yet the "gravitational waves" in this case have spin zero rather than spin 2 though the coupling to matter is still spin 2 like (minimal coupling to an order two tensor field) and the exchange of such waves between two masses is not expected to generate any additional gravitostatic interaction after quantization (additional to the one described in Section 6.1).

After requiring the action to be extremum we get a single equation for our background single degree of freedom:

$$3A\left(-\frac{\ddot{A}}{A}+\frac{1}{2}\left(\frac{\dot{A}}{A}\right)^2\right)-\frac{3}{A}\left(\frac{\ddot{A}}{A}-\frac{3}{2}\left(\frac{\dot{A}}{A}\right)^2\right)=n\pi G(A^2(\rho-3p)-\frac{1}{A^2}(\tilde{\rho}-3\tilde{p})). \tag{12}$$

The scale factor $a(t)$ definition is as usual $A(t) = a^2(t)$. When $a(t) = 1$, the conjugate metrics identify to each other and to Minkowski allowing to reconnect the content of the two sides. It is thus natural to assume an almost exact compensation, i.e., the same initial global density of energy and pressure on our and conjugate side, an easy way to explain the origin of the matter-antimatter asymmetry, a small initial excess of baryons on our side resulting in the same relative small excess of anti-baryons on the conjugate side just after their separation.

The initial solution is

$$A \approx 1 \Rightarrow \ddot{A} = \frac{\dot{A}^2}{A} \Rightarrow a = \mathrm{e}^{\frac{t-t_0}{T_{\mathrm{ini}}}}. \tag{13}$$

We notice that $a(t) \approx 1$ implies $t \approx t_0$, the origin of times.

As long as both sides remain hot, the source terms both vanish and the conjugate worlds have simple evolution laws in the particular ranges $a(t) \ll 1, a(t) \gg 1$. Indeed, the scale factor evolution is then driven by the following

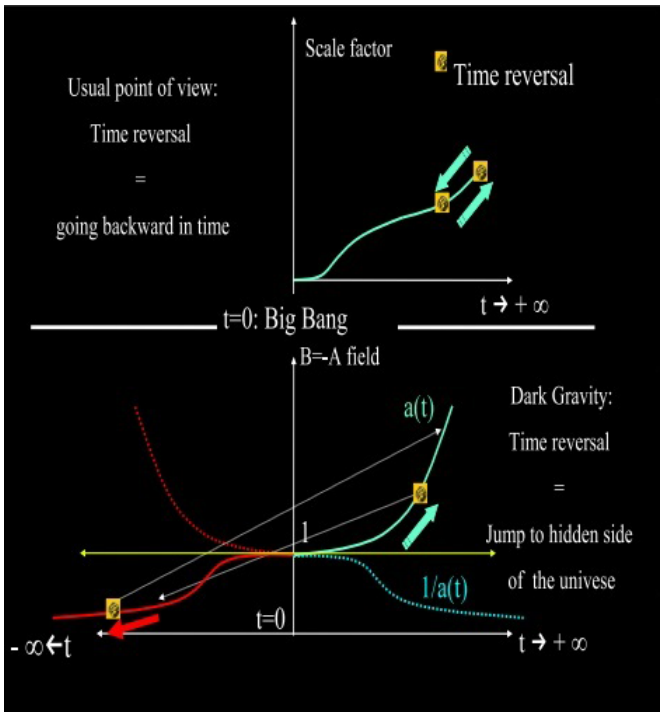

Figure 1. Time reversal in DG vs RG, plotted curves are not realistic.

differential equations:

$$a \ll 1 \Rightarrow (1\ddot{/}a) = 0 \Rightarrow a(t) = \frac{T_{\text{hot}}}{t_0 - t}, \quad \text{where } t < t_0, \tag{14}$$

$$a \gg 1 \Rightarrow \ddot{a} = 0 \Rightarrow a(t) = \frac{t - t_0}{T_{\text{hot}}}, \quad \text{where } t > t_0. \tag{15}$$

If one or both are evolving in a cold era, there is a dominant source term determined by the content of the side with greater scale factor. The differential equations read:

$$a \ll 1 \Rightarrow (1\ddot{/}a) = \frac{-n\pi G\rho_0}{6} = \frac{2}{T_{\text{cold}}} \Rightarrow a = \frac{1}{\left(\frac{t-t_0}{T_{\text{cold}}}\right)^2 + K}, \quad \text{where } t < t_0, \tag{16}$$

$$a \gg 1 \Rightarrow \ddot{a} = \frac{-n\pi G\rho_0}{6} \Rightarrow a = \left(\frac{t - t_0}{T_{\text{cold}}}\right)^2 + K, \quad \text{where } t > t_0, \tag{17}$$

where ρ_0 is the unknown density at t_0. Of course the integration constants t_0, T_{ini}, T_{hot}, T_{cold} and K of the approximate solutions in the different ranges are a priori not the same but must be non trivially related to each others and to ρ_0.

The harvest is already impressively successful! The first good news is that we can check in a straightforward way that $t - t_0 \rightarrow -(t - t_0)$ implies $A \rightarrow 1/A$ i.e. remarkably, we have $A^{-1}(-t) = A(t)$ setting $t_0 = 0$. The conjugate universes are really linked by time reversal, one of our initial goals! One is expanding and the other contracting. But here time reversal does not mean going backward in time anymore. As shown in Fig. 1, reversing time means jumping to the time $-t$ of the conjugate universe where one can remain for sometime before jumping back which can never make you reappear in the past there.

From now on we shall assume that *K* is negligible in the formula for the scale factor cold evolution. Then the coordinate transformations to the more familiar standard cosmological time t' is much simpler. We also set the arbitrary t_0 to 0 and for the sake of simplicity "forget" the other integration constants. We discover that not only our universe can be accelerated thanks to a t'^2 evolution (equivalent to $\frac{1}{t^2}$ after the coordinate transformation from *t* to $t' = -1/t$) for the scale factor without any need for a cosmological constant or dark energy component, not only can it also decelerate thanks to a $t'^{2/3}$ solution (equivalent to t^2 after the coordinate transformation from *t* to $t' = t^3$) as in standard cosmology in the matter dominated era but we also have a standard $t'^{1/2}$ evolution (equivalent to t after the coordinate transformation from *t* to $t' = t^2$) again as in standard cosmology for the radiative era. However, the transition between the decelerated expansion to the recent accelerated expansion regime at the so called turnaround red shift where the universe was between 4 and 7 billion years younger than now requires that coming back to the conformal time we had a sudden (discontinuous) transition from $t^2 \ll 1$ to $1/t^2 \ll 1$, which implies that time reversal occurred and the two conjugate metrics exchanged their roles. But t'^2 is known to be still expanding so t' increases

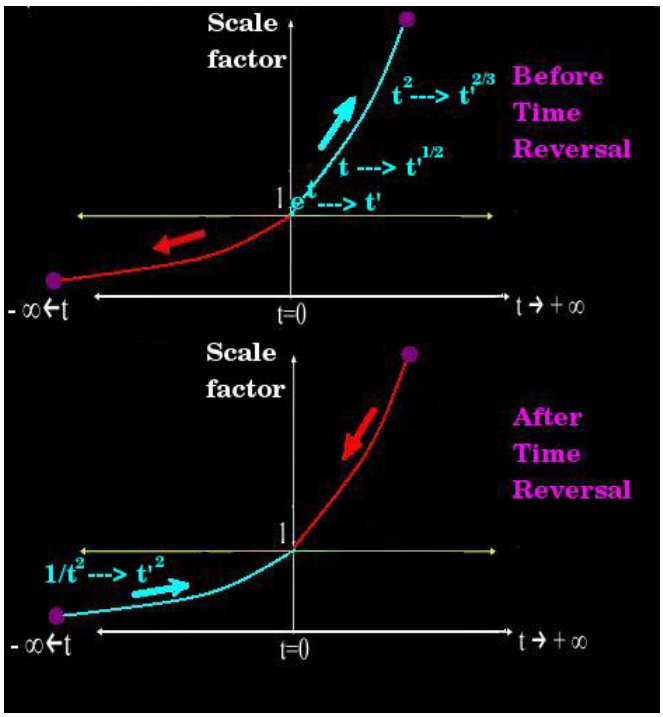

Figure 2. Evolution laws and time reversal of the conjugate universes, our side in blue.

and consequently $-t$ decreases and returns to zero so $1/t^2$ must still be expanding (as did t^2). All this is summarized in Fig. 2.

Now one needs to understand why the huge discontinuous transition from $t^2 \gg 1$ to $1/t^2 \ll 1$ did not have any observational effect. Indeed the same kind of transition if it had been continuous would have produced huge red shift anomalies. This is where the new rules describing the effect of genuine gravitational field discontinuities on various fields minimally coupled to them must be understood. The usual differential equations based on the hypothesis that all fields are C∞ clearly cannot help us to understand the transition. But the evidence is there that only the red shift derived as usual from the continuous variation of the cosmological field before and after the discontinuous transition did have observational effects, not the transition itself. This is as if the effect of the discontinuity was a mere renormalization of the field rather than a time variation and we know that indeed the renormalization of a gravitational field has no observational effect. Also notice that the Hubble expansion rate is the same just before, $H(t) = 2/t$, and just after, $\tilde{H}(t) = -H(-t) = \frac{-2}{-t}$ (since (a(t),dt) $\Rightarrow$ (a(-t)=1/a(t),-dt)), the transition.

Now, coming back to the standard cosmological time we can require that the total age of the universe must be $1/H_0$ as in the standard model (beware that we now change our notations: subscript zero refers to the present time, and t to the standard time). This total age is the sum of the duration Δt_2 of the decelerating regime from the decoupling red shift $\gg 1$ to the transition redshift z_{tr}, given by $\Delta t_2 = (2/3)\frac{1}{H_{\text{tr}}}$, and the duration Δt_1 of the subsequent accelerated t^α regime given by

$$\frac{\alpha}{H_0}\left(1 - \frac{1}{(1+z_{\text{tr}})^{1/\alpha}}\right).$$

Knowing that H_{tr} is related to H_0 by $H_{\text{tr}} = H_0(1+z)^{1/\alpha}$ it is straightforward to simplify $\Delta t_1 + \Delta t_2 = 1/H_0$ to get:

$$z_{\text{tr}} = \left(\frac{2/3 - \alpha}{1-\alpha}\right)^{\alpha} - 1. \tag{18}$$

One checks that our predicted $\alpha = 2$ gives $z_{\text{tr}} = 0.78$ in perfect agreement with the best current estimation $z_{\text{tr}} = 0.77 \pm 0.18$ [17]. This confirms that DG cosmology can perfectly mimic GR cosmology without inflation nor a cosmological constant as regards the scale factor evolution. The transition redshift is expected not to be everywhere exactly the same due to local perturbations so that integrated over large regions, the resulting transition is likely to be observed significantly smoothed by this dispersion of z_{tr}.

Perhaps we can go a little further considering that we have actually obtained a large family of cosmological solutions corresponding to different initial ρ_0 and integration constants. All these universes have a cyclic evolution as in Fig. 2, but some of them will remain in the regime $a(t) \ll 1$ where $a(t)$ is exponential and $a(t') \propto t'$ throughout the cycle. For each such universe, at any time t' its age is given by exactly $1/H(t')$. This is the same formula as the one satisfied by our universe at the present time only by chance! We are therefore tempted to postulate that all universes are constrained to satisfy exactly the same formula giving their age as $1/H_0$ at the end of their completed cycle when returning to and all crossing each others at $t = 0$. Then the coincidence that the total age of our universe is exactly $1/H_0$ at the present time would just be the translation of another amazing coincidence: we are presently almost exactly at the end of a cosmological cycle! This coincidence might be correlated with another extreme coincidence: the present time is also the first time in the history of the universe when human kind has reached a degree of development allowing to understand and may be to take advantage of this! Indeed, being near $t = 0$ also means that various regions of the universe are in a kind of metastable state. These have to choose between $a(t)$ and $1/a(t)$ for the next cosmological cycle and the discrete jump at the frontier between two such regions can be relatively very small because we are very close to $a(t) = 1$. May be this speculation will make more sense later when discussing LENR.

What remains to be investigated is whether the anti-gravitational effects of the matter from the conjugate side can do a better job than Dark Matter at all scales and any epoch of the history of our universe. The situation is very promising from both galaxy simulation studies by JP Petit and my analysis of well known anomalies of Dark Matter models at the galactic scales see [2] Section XX.e. At larger scales it seems difficult to decide between DM and conjugate matter given that they tend to perfectly mimic each other in the linear domain.

Of great importance is the fact that the background metric in DG applies to all scales and not only to the largest scales. For instance the solar system is also expanding (this is not the case in GR [16]) and to avoid conflicts with precision tests probing effects equivalent to a variation of the gravitational constant *G*, an extension of DG is required and was postulated that would result in the electromagnetic field being also affected by the scale factor. A bridge between gravity and electromagnetism takes shape, this being already favoured by the mere fact that our theory is now also a theory having a flat space-time background so that $g_{\mu\nu}$ does not have anymore the exceptional status it acquired in GR and that made it very different from usual other fields such as A_μ.

7. Discontinuities of the Background Field

According to Eq. (12), our side of the universe could have evolved in two possible ways, expanding or contracting in this coordinate system starting from $t = t_0$ where the total source term vanished and the conjugate metrics were equal. But local initial density fluctuations (net source term slightly positive or negative) might have determined how the background decided to evolve in different regions of the universe. This is just similar to the situation we encounter when there is a spontaneous symmetry breaking, a phase transition resulting in different vacuum expectation values for a field in various regions. In other words, one single solution $a(t)$ for the scale factor might not be at work everywhere in our side of the universe. Some regions might instead be evolving according to the other solution $1/a(t)$ implying that the conjugate background metric exchange their roles from one to the neighbour region but then also a genuine discontinuity of this background field at their common frontier. Remember that indeed, it is rather the spontaneous symmetry breaking of a discrete time reversal symmetry that we have to deal with in this case. The background field is a two valued field that can only jump from one value to the other T-conjugate one.

What kind of new phenomenology could we expect from such discontinuities? This was the subject of our article [6] where we focused on three main effects. First, if highly relativistic particles take advantage of these discontinuities which are at the same time metric points and switches to transit from one universe to the conjugate one, these particles would appear to propagate in the conjugate metric faster than our local speed of light. The second effect appears if we compare ticks of two identical clocks separated by a discontinuity: in one region times accelerates as $a(t)$ and in the other region times decelerates as $1/a(t)$ so from the point of view of one clock the other will be seen to accelerate or decelerate at a rate equal to twice H_0. This is exactly (quantitatively) the so called Pioneer effect! The third kind of effect is the one we want to investigate in more details now. Discontinuities of our conformal background metric imply potential barriers able to accelerate massive particles crossing them (the energy gained or lost is proportional to their mass) so these could be new sources of energy for LENR phenomena. However these should be totally transparent to light or other massless particles.

8. Summary Statement

Serious experimentalists in Cold Fusion, when they are quite fed up because of the plethora of ad hoc theories flooding the market, tend to say that to make good physics one should not be imaginative. What one needs is to respect all the experimental data, which are indeed already very much constraining in the field of LENR given how many variants of the initial experiments and effects we have to explain at the same time. Of course this is true, but what these experimentalists do not suspect or tend to neglect is that almost all these models are already born dead by very simple

purely theoretical arguments. Even in theoretical physics there is actually almost no place for imagination. First the game is not to reinvent everything but instead we have to stick to the accepted physics until we can point to a hidden hypothesis that deserves to be put in question or a forgotten solution. Our starting point was that the negative energies were not understood properly but discarded out of hand. To understand them we need to rehabilitate Unitary Time reversal in QFT and a complete revolution of our understanding of time reversal in a gravitational framework but a revolution that unsurprisingly turned out to be so constrained that a single solution were dictated to us by the structure of the problem. Down the road we find that there is another strong assumption of all field theories that we should also put in question: the continuity of all fields (even assumed C infinite in Lagrangian theories). But if we allow ourselves to relax the everywhere continuous hypothesis, it is only because we are strongly justified to do so by the new symmetry of our DG theory, a time reversal that we are now able to really treat as a discrete fundamental symmetry even in a gravitational framework. The plan is especially not to brush off all the physics which has proven itself, of continuous fields that relied on infinitesimal calculus! These laws will still apply almost everywhere i.e. in the bulk of spatial regions at the frontier of which new complementary supplemented rules will apply for discontinuities (see Fig. 3).

Anyway, because this new step is an extraordinary one, it needs extraordinary justifications. This is why we think it is useful to take some time here to explain why we believe discontinuities are one of the missing keys for a better understanding of our Universe.

9. Theoretical Motivations for Discontinuities

9.1. Classical relativistic field theories in a nutshell: encounter of the fourth kind

Classical Relativistic Field Theories were the triumph of four ideas: first it was possible to reach a mathematical quantitative and accurate description of almost all known phenomena. Second the whole theoretical construction can be derived from a very small number of principles: it is extremely economic which also ensures its predictive character. Third, both the principles and the theoretical construction that follows do not conflict much with common sense, our familiar conceptions about the real world (it is much easier to learn how to live with SR than with QM). Fourth,

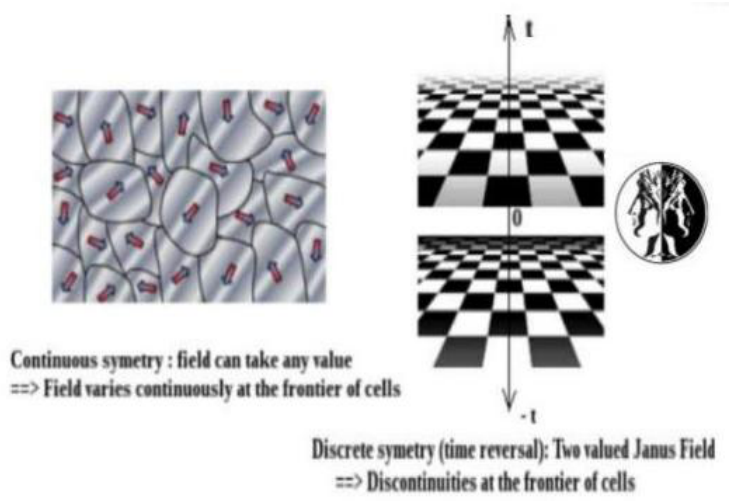

Figure 3. Discrete symmetry domains vs continuous symmetry breaking domains.

the principles themselves do not appear arbitrary but would seem to be implied by a meta-principle which could be summarized in the mere sentence: "science must be possible".

The advent of QM reinforced the two first ideas by extending our understanding to the micro-world with very few new principles, disproved once and for all the third and left the fourth in a worrying status.

To clarify the last point, let us outrageously summarize our understanding of how classical relativistic field theories could have been obtained. To describe the container of everything we give ourselves three space coordinates and one time coordinate. Everything in the content will be described in terms of fields, i.e., just one or several numbers at each point of space and time. Nothing is more refined than the idea that at the roots of everything you do not have water (as would have argued Thales), nor fire (à la Heraclitus) nor even atoms (à la Democritus) but just . . . numbers.

But probably because this was not simple (unified) enough we require that the Transformation between two Galilean frames should be rather of Lorentzian than Galilean type (no other choice according modern axiomatizations of SR) because this is the only choice that really allows to unify the four space-time coordinates in a single multi-component object (x, y, z, ct) but this requires the introduction of an invariant universal finite speed c. From this follows the whole theory of SR. In particular the structure of the container, our now unified space-time, requires the content, the fields, to belong to well defined representations of the Lorentz group, i.e. our numbers must be arranged into single or multi-component objects, our now familiar scalar, four-vector and higher order tensors, Dirac fields and so on. The next step is to ask what are the laws of physics that these fields should obey. Of course such question presupposes that we believe in a kind of meta-principle: that science is possible. This in turn implies that there must be universal laws valid everywhere and at any time. Obviously if we had to reestablish the laws at each new location or each new morning, science would not be possible. The requirement needs to be generalized to any kind of space-time transformation that should leave the fundamental equations invariant. Science is possible also implies that we are not in a trivial world: things must occur, fields must be allowed to vary, derivatives are needed. But science is possible also implies that the laws should not be over-complicated if we want to be given some chance to discover them so let's ask no more than two derivatives in all terms of our fundamental equations. Now just knock the door of your favourite mathematician and ask the generally covariant laws with no more than two derivatives and he will give you all our familiar laws for a massless or massive four-vector Field, the GR laws for the order two tensor field of gravity and, he might also give you a very powerful recipe to get the laws, the extreme action principle. Without exaggerating too much, that is the very impressive feeling that you might be left with after studying Classical Field theories: the mere requirement that science must be possible could have led pure thought to discover the laws without even performing a single experiment!

9.2. Two parallel paths: from DG to QM, from DG to LENR

Given how unexpected and weird were the new rules introduced by QM, the Planck Einstein quantization relations and the non local and non deterministic collapse of the wave function, it was clear from the beginning that considering these new rules as principles would irremediably and severely maul our fourth idea that the principles of our fundamental theories should not be completely arbitrary. Yet when theoreticians progressively realized that they will have to give up forever the idea of a local theory behind QM after many experiments confirmed the reality of the "spooky action at a distance" in the words of Einstein, they threw the baby out with the bath water, they gave up the fourth idea together with the third.

Indeed, almost no effort was engaged to explore a deeper world with new discontinuous and non local laws and to discover less arbitrary principles (themselves almost necessary starting from the meta-principle that science must be possible) from which the QM rules could have been hopefully derived. Instead the effort was focused on unifying the interactions and trying to apply quantization as we (do not) understand it to gravity which resisted up to now.

In DG the context is the best one could imagine to start such exploration:

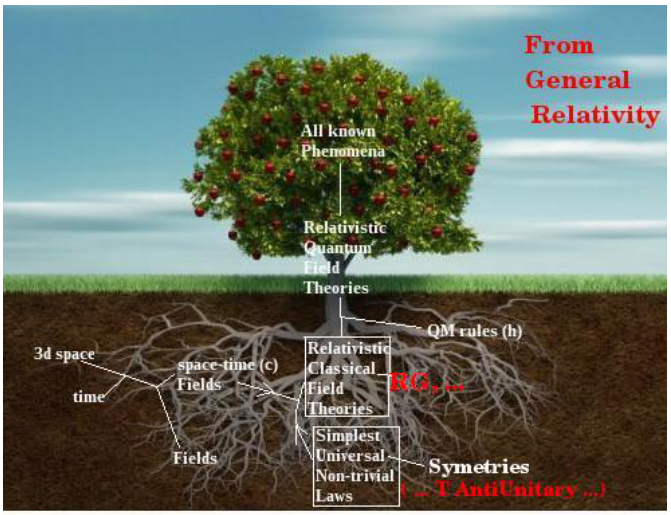

Notice: Fields assumed to vary continuously
Problems: - QM and GR are not compatible
- Weird non trivial choice for Time reversal (Anti-Unitary)
- QM principles appear completely arbitrary and weird

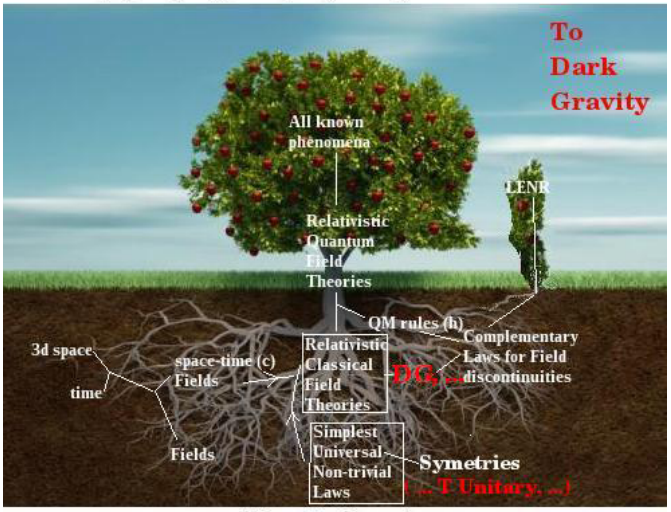

Unitary Time Reversal
> GR is modified to be invariant under time reversal ==> discontinuities are natural
> Modified GR in the bulk + laws for Field discontinuities at domain frontiers
> Hopefully the new GR will be more compatible with QM
> QM rules can be derived from more fundamental non local laws for discontinuities

> A new tree: LENR phenomena directly following from field discontinuities

Figure 4. Synopsis.

- Discontinuities and our non propagated gravity have all to be the missing keys to understand where discontinuous and non local rules of QM come from and to hopefully predict the value of the Planck constant, in other words, compute the fine structure constant α.
- Rehabilitation of negative masses allows us for the first time to imagine a stable structured vacuum based on alternating positive and negative masses, a new actor hopefully responsible for the non local QM collapse, and standing for the creation and annihilation operators of QFT.
- LENR phenomena could be the direct consequences of the physics of discontinuities allowing to probe a deeper level of reality without conflicting with the accepted physics that results from the quantization of our classical field theories, QM being the other indirect parallel consequence of the physics of discontinuities.

Moreover let us stress again that being a theory with a flat space-time background and with a not so exceptional field (apart its Janus Character), DG gravity might be much better positioned than GR gravity to be quantized if necessary or unified with other interactions. Figure 4 is a synopsis of the ideas developed in the previous sections.

10. LENR, the Whole Experimental Evidence

None of the following LENR main signatures, the so called miracles, should be ignored or neglected.

(A) Large excess Power (XP) not possibly of chemical origin with very low levels of nuclear radiations (alpha, beta, gamma, neutrons) as compared to what would be expected from nuclear processes producing the same amount of energy.
(B) Transmutations and isotopic anomalies in cold conditions.
(C) Observation of a new category of incredible objects which behaviour seems almost impossible to understand without postulating new physics (for instance caterpillar traces left by micron sized magnetic and radiating objects able to fly meters away from their source, to go through dense materials, to explode and release much energy in them, and so on) objects which were discovered by many scientists independently (Matsumoto, Dash et al., Shoulders, Lewis, Savvatimova, Urutskoev et al. , Ivoilov and other groups) in many kind of experiments involving macro or micro electric discharges and independently named Evos, EVs, Ectons, Plasmoids, Ufos, Leptonic Monopoles, Charged Clusters, Nucleon Clusters, Micro Ball Lightning, ... [18] and all references therein.

Any idea proposed to explain (A) or (B) but neglecting (C) is almost certainly wrong because it is unlikely that two kinds of very different new theoretical ingredients are needed, one to explain (C) and another to explain (A) and (B), while the detections of the two kind of effects are clearly related. Indeed, typical transmutations of LENR (without high energy radiation and leading to stable nuclei only) have often been reported in association with the observation of strange tracks, and often in the tracks themselves. There is even an annual conference called Russian Conference on Cold Nuclear Transmutation and Ball-Lightning (RCCNT and BL) and regularly there also have been presentations on Ball Lightning and strange tracks at the ICCFs. The properties of these objects are so unimaginable that even if we could produce a theory to address (A) or (A) and (B) pushing standard physics to its limits to get unusual screening effects or energy concentrations in condensed matter, it seems extremely unlikely that it will explain at the same time observations of the third kind (C). On the other hand if you are able to provide an explanation for (C), you might be more lucky to elucidate (A) and (B) at the same time. Clear sightedness thus recommends that we should first gather the detailed evidence about the strange objects that we shall call micro ball lightnings (mbl) following the interpretation of [18], that though much smaller than their sisters produced in lightning storms, these are probably of the same nature given that in both cases we have to explain the long term stability of an object concentrating electromagnetic energy, luminous and charged appearing as the result of a more or less powerful electrical discharge. Apparently the

more powerful the discharge, the greater and longer lived the ball lightnings. We include micro-discharges near metal surfaces in simple electrolysis experiments or inside metal cracks (Ni, Pd) in experiments where these discharges can result from either the metal surface being submitted to mechanical, thermal or EM pulse shocks or the cracks to successive loading and de-loading of H or D or to a current flow that these cracks block, triggering micro-discharges. We also leave open the possibility that the universal trigger might just be a concentration of charges implying a local increase of the electrostatic energy since such conditions can both lead to discharges or be created by them.

11. From Field to Temperature Discontinuities

The challenge is thus the same as it is for macroscopic ball lightning; it is to find a mechanism able to confine a significant amount of energy in the form of heat (the temperature inside is at least of 1000°) and resist the pressure during the whole lifetime of for instance a 6 μm sized mbl (between 10 and 0.01 μs, [21]) and to explain how such

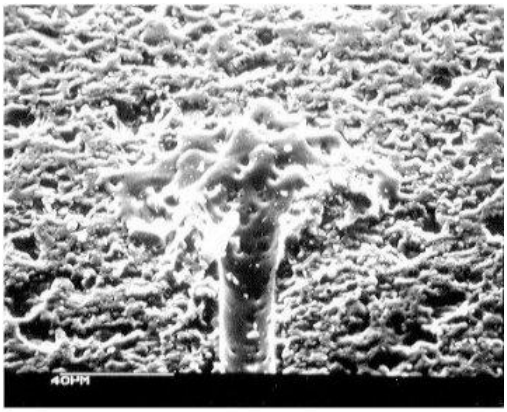

Entrance cross section of EV borehole in aluminum oxide showing sloshing cycles.

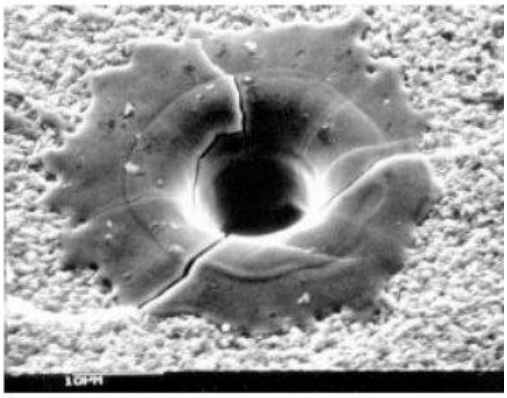

SEM micrograph of EV entrance into lead glass showing wave action of sloshing.

Figure 5. Boreholes left by mbls.

a macroscopic collection of a huge number of particles can behave as a single object leaving a well defined track in nuclear emulsions or boreholes in matter. The stability problem is even worse if you take seriously the results from various researchers [20,21] strongly suggesting that the mbls also carry a huge electric charge, because you then have to explain how these can resist the corresponding electrostatic repulsion between an incredible concentration of charges of the same sign.

Let us cite the ground breaking result obtained by Shoulders after analysing boreholes left by mbls: "The borehole is fairly clean for a process that is capable of fluidizing a material with a melting point of 2600°C and projecting it to an unholy velocity. In fact, when a special test is set up to determine the thermal gradient at the edge of the borehole, one comes to an astounding conclusion: either a gradient of over 26,000°C/μm exists here, or this is a non-thermal process!". Can we imagine a better signature for a field discontinuity than this evidence for a temperature discontinuity (Fig. 5)?

We are led to understand the mbl as a macroscopic object, i.e. a huge collection of particles with an initial density determined by the medium where it formed (gas, liquid, and solid) surrounded by a discontinuous gravitational potential which can accelerate in a centripetal way all massive particles encountered up to an energy proportional to their mass and then trap them inside, resisting both pressure and electrostatic repulsion between particles of the same charge trapped in the volume delimited by the discontinuity. The discontinuity is of course one possible source of the particles kinetic energies and hence temperature inside the mbl. But how could the energy escape out of the mbl and be measured as heat (XP) outside if the energetic particles are all trapped inside? Again the answer is simple. The kind of gravitational potential barrier implied by a discontinuity of the background field has no effect on massless particles (conformal metric), so any photon can cross it and escape (hence the name Ball Lightning). Thus the radiative cooling of the mbls can take place efficiently, implying that these are able to heat their environment but only radiatively.

The mbl is also charged and it is actually the electrostatic density of energy implied by this charge that reached the threshold that triggered the apparition of the discontinuity. For instance, an electrical discharge impact might generate a very short-lived concentration of charges of the same sign which is of course electrically very unstable and should disperse very fast if a discontinuous potential suddenly appearing did not trap them, stabilizing the object for a much longer time. The mbl would therefore be stabilized as long as it is able to keep the charge that gave birth to it.

Let us specify our understanding of the most likely origin of this electrostatic energy threshold. The source term in Eq. (12) determines whether the background will choose the $a(t)$ evolution or the $1/a(t)$ evolution. It just depends on which contribution is the greater, our side positive or the conjugate side negative. If we are in a vast region dominated by the conjugate side source term then a local concentration of energy on our side, an energy that fills the available space as is the energy of the electromagnetic field rather than concentrated in points (as is the energy of massive particles), as soon as this new contribution locally exceeds the conjugate side one, the background will flip in this region to the other regime, producing a discontinuity with amplitude $a(t) - 1/a(t)$ sitting exactly at the surface frontier between the external area where the conjugate side still dominates and the internal one which is enclosed by the discontinuity. Of course this surface is defined by the vanishing of the total source due to the exactly compensating terms from our and conjugate side. As we explained earlier the dynamical background components $a(t)$ and $1/a(t)$ are expected to be rather close to each other in our cosmological epoch. If the difference is of the order of 10^{-9} the potential barrier implied is 20 eVs for nucleons and of the order of 10 meVs for electrons.

Since the probability of reaching the crucial threshold is determined by the local density of energy on the conjugate side on which we have no control and no knowledge, but also on potential gravitational energies implied by the position of massive local objects (planets, sun), and since these are expected to fluctuate in time, it is not surprising that eventually, cold fusion COPs are so erratic and unpredictable.

12. Fate of mbls: the Fast Case

Because the discontinuous potential barrier is two thousand times more effective for the more massive nucleons than it is for electrons, it turns out that it is much easier to keep alive positively charged mbl than negative ones. Indeed inside the mbl any interaction between the cold electrons (accelerated to 10 meV) and much hotter nuclei (accelerated to 20 eV) will likely boost the electrons to an energy much above the 10 meV mbl barrier for them. Thus eventually the electrons tend to be ejected out of the mbl while the nucleons are trapped much more efficiently because the potential barrier is much higher for them. This would result in a very unstable initially negatively charged mbl (remember an mbl must keep its charge to stay alive) unless the radiative cooling of the nucleons is much faster than the rate at which the hot nucleons interact with the cold electrons (the crucial physical parameter here is probably the plasma density). On the other hand stability should be granted for the positively charged mbls in vacuum. Indeed, in this case, the electrostatic attraction by the protons prevents the electrons to escape too far from the mbl even if they have sufficient energy to overcome their discontinuous potential barrier.

But of course, in real life conditions, mbls can only rarely be considered isolated from surrounding matter of their environment, as if they were in vacuum. As a consequence of their charge the mbls will be attracted and will attract any opposite available charges around and absorbing them will tend to recover neutrality. Losing its net charge in this way any mbl is expected to soon collapse and "evaporate" as it recovers neutrality. Eventually, any mbl, either positively or negatively charged is unstable if it is not strictly isolated.

Two fate scenarios are possible, a fast and slow one. Let us list the steps involved in the most common fast collapse:

- As the mbl neutralizes, at any place where the density of electrostatic energy has decreased below the threshold defined by the conjugate density of energy the background has returned to its exterior value which therefore gains ground on the volume of the mbl. In other words, the mbl collapses.
- For a fast input of opposite charges and hence fast neutralization, because of the mechanical work that the discontinuity gives to the mbl interior plasma during the collapse, the heat accumulates too fast in the mbl to allow it to radiatively dissipate this heat.
- The kinetic energies of the particles inside the mbl increase up to the point where these can overcome the discontinuous barrier and escape. The lost of its charge as it seems to "evaporate" in this way also accelerates the collapse of the mbl up to total disappearance.
- In such process it is still only the radiative losses that are responsible for heating the environment and the XP because the particles escaping the barrier are instantaneously cooled to the exterior temperature. The very origin of this excess energy is neither directly chemical nor nuclear so far. It is rather the potential energy implied by the discontinuity, and the mechanical compressional work performed by this discontinuity both turned into radiation (light). Because the Noether theorem does not apply any more for discontinuous fields, the energy is a priori not locally conserved in such process but still might be globally conserved.

13. Fate of mbls: the Slow Case

13.1. The slow collapse

The slow collapse is probably exceptional but much more energetic as it triggers nuclear reactions. If the collapse is sufficiently slow, such a small object as is the mbl can radiatively dissipate its heat faster than it is produced so that the mbl can remain cold during the collapse. The particles kinetic energies now remain insufficient to escape the potential well. Thus the mbl keeps its content and compresses it up to huge densities. For this to be possible a first necessary condition is probably that the positively charged mbl is magnetically trapped in a metal crack or trapped in an insulating material or any area where it is slowly fed with electrons and recovers neutrality extremely progressively. A magnetic trap may rely on the extremely magnetic properties of the mbl that we shall investigate

in the next section. What also makes it possible to reach huge densities is that the effect on a given test nucleus of even a small amplitude discontinuity always overcomes the repelling potential of another neighbour nuclei whatever its amplitude which indeed becomes huge when the other nucleus gets closer and closer [22]. Actually it is only by reaching enough kinetic energy that a nucleus can overcome a discontinuous barrier, but for this to be possible, this nucleus needs its huge repelling potential energy implied by the compression, to be converted into enough kinetic energy. This is not the case because the nuclei do not have enough place to move and their thermal vibrations are efficiently dissipated by the mbl as we already explained in this slow scenario.

As the nuclei get closer and closer the electron wave packets tend to more and more overlap each others and must shrink to respect Pauli exclusion principle so we are approaching the picture of the black dwarf: nuclei very close to each other in a cloud of electrons with much higher "Heisenberg kinetic energies". In this case an electronic screening effect can take place because the electronic density of the sea of electrons also increases in between any two nuclei as these approach each other. At this level the degeneracy pressure of the electrons is not yet beaten by the discontinuity but the proximity of the nuclei and the electronic screening makes possible a variety of nuclear multi-body reactions between all the trapped nuclei that will eventually lead to the more stable reachable states. As in a white dwarf everything might eventually be turned into Ni^{62}. Reaching higher mass nuclei thanks to an mbl increased density is not insured because again if the release of energy is too sudden the mbl will heat too fast and lose its content as in the fast collapse scenario which anyway is expected to occur sooner or later.

13.2. Clean nuclear energy

Mbls are actually very common objects expected in any kind of electrical discharges or any phenomena producing local concentrations of charges having the same sign, such as for instance capacitors, point effects, biological membranes, the impact of a target by a narrow beam if the charges are not cleared out efficiently. It is the very revolutionary nature of these objects that escaped the attention of mainstream physicists for decades mainly because it is so unexpected. One of the most impressive kind of observations are those revealing many types of transmutation or nuclear fusion products clearly associated with these objects and their various traces and pitches these left in the materials met on their path. We explained in the previous section that the mbl understood as a kind of micro black dwarf, the fate of a slowly collapsing gravitational discontinuity, is the ideal candidate to trigger the chain of multi-body reactions that will lead to the most stable and more easily reachable nuclei: He^4, Ni^{62} and so on. Stable means that we already understand why eventually the residuals of CF reactions are not radioactive. What would seem to be a priori more challenging is to explain why the nuclear reactions inside the mbl themselves do not produce large fluxes of high energy particles: α, β, γ, neutrons in the MeV range for which the discontinuity potential barrier is negligible. We already discussed this problem in [6] and concluded that most highly energetic particles produced in the mbl, included neutrons, should be thermalized well before they are able to reach the surface of the object. For instance a 10-micron mbl with the density $d = 1$ of condensed matter at birth, once compressed to a nanometer size, will have a density d over 10^{12} and neutron mean free path of the order of 10 fm, hence so much smaller than the mbl, that only very exceptional neutrons produced near the surface of the mbl can be radiated at high energies. The conclusion a fortiori also applies to all other nuclear radiations with even smaller mean free paths. Eventually most of the energy produced in the mbl should be radiated electromagnetically by at most soft X-rays (10 eV) except there may ultimately be more or less explosive fast dispersion of the mbl if a chain of nuclear reactions is triggered.

14. Other Extreme Properties of mbls

Traces of mbls have been reported revealing objects of various sizes [19] as they propagate through various materials. This, along with the specific properties of these traces confirms that we are seeing a macroscopic object, not any kind of

elementary particle, and yet an extremely penetrating one able for instance to pass through two meters of atmospheric air and two layers of black paper. This would be very hard to explain if we did not understand that a mbl is not merely a micropiece of hot matter which would be arrested immediately by any dense obstacle. Of course its surface discontinuity can fuse, evaporate or even turn all the material encountered into a plasma which might help penetrating a solid for instance. But this is not enough! The question is how is an mbl able to propagate such a long distance in a dense medium and interacting so much with it without apparently slowing down, as if its motion was not resisted at all. We already have the answer. The whole material content of the mbl is actually enclosed by the discontinuity, which itself is completely driven by its minority of charged particles in excess that defines the distribution of the electrostatic energy that gave birth to the mbl. If some of these charges during a small time interval interact and are deviated or slowed down, the majority of the other charged particles do not interact (being elementary particles these are much less likely to interact than a macroscopic object) still carrying the discontinuity at almost uniform speed, discontinuity that is able to permanently refocus, gather and re accelerate the latecomers and dispersing ones. Moreover these charged particles being elementary are individually extremely sensitive to any external electromagnetic field because of their huge charge over mass ratio q/m and so is the cluster of these charged particles, thus the mbl as a whole even though it has a much smaller Q/M being essentially neutral as any macroscopic quantity of matter.

We are indeed faced with an extraordinary macroscopic object able to react to external EM fields or propagate through matter almost the way elementary particles do. Many searchers reported those incredible tracks left by mbls showing sharp angle turns manifesting huge accelerations as if the mbl as a whole did not have any inertia and could be accelerated as efficiently as each single electron in the electrical field (inside a mbl plasma the much greater mobility of the electrons relative to the ions suggests that the electrons are the main drivers of the mbl)! Phenomenal accelerations of a macroscopic object is made possible by mbls but these can also describe circles at high cyclotron frequencies in a

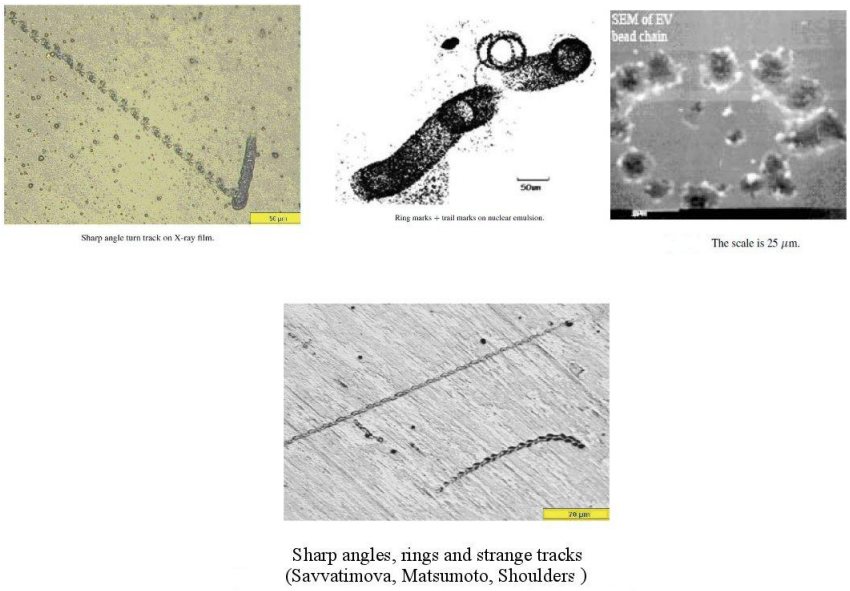

Figure 6. Inertia anomalies and strange traces.

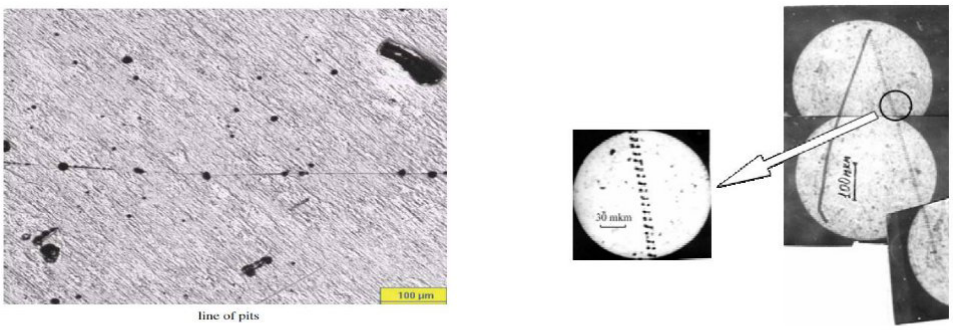

Figure 7. Caterpillar and dotted line traces.

magnetic field as was also observed [18]. Various strange traces can be seen in Fig. 6.

Such kind of observations might have created the illusion that the mbls manifesting so huge Q/M ratios were clusters of an incredible number of electrons, though this interpretation is hardly tenable.

For all the previous reasons, the mbls are obviously extremely effective charge carriers in a wire submitted to a voltage and therefore able to produce dramatic falls in wire resistivity as is also regularly reported in cold fusion experiments even up to the destruction of the wire.

At last, the mbls being very charged and, due to the conservation of angular momentum during their collapse, also rotating at high angular velocity, these are expected to be extremely magnetic. So it is not so surprising that such objects can be trapped in ferromagnetic materials [19].

Eventually let us not forget that discontinuities in DG are connecting the two sides of the universe. This is why the material content of the mbl might oscillate between our side of the universe and the conjugate side (the antimatter universe) via the peripheral surface discontinuity of the mbl so that the mbl may have an alternating luminosity from one side (the observer side, i.e. our side) point of view, hence leave those strange caterpillar or dotted line traces in emulsions as described in [19] for instance (see Fig. 7).

15. Conclusion

The review on Dark Gravity given in the first part of the article was necessary to clarify and present in the most intuitive way, avoiding the mathematical formalism already developed elsewhere, the main steps toward an anti-gravitationally stable extension of General Relativity with Time Reversal treated as a fundamental discrete symmetry even in a gravitational context, and its naturally expected associated field discontinuities. Having established this stable extension of General Relativity, we can then list many key observations of LENR and show that each one is an almost perfect signature of the physics of these discontinuities. By the way we were also able to derive a correct transition red shift from deceleration to acceleration of our Universe, showing thereby that our DG cosmology can perfectly mimic the LCDM one as for the scale factor evolution without the free parameters associated to DM, DE, Inflation.

References

[1] F. Henry-Couannier, *Int. J. Mod.Phys.* A **20**(NN) (2004) 2341–2346.

[2] F. Henry-Couannier, *Global J. Sci. Frontier Res.* A **13**(3) (2013) 1–53.
[3] J.P. Petit, *Astr. and Sp. Sci.* **226** (1995) 273.
[4] M. Milgrom, *Monthly Notices Roy. Astronomical Soc.* **405** (2) (2010) 1129–1139.
[5] S. Hossenfelder, *Phys. Rev. D* **78** (2008) 044015.
[6] F. Henry-Couannier, *J. Nucl. Phys.* 2014. http://www.journal-of-nuclear-physics.com/?p=838.
[7] F. Henry-Couannier,, Dark Gravity, *Global J. Sci. Frontier Res.* F **12**(13) (2012) 39–58.
[8] S. Weinberg, *Quantum Field Theory*, Vol. 1, Cambridge University Press, New York, 1995.
[9] A.D. Linde, *Rep. Prog. Phys.* **47** (1984) 925.
[10] A.D. Linde, *Phys. Lett.* B **200** (1988) 272.
[11] J.P. Petit, *C.R. Acad. Sci.* **t.285** (1977) 1217–1221.
[12] J.P. Petit and G. ĎAgostini, *Astr. and Sp. Sci.* **354** (2014) 611–615.
[13] S. Hossenfelder, 2014, Advertisement break in
http://backreaction.blogspot.fr/2014/11/negative-mass-in-general-relativity.html.
[14] R.J. Gleiser and G. Dotti, *Classical Quantum Gravity* **23** (2006) 5063–5078.
[15] R. de Sangro, G. Finocchiaro, P. Patteri, M. Piccolo and G. Pizzella, *Eur. Phys. J.*C **75** (2015) 137.
[16] M. Carrera and D. Giulini, European Space Agency, the Advanced Concepts Team, Ariadna Final Report 04-1302, 2005.
[17] S. Cappozziello et al., *Phy. Rev.* D **90** (2014) 044016.
[18] E. Lewis, *J. Condensed Matter Nucl. Sci.* **2** (2009) 13.
[19] L.I. Urutskoev and V.I.Liksonov, *Ann. Fond. Louis de Broglie* **27**(4) (2002) 701.
[20] K. Shoulders and S. Shoulders, Charge Clusters in Action, 1999.
[21] M. Rambaut, *J. Condensed Matter Nucl. Sci.* (2006) 798–805.
[22] F. Henry-Couannier, 2015, Geogebra Animation Online
https://tube.geogebra.org/student/m1236323.

J. Condensed Matter Nucl. Sci. 18 (2016) 24–35

Research Article

Study on the Phenomenon Reported "Neutron Generation at Room Temperature in a Cylinder Packed with Titanium Shavings and Pressurized Deuterium Gas" (3)

Takayoshi Asami*,†

Research Institute of Innovative Technology for the Earth, 9-2 Kizugawadai, Kizu-cho, Soraku-gun, Kyoto 619-0292, Japan

Giacomo Giorgi and Koichi Yamashita

Department of Chemical System Engineering, School of Engineering, The University of Tokyo, 7-3-1 Hongo, Bunkyo-ku, Tokyo 113-8656, Japan

Paola Belanzoni

Dipartimento di Chimica, e Biologia e Biotecnologie & Istituto di Scienze e Technologie Molecolari del, CNR c/o Dipartmento di Chimica, Biologia e Biotecnologie Università di Perugia 06123, Italy

Abstract

In this paper, the authors have intended to ascertain the driving force for an adsorbed deuterium atom or a deuteron to collide in titanium crystal. Recent simulation analysis results, related to the predicted cluster or cell models of deuterium atoms adsorbed in titanium crystal, together with the related calculations by Coulomb formula and Yukawa formula were investigated. Coulomb force working between deuteron–deuteron (d–d) particles is compared with the nuclear force working between them. The change of the force to each of them is evaluated in accordance with the distance between them, near the surface of the atomic nucleus. Taking into account the results of previous studies, it seems that nuclear fusion will occur occasionally without adding any specified energy. We think that there is a possibility of a collision of free deuterons through the medium of a negative charge in a deuterium atom in ligancy 2. On the other hand, we think that if a suitable amount of energy, which is far smaller than that of high temperature nuclear fusion, such as the irradiation of the alternative electromagnetic wave, for example, is supplied to adsorbed deuterium atoms and desorbed deuterons in the titanium (Ti) shavings packed in the experimental cylinder under a pressurized or evacuation condition with a suitable temperature rise, then there also will be a higher probability of nuclear fusion being achieved.
 ISSN 2227-3123

Keywords: Adsorption, Coulomb force, Desorption, Deuterium, Nuclear force, Titanium

*E-mail: : takaysami@yahoo.co.jp

†Retired.

 ISSN 2227-3123

1. Introduction

In the previous paper [1], we analyzed the state of deuterium atoms in the tetrahedral cage of titanium crystal using the first principle molecular orbital calculation and proposed a method to promote the neutron generation.

Recently, Giorgi et al. [5,6] have given a theoretical explanation for the formation of a combination in an electron deficient metallic system with a hydrogen (or deuterium) atom in ligancy 2, that is to say, a 3-center-2-electrons, (3c-2e) bond in the collisional mechanism which has lead to the reported neutron generation.

Furthermore, Giorgi et al. have found a metastable model including (3c-2e) bonds with respect to the structure of one octahedral subcell belonging to the hexagonal close-packed (hcp) titanium lattice. As a result of this research, we can recognize that the adsorbed deuterium atoms form a compound of deuterium atoms in ligancy 2, in many locations of titanium crystal.

In this paper, we intend to ascertain what the driving force for a deuterium atom and a deuteron to collide with one another is and what the driving force for nuclear fusion to occur is, comparing it with Coulomb force and the nuclear force working between d–d particles.

2. The Behavior of Deuterium Atoms Adsorbed in Ti Shavings

The only energy change in the process of neutron generation in the previous experiments [2–4] has been the temperature rise under a pressurized or evacuation condition. The kinetic energy change of the adsorbed deuterium atom from liquid nitrogen temperature to room temperature is ca. 26 meV.

We doubt that such a small amount of energy can make deuterium atoms overcome their repulsive force, collide with one another and then create nuclear fusion. We expect the energy of the temperature rise will only open a door to a collisional space by means of a chemical bonding environment in which a deuterium atom and/or a deuteron can collide.

To explain this concept, we think that quantitative evaluations of charge value per each deuterium atom and the working energy between deuterium atoms are necessary.

In the recent theoretical analysis, Giorgi et al. [5] have reported the impact of the deuterium adsorption on the final stress of the cell. They calculated the stress impact given by the formation of the titanium atoms combined with a deuterium atom in ligancy 2 ((3c-2e) bond) to the titanium supercells (16 and 54 atoms, respectively) and analyzed the bond formation of an electron deficient titanium matrix. Difference between the full (ions + lattice) and partial (ions) optimization [5]. T_d: tetrahedral cage, O_h: octahedral cage.

The calculated result referred to in Table 1 [5] indicates that the energy variation in the tetrahedral cage (in the matrix composed of 54 titanium atoms) is 0.028 eV. A matrix; the size of 54 titanium atoms is large enough not to give a sizable effect to the ΔE value evaluation. So, even if we calculate the ΔE value in a larger matrix, it seems that its ΔE value will not be much different as compared to 0.028 eV.

On the other hand, Ti shavings used in the previous experiments [2–4] seem to compose of a far larger size than that of 54 titanium atoms. This calculated ΔE value, 0.028 eV, is very close to the value of the input energy, ca. 0.026 eV, caused by the temperature rise under the pressurized or evacuation condition. It appears that this energy generated by the temperature rise under the pressurized or evacuation condition is used by a deuterium atom to enter into or leave the titanium crystal lattice. Therefore, when it intends to vacate the cage or a deuterium atom in another location intends to move from its location to go to the gaseous region, its electron is taken by the titanium atom and/or surrounding titanium atoms and it will become a deuteron. After that, a collision is likely to occur between a deuteron and a deuterium atom in ligancy 2, by means of a small amount of kinetic energy, for example, alternative electromagnetic energy, and by the medium of its negative charge.

If the specified condition regarding temperature, pressure and titanium metal adsorbed deuterium gas are prepared suitably, neutron generation automatically proceeds without any additional energy required except for a temperature

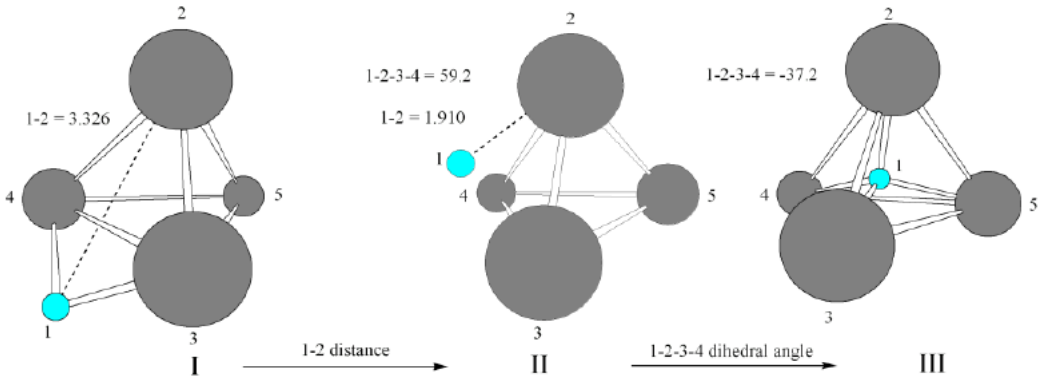

Figure 1. Set up of the trajectory of D atom entering the tetrahedral cage: the two steps approach showing the two different reaction coordinates [6].

rise under a pressurized or evacuation condition, as witnessed in past experimental reports.

Giorgi et al. performed the Density Functional Theory (DFT) study of deuterium entering a titanium tetrahedral cage [6]. In this study, the geometry of the initial Ti_4D^+ system, with the D^+ atom outside the cage, in this case a quintet spin state, and they calculated the deuteron charge from outside of the cage to the inside of the cage. Concerning the tetrahedral cage they indicated the outside–inside trajectory of the D^+ atom, provided a two step set up as indicated in Fig. 1.

In Fig. 1, Giorgi et al. have calculated the energy vs. the D^+–Ti(1–2) distance for the first step of the D^+ approach to the Ti_4 cage (from structure I to II) and calculated the energy vs. the D^+–Ti–Ti–Ti (1–2–3–4) dihedral angle for the second step of the approach to the Ti_4 cage (from structure II to III in Fig. 1).

The second step results are reported in Table 2 and show that if there is a deuterium atom in the cage, a deuterium atom in ligancy 2 outside the cage cannot enter into the cage without providing necessary energy, because they both have the same charge sign and therefore will not collide. Accordingly, we conclude that nuclear fusion will not occur inside the cage.

Table 1. Energy variation as function of adsorbed deuterium atoms. ΔE represents the difference between the full (ions + lattice) and partial (ions) optimization [5].

	ΔE (eV)
2×2×2(16 atoms)	
Ti	0.05
Ti+2D 2(3c-2e)T_d	0.12
Ti+2D 2(3c-2e)O_h	0.07
3×3×3(54 atoms)	
Ti	–
Ti+2D 2(3c-2e)T_d	0.028
Ti+2D 2(3c-2e)O_h	0.013

T_d: Tetrahedral cage, O_h: Octahedral cage.

Table 2. Calculated the Voronoi deformation density (VDD) atomic charges on D during the second step of the trajectory from outside to inside the cage (from structure II to III in Fig. 1) [6].

1–2–3–4 dihedral angle (degree)	VDD atomic charge on D (e)
50	−0.149
40	−0.29
30	−0.439
20	−0.554
10	−0.630
0	−0.693
−10	−0.744
−20	−0.760
−30	−0.781

To clarify the mechanism of the neutron generation here, we assume that there are three regions in the system of deuterium gas and Ti shavings packed in the cylinder (here after referred to as "titanium-deuterium system", or "Ti–d system"), as indicated in Fig. 2.

- Region I: The part of Ti shavings excluding their surface part. Presumedly there are deuterium atoms in the stable location here.
- Region II: Surface part of Ti shavings, the region presumed to be where almost all the adsorbed deuterium atoms in ligancy 2 are.
- Region III: Gaseous phase region of deuterium between Region II and the inside of the cylinder wall.

We studied two cases of neutron generation based on the experimental results.

Case 1

This case inspects the neutron generation in the pressurizing condition [2–4], it pays attention to the pressure and temperature condition in the cylinder in the experiment.

Referring to a pressure-composition isotherm adsorption diagram for Ti–H_2 (assuming that this diagram is almost equivalent to the Ti–D_2 diagram) with the parameter temperature in Fig. 3 [7], we assume that the location when the

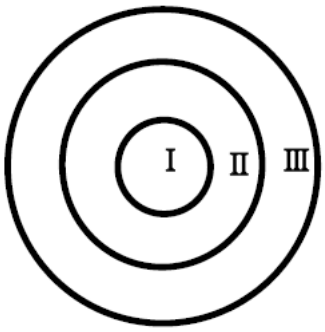

Figure 2. Spatial partition for the analysis of the neutron generation mechanism in the Ti–d system (Region I, Region II, Region III).

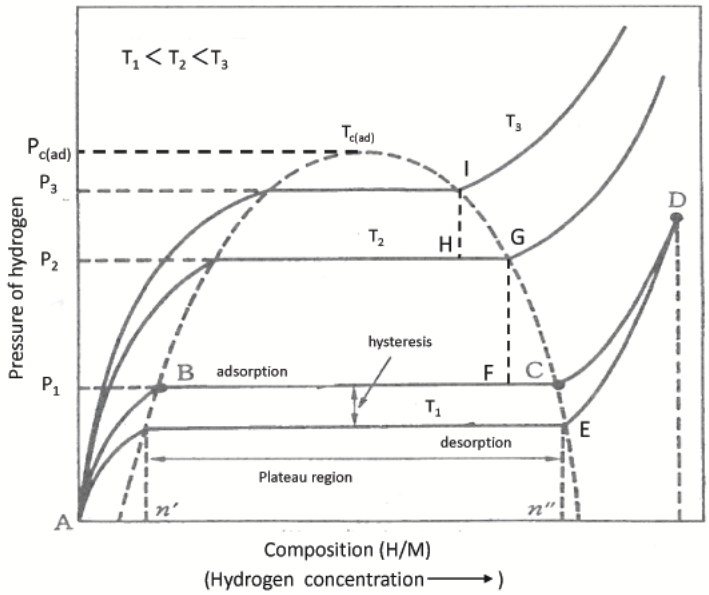

Figure 3. Pressure-composition isotherm adsorption diagram for Ti–H_2 with the parameter temperature in the adsorption diagram [7]. Where $P_i(i = 1, 2, 3), T_i(i = 1, 2, 3), P_{\text{c(ad)}}$ and $T_{\text{c(ad)}}$ denote pressure, temperature, critical pressure and critical temperature, respectively.

experiment starts is at point "C", as indicated on the curve, and the temperature is T_1 and after that, the temperature rise is from T_1 to T_2. At that time, the location of the saturation point moves from point "C" to "G".

As a result, the length of the plateau region shortens. This means that the saturation region of adsorption will shorten and the deuterium gas in the shortened portion, $\overline{CF}$, is equivalent to the deuterium gas desorbed from Ti shavings. When deuterium atoms in ligancy 2 desorb from the Ti shavings, it appears that some portion of their electrons must be taken by the titanium atoms which have adsorbed D atoms and/or the surrounding titanium atoms and become deuterons. They leave from Region I and/or Region II and enter Region III. When deuterons leave Region I and/or Region II, there is the possibility of collision with a deuterium atoms in ligancy 2 and a desorbed deuteron through the medium of their negative charges.

Case 2

Referring to the curve indicated in Fig. 3 and assuming that the experiment starts from point "G", and we change the pressure condition from P_2 to P_1 providing that the temperature T_2 is kept or only risen by a suitable temperature, theoretically; all the portions of adsorbed and saturated deuterium gas must be desorbed in accordance with the characteristics of the curve. It seems that at that time at least, the electrons of some of the desorbed portion of deuterium atoms must be taken by the titanium atoms, as in Case 1.

The working condition in the cylinder in this experiment is the evacuation condition as in neutron generation [4].

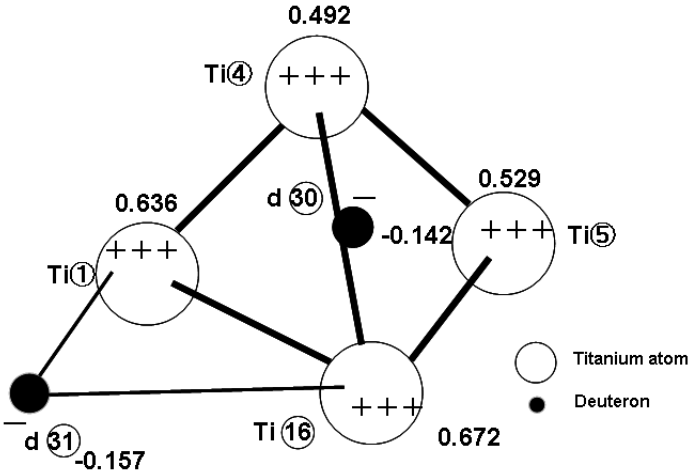

Figure 4. Atomic charge value (bold) in the cluster model 3, in the previous paper [1], a deuterium atom and a deuteron are located inside and outside the cage, respectively.

3. Working Force and Potential Barrier between Two Particles (d–d)

3.1. Working force

Providing that the condition indicated in Fig. 4 is assumed, we think that it is important to consider how strong or large the estimated force (or potential barrier) is between a deuterium atom outside the cage and a negatively charged deuteron inside the cage. We should therefore try to evaluate the numerical value.

Providing that a deuterium atom in ligancy 2 and a deuteron with a negative charge are located at the inlet and inside the cage as in Fig. 4, we can evaluate the working force between them applying Coulomb formula.

$$F = (1/4\pi\varepsilon_0)(qq'/r^2), \tag{1}$$

where F, ε_0, q, q' and *r* denote Coulomb force, vacuum dielectric constant, charge (q, q') and the distance between the two charges, respectively.

Providing that d31 is detected only in the inlet of the cage in Fig. 4; the distance *r*, between q30 and q31 would be ca. 0.604 Å in a tetrahedral cage without distortion and the charge of d30, q30 would be -0.142 eV (q30 $= -0.142 \times 1.602 \times 10^{-19}$ C). If we assume that the charge value does not change at the inlet of the cage, then the charge of a deuterium atom in the front of the inlet of the cage, with a charge of d31, q31 would be -0.157eV (q31 $= -0.157 \times 1.602 \times 10^{-19}$ C) [1], Coulomb repulsive force between them at the inlet should be about 1.41×10^{-9} N (1.44×10^{-10} kg force).

The minimum necessary energy for two deuterons to collide should be greater than that of the potential barrier. When we make d31 collide with d30 by accessing the distance between them from l to D_{d}, where l and D_{d} denote the optional distance and a pion-range or shorter distance than l between them, respectively; and if we substitute the value of each charge q30 and q31 to Eq. (2), respectively, then the energy necessary to make d31 collide with d30 is calculated from

$$W = \int_{D_\mathrm{d}}^{l} (1/4\pi\varepsilon_0)(\mathrm{q30q31}/r^2)\,\mathrm{d}r = (1/4\pi\varepsilon_0)(\mathrm{q30q31})[-1/r]_{D_\mathrm{d}}^{l}. \tag{2}$$

3.2. The potential barrier for two particles to overcome based on Coulomb formula in order to collide

The potential barrier in each condition is calculated in the following.

(1) The potential barrier between two deuterons with the same charge sign and 1 eV each, stems from the following conditions.

The evaluated energy is the worked energy $W_{\text{d-d}}\,(1)$, that two deuterons each accessed from infinite to the distance, $D_\mathrm{d}(D_\mathrm{d} \sim 5.4$ fm).

If two deuterons approach 1.4 fm, the gap between them, is a pion-range, and these two particles will collide with subsequent nuclear fusion. Providing that the radius of a deuteron is 2 fm and the pion-range is 1.4 fm, and we substitute $D_\mathrm{d} = 5.4$ fm and $l = \infty$ to Eq. (2), the calculation result is as follows:

$$W_{\text{d-d}}(1) = (1/4\pi\varepsilon_0)\,(1.0)(1.602 \times 10^{-19})(1.0)(1.602 \times 10^{-19}) \times [-1/r]_{D_\mathrm{d}}^{l} = 267\ \mathrm{keV}. \tag{3}$$

This value is equivalent to the potential barrier in this condition and coincides fairly with the value in Tanimoto's paper [8].

(2) The potential barrier for two deuterium atoms to overcome in order to collide is associated with the following conditions.

We must assume that each charge value of q and q′ is 1.0 and -0.157 eV, respectively, and each charge value does not change while two particles have access to the distance, 25 fm.

(As the distance between two deuterons is ca. 25 fm, the nuclear force between them is nearly equal to zero, we therefore selected this value.)

(a) When one particle is a deuterium atom in ligancy 2 and another particle is a deuteron

We assume that each charge value of q and q′ is 1.0 and -0.157 eV, respectively. The worked $W_{\text{d-d}}(2)$, accessed from $l = \infty$ to $D_\mathrm{d} = 25$ fm is calculated below. It is likely that this energy can be accessed as long as a deuterium atom in ligancy 2 does not change its negative charge before a collision.

$$W_{\text{d-d}}(2) = (1/4\pi\varepsilon_0)(-0.157)(1.602 \times 10^{-19})(1.0)(1.602 \times 10^{-19}) \times [-1/r]_{D_\mathrm{d}}^{l} = -41.92\ \mathrm{keV}. \tag{4}$$

(b) When two particles are deuterons

The potential barrier between two deuterons at a distance ca. 25 fm is calculated in the following.

$(I = \infty, D_\mathrm{d} = 25$ fm)

$$W_{\text{d-d}}(3) = (1/4\pi\varepsilon_0)(1.0)(1.602 \times 10^{-19})(1.0)(1.602 \times 10^{-19}) \times [-1/r]_{D_\mathrm{d}}^{l} = 57.7\ \mathrm{keV}. \tag{5}$$

These calculation results indicate that the difference in the combination condition between a titanium atom and a deuterium atom makes the superficial charge value of a deuterium atom change. As a result, the potential barrier also greatly changes.

However, the evaluation of the force between two particles in the region where the nuclear force influences them, is not included in the previous calculations and neither is the possibility of the access to the distance, (25 fm) between two particles.

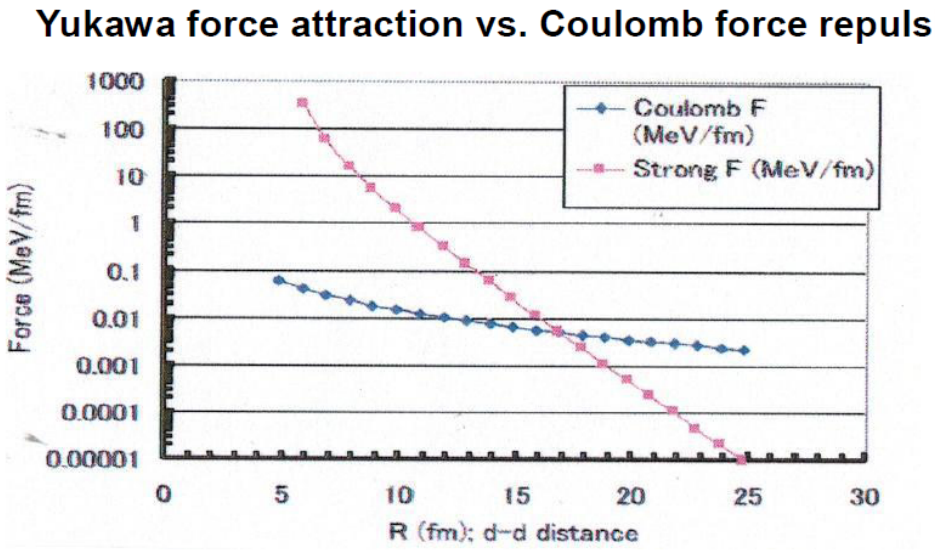

Figure 5. Comparison of repulsive force by Coulomb force and attractive force ("Yukawa force attraction" or "Strong F" in Fig. 5) by nuclear force between two deuterons. Attractive force is calculated by an improved Yukawa formula [9].

4. Coulomb Force and Nuclear Force between d–d Particles

According to the reports of Takahashi [9,10], the comparison of the nuclear force (Yukawa force) and Coulomb force in the near nucleus surface is indicated in the graph, in Fig. 5.

In previous reports [9,10], the nuclear force between d–d results attractive. Figure 5 indicates that Coulomb force (repulsive force) is stronger than the nuclear force between d–d until the distance is nearly equal to ca. 17 fm. The attractive nuclear force works for two deuterons so as to be inversely proportional to the distance between them. On the other hand, nuclear force only works a bit until two deuterons access to ca. 25 fm. When the two deuterons access to ca. 17 fm, the absolute values of repulsive and the attractive forces are nearly the same and after closer access, the attractive force exceeds the repulsive force.

Two curves indicate that if we can add a suitable amount of energy at a specified distance between two deuterons when the nuclear force exceeds the repulsive Coulomb force to an accessing deuteron, then they will be able to collide each other, even if each of the two particles have the same charge, 1 eV.

Using the original Yukawa formula regarding nuclear potential, the formula of nuclear force between each nucleus is introduced in the following:

$$F_n = -ge^{\kappa r}(1/r^2 + \kappa/r), \tag{6}$$

where g and κ are constants. (Constants g and κ are produced by fitting them to the improved Yukawa formula, $g = -8.501 \times 10^4, \kappa = 0.804$.) r is the distance between two nuclei (fm) and F_{n} is the nuclear force (MeV/fm). The results of the calculations regarding $F_{\mathrm{n}}, F_{\mathrm{lig2}}$ and F_{c} are indicated in Fig. 6. Where $F_{\mathrm{n}}, F_{\mathrm{lig2}}$ and F_{c} denote nuclear force and Coulomb forces between d-d including a deuterium atom in ligancy 2 and pair charge values of each force are F_{n}: (1 eV, 1 eV), F_{lig2}: (1 eV, -0.157 eV) and F_{c}: (1 eV, 1 eV), respectively.

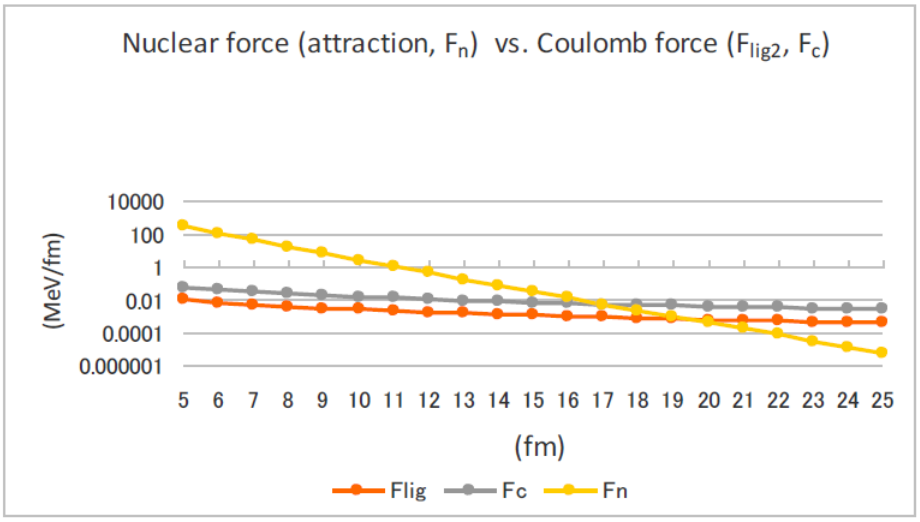

Figure 6. Comparison of Coulomb forces and attractive nuclear force. All the forces are indicated in their absolute values. F_{n}: nuclear force (attraction), F_{c}: Coulomb force (repulsion), F_{lig2}: Coulomb force (attraction).

In the Ti shavings adsorbed deuterium atoms, there are deuterium atoms in ligancy 2 in a Ti–d system which locally forms polar compounds. So if the suitable alternative electromagnetic wave is irradiated to a Ti–d system, desorbed deuterons and deuterium atoms in ligancy 2 must periodically move changing in opposite directions of each other with a positive and negative charge respectively in accordance with the frequency change.

It appears that the electron deficient titanium atoms constrain the electrons of deuterium atoms or take them. As a result, it means that the potential barrier will change. It seems that the absolute value of energy to add may only be a little bit or it may not be necessary at all by the tunnel effect, if the nuclear force is equal to or greater than the repulsive Coulomb force at ca. 17 fm. Even if two particles each have the same charge, 1 eV, the nuclear force will dramatically increase in inverse proportion to the distance between two nuclei.

For two particles to collide, we think that it is preferable to add additional energy to an accessing deuteron. However, it is most important to note how a deuteron will be able to access distance $<$ 17 fm from a deuterium atom in ligancy 2, without changing either charge.

5. The Presumed Nuclear Fusion Process in the Titanium Crystal Adsorbed Deuterium Atoms

When deuterium gas and titanium crystal adsorbed deuterium atoms are in an equilibrium state under a suitable pressure and temperature, even a slight temperature rise will break this equilibrium state and they will proceed to a new equilibrium state. As a result, it seems that the electrons of some portion of the desorbed deuterium atoms in Regions I and II (Fig. 2) are then taken by the titanium atoms or by the surrounding titanium atoms at desorption and proceed to Region III via Region II, where there should be a large quantity of deuterium atoms in ligancy 2 at saturation.

The authors envision that if the charge sign of the deuterium atom becomes positive and Coulomb force, based on the above mentioned concept, works between the deuterium atom in ligancy 2 outside the cage and the deuterons which move from Regions I and II, and the suitable amount of energy by alternative electromagnetic wave is irradiated,

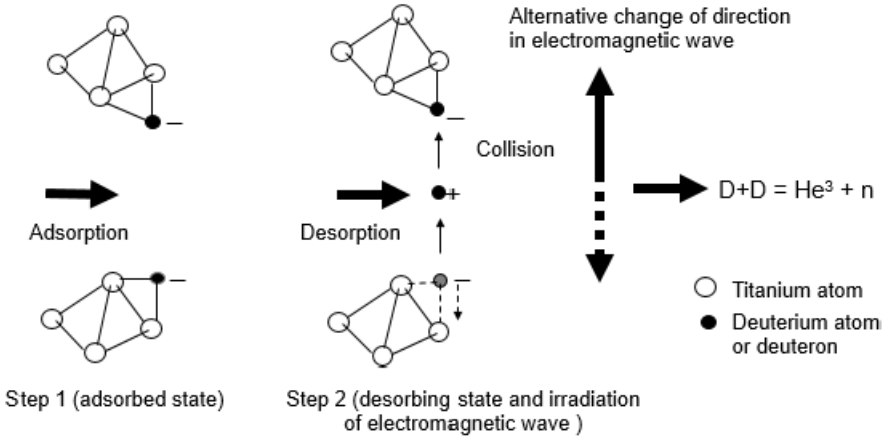

Figure 7. NFP model 1 in the titanium crystal adsorbed deuterium atoms.

there is a high possibility of a collision.

If the additional energy to overcome the repulsive force by Coulomb force before entering into the superior field of the attractive nuclear force in the near surface of the nucleus is added at the distance l for example, $17 < l < 25$ fm, to such a non-equilibrium condition in the Ti–d system, especially to free deuterons, it appears that there will be a higher probability of nuclear fusion being achieved because the nuclear force in d–d is attractive.

Nevertheless, it seems that if the deuterium atom in ligancy 2 with the charge -0.157 eV, does not lose its negative charge until the distance between it and the accessing free deuteron is less than ca. 17 fm, then the two particles will be able to collide with each other. After these particles access a distance closer than ca. 17 fm, the attractive nuclear force will begin to work, even if the charge of the deuterium atom in ligancy 2 changes from -0.157 to 1 eV.

Evidently, it is unconceivable for a free deuteron to directly enter into the plane within the orbit, including the nucleus and its related electron, without being given suitable kinetic energy, because each particle may change its charge and the power balance between them at that time would be unstable.

Presumed nuclear fusion process (here after referred to as "NFP") models in the titanium crystal adsorbed deuterium atoms are indicated in Fig. 7 (NFP model 1) and Fig. 8 (NFP model 2).

To accurately evaluate the energy required to increase the probability of nuclear fusion, we think that the information of the electron orbit and each charge of atoms relating to the deuterium atom in ligancy 2 are necessary, especially, the orbit form and each radius length in periapsis and apoapsis. Based on these information, the energy needed for nuclear fusion to occur will be calculated.

In NPF model 2, we think there may be a possibility of double or triple collision of deuterons.

The most important matter is how accessible the minimum distance between two particles is, after the collision with a negative charged deuterium atom in ligancy 2. Then, if the distance of two particles is within the attractive region that is stronger than that of the repulsive region, there will be chance of nuclear fusion.

6. Conclusion

Based on computational results and published reports, we have investigated the possibility of the nuclear fusion in titanium crystal.

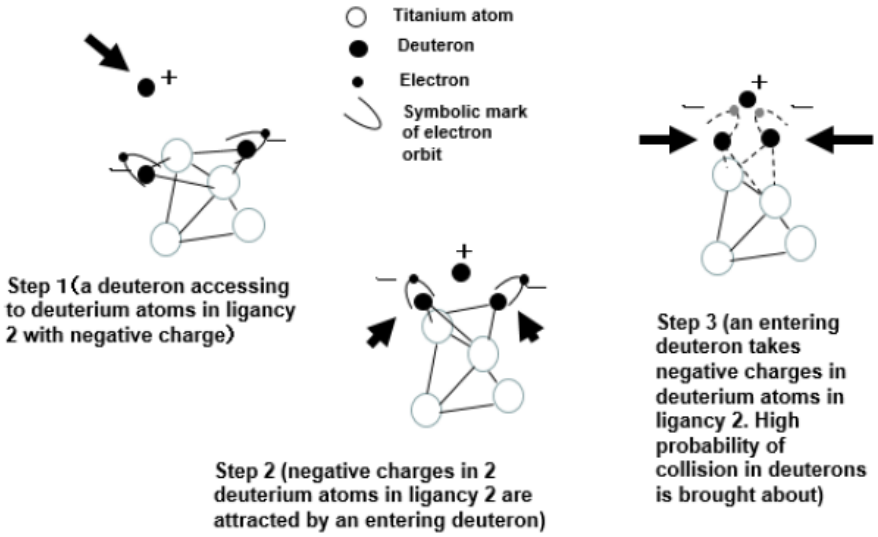

Figure 8. NFP model 2 in the titanium crystal adsorbed deuterium atoms.

We thought that the temperature at which a non-equilibrium state occurs was not at one single specific value, but that there were several temperatures which are lower than the temperature $T_{c(ad)}$ indicated in Fig. 3. This presumption confirms the past experimental results [3,4]. That is, that there are several conditions in which a non-equilibrium state occurs in both pressurization and evacuation conditions.

Regarding a non-equilibrium state, firstly, deuterium atoms locally form a polar compound in ligancy 2 with titanium atoms in titanium crystal and each deuterium atom in ligancy 2 has a negative charge. Under the pressurized or evacuation condition and with an additional suitable temperature rise, it appears that some portions of adsorbed deuterium atoms desorb from the titanium atoms and they become deuterons with a positive charge.

Secondly, as there are some particles (deuterons) which have a positive charge within them and others (deuterium atoms in ligancy 2) that have a negative charge inside, and providing that these charges do not change, they are then able to access one another within the working region of Coulomb force.

According to Takahashi's report, the nuclear force between d–d is attractive and it is nearly equal to the repulsive Coulomb force at the distance of ca. 17 fm at the dividing distance of ca. 17 fm when they have the same charge, +1 eV. For larger distances ($>$ 17 fm), the repulsive Coulomb force is stronger than the attractive nuclear one [9,10].

We think that even if the charge sign of a deuterium atom in ligancy 2 is changed during the accessing process of a deuteron, the added suitable amount of energy and the nuclear force will be able to overcome the repulsive Coulomb force and the two particles will be able to access each other, therefore colliding and nuclear fusion will be achieved.

To promote the nuclear fusion effectively, a necessary amount of energy needs to be added to the desorbed deuterons to overcome the Coulomb force and it needs to be determined by means of a more detailed theoretical and experimental setup.

To increase the probability of nuclear fusion in a Ti–d system, we now believe that it is necessary to add a suitable amount of energy. As a possible means to provide energy, the irradiation of an alternative electromagnetic wave energy is a possibility we would like to confirm in a future experiment.

Addendum

The authors had the information of a case study which was to reserve the hydrogen in a cylinder for the use of a fuel tank of an automobile.

At that time, we intended to similarly apply the example of a reservation cylinder of acetylene. In the cylinder, we packed Ti–Fe alloy grain with 5–10 mm equivalent diameter size to adsorb hydrogen gas instead of diatom earth and acetone.

When we reserved the hydrogen gas, we found that at first the adsorption quantity of the hydrogen was smaller than after conducting the adsorption and desorption operation several times. Therefore, it is recommendable that preliminary adsorption-desorption operations are executed before starting the adsorption operation. For example, the pressurizing and depressurizing of hydrogen in the cylinder can be repeated between ambient pressure and 2.5 MPa. After this operation, the adsorption quantity of hydrogen will increase greatly.

The authors think that this tendency is also the same in Ti shavings as that of the Ti–Fe alloy grain. In the experimental operation, caution is necessary as repeatedly pressurizing and depressurizing will cause the pulverizing of the Ti–Fe grain. This pulverized Ti–Fe powder sticks inside the piping. So, it is recommendable to equip a filter at both the inlet and the outlet of the cylinder packed with Ti shavings.

Acknowledgements

The authors wish to express sincere gratitude to Dr. Akito Takahashi, Emeritus Professor of Osaka University and Dr. Noriaki Sano, Associate Professor of Kyoto University, for their valuable suggestions and discussions on the manuscript.

References

[1] T. Asami and N. Sano, Study on the Phenomenon Reported "Neutron Generation at Room Temperature in a Cylinder Packed with Titanium Shavings and Pressurized Deuterium Gas"(2), *J. Condensed Matter Nucl. Sci.* **9** (2012) 1–9.

[2] A. De Ninno and F. Scaramuzzi, ENEA-Area Energia e Innovazione, Dip. Sviluppo Tecnologie di Punta, Centro Ricerche Energia Frascati, CP 65, I-00044 Frascati, Italy, *AIP Conference Proceedings*, Anomalous Nuclear Effects in Deuterium/Solid Systems, PROVO, UT, (*Emission of Neutron Bursts from a Titanium–deuterium Gas System in a High-efficiency Low-background Experimental Setup*), Vol. 228, 1990, pp. 122–129.

[3] [3]H.O. Menlove, M.M. Fowler, E. Garcia, A. Mayer, M.C. Miller, R.R. Ryan and S.E. Jones, Highlights of Papers Presented at the Workshop on Cold Fusion Phenomena, *The Measurement of Neutron Emissions from Ti plus D_2 Gas*, Santa Fe, New Mexico, May 23–25, 1989, p. 13.

[4] A. De Ninno, A. Frattolillo, G. Lollobattista, L. Martinis, M. Martone, L. Mori, S. Podda and F. Scaramuzzi, *Evidence of emission of neutrons from a titanium–deuterium System*, *Europhys. Lett.* **9**(3) (1989) pp. 221–224, ENEA, Dipartimento TIB, U.S. Fisica Applicata, Centro Ricerche Energia Frascati, 65-00044, Frascati, Rome, Italy, 1 June 1989.

[5] G. Giorgi, P. Belanzoni, T. Asami and K. Yamashita, Neutron generation via the mechanism adsorption of pressurized deuterium on an electron deficient titanium matrix, An MD-DFT combined analysis on the mechanism of the Ti–D bond formation, *Int. J. Hydrogen Energy* **37** (2012) 18959–18971.

[6] G. Giorgi, P. Belanzoni, T. Asami and K. Yamashita, On the dual deuterium/deuteron nature of D charge distribution in the Ti host matrix: A DFT analysis, *Int. J. Hydrogen Energy* **38** (2013) 16477–16484.

[7] Y. Ohsumi, *Hydrogen Adsorption Alloy (Suiso Kyuzo Gokin)*, Chapter 2 (Agune Gijutsu Senta Corp. Ltd., Tokyo, 2000), p. 33.

[8] M. Tanimoto, Review of recent studies on cold fusion, *J. Japan Soc. Energy and Resources (Enerugi Shigen Gakkai Shi)* **10**(5) (1989) 400–407.

[9] Akito Takahashi, Physics of cold fusion by TSC theory, *J. Phys. Sci. Application*, **3**(3) (2013) 191–198.

[10] Akito Takahashi, Fundamental of rate theory for CMNS, *Proc. ICCF 19*, to be published in J. Cond. Matt. Nucl. Sci. (see http://vixra. org/author/akito takahashi [13]).

J. Condensed Matter Nucl. Sci. 18 (2016) 36–49

Research Article

A Technique for Making Nuclear Fusion in Solids

R. Wayte*

29 Audley Way, Ascot, Berkshire, SL5 8EE, England, UK

Abstract

A technique is described for making nuclear fusion at room temperature by compressing a powder mixture comprising a deuteride and catalytic material. The result is explosive beyond known chemical reaction for the materials.
 ISSN 2227-3123

Keywords: Nuclear fusion, Solid state

1. Introduction

It is understood worldwide that efforts must continue to develop nuclear fusion as an energy source. One process involves inertial confinement fusion wherein a pellet of deuterium and tritium fuel is compressed strongly by lasers, see https://lasers.llnl.gov/science/icf, http://www-lmj.cea.fr/en/experimental/index.htm. This and other techniques are being pursued in order to prevent a global warming catastrophe and the riotous consumption of the remaining oil.

A significant number of established trustworthy scientists have pursued cold fusion [1], and published papers in the proceedings of 18 International Conferences on Condensed Matter Nuclear Science and elsewhere [2–4]. However, a problem of reproducibility remains, and the absence of expected fusion products like neutrons and γ-rays is puzzling. Experiments point to some obscure new phenomenon involving serendipitous trace catalysts.

In this paper it will be claimed that by strongly compressing a deuteride and catalyst mixture, one type of nuclear fusion has been induced (E.B., private communication). Repeatability is no longer a problem, and there should be a way of making this process commercially viable using inertial confinement in particular.

Section 2 describes current experimental techniques to produce nuclear reactions. Section 3 covers experiments with hydride in place of deuteride. Section 4 describes different mechanical designs. Section 5 offers explanations for the chemical processes involved. Section 6 proposes ways to develop a commercial energy generator. Section 7 summarises the work, and ends with a note of caution.

*E-mail: rwayte@googlemail.com; Tel.: +44-1344883352.

 ISSN 2227-3123

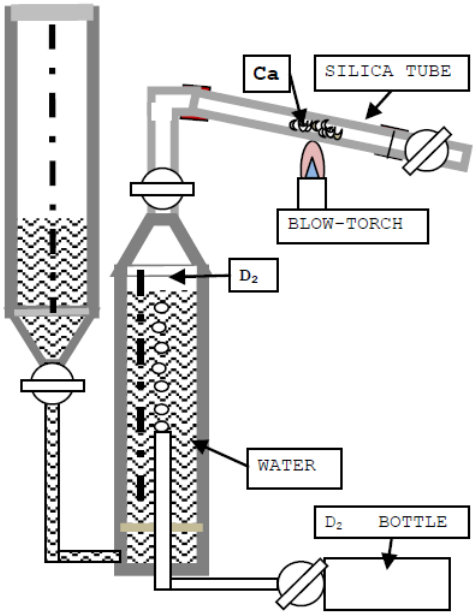

Figure 1. Apparatus for preparation of calcium deuteride from calcium turnings and deuterium gas.

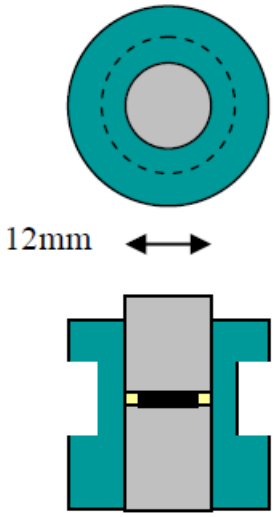

Figure 2. Original compression cell design consisting of two chrome steel roller bearings in a steel sleeve with solder seal to contain the fuel powder and gases.

2. Experimental Methods

The techniques developed for demonstrating the claimed nuclear fusion are on a small scale, but generate strong explosions. Many varied experiments have been performed in order to understand the effect and gain reproducibility.

2.1. Fuel preparation

First of all, a quantity of calcium deuteride was produced by heating calcium turnings in a flushed-out closed silica tube containing deuterium gas supplied by a manometer assembly, see Fig. 1. The used volume of deuterium was measured in order to estimate the final purity of the calcium deuteride at around $CaD_{1.75}$ as if some CaD was also produced. The lumps of $CaD_{1.75}$ were then ground to a fine powder with mortar and pestle, and thoroughly mixed with similar weights of red phosphorus and manganese powders, to yield the "primary fusion fuel". Typical particle sizes of the powders have been in the range 20–75 μm, while the weight proportions of the ingredients have been varied around 1:1:1.

Subsequent experiments using the deuteride of magnesium, strontium, barium, lithium and sodium in place of calcium deuteride have also provided results, suggesting that efficient deuterium fixation is the key necessity. Likewise, other transition metals have been found to work in place of manganese to some degree; as was confirmed by mixing the calcium deuteride and red phosphorus with each one of the following powders: scandium, titanium, vanadium, chromium, iron, cobalt, nickel, copper, zinc, yttrium, zirconium, niobium, molybdenum and cadmium. By inference, a metallic particle surface is required, with its high electron density and ionic lattice.

Figure 3. Two typical results of fusion ignition, wherein the local gas pressure has forced a wedge of steel downwards through the lower bearing, splitting it apart. One of the wedges is shown at top left, and sitting on the appropriate bearing in the lower views. It is triangular in cross-section, roughly 4 mm $\times$ 1 mm $\times$ 2 mm deep.

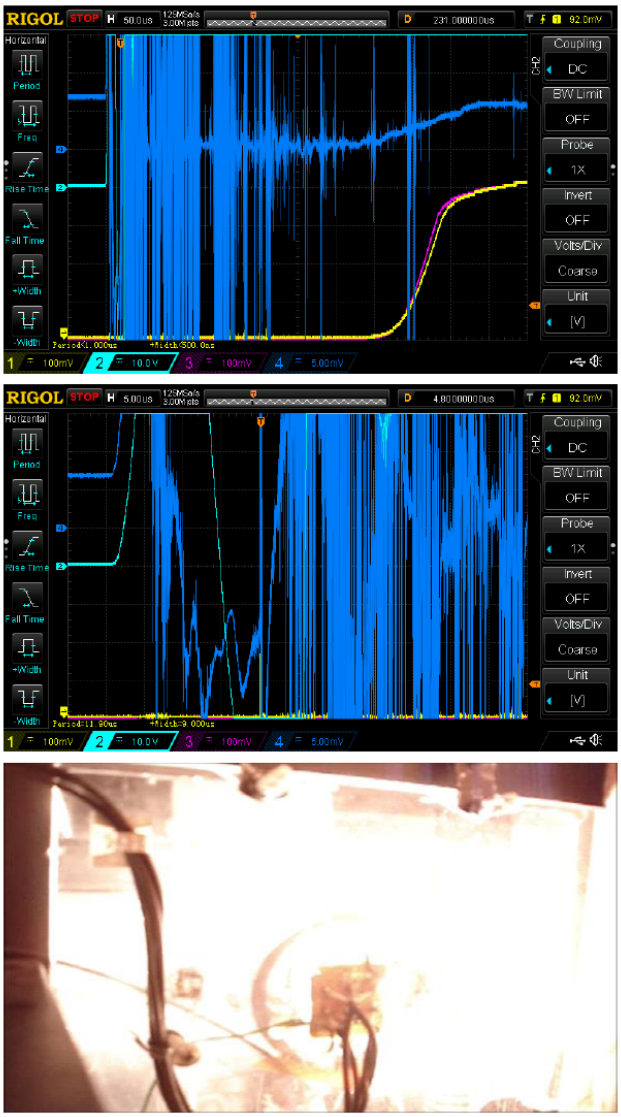

Figure 4. Oscilloscope traces for one very strong explosion, shown at 50 and 5 μs/division temporal resolution (use zoom 200% to view details). Blue trace is the load-cell output showing how the press applied load at 20 tons is increased above 40 tons by the explosion lasting only for 8 μs, followed by total fall-off and strong mechanical ringing. Turquoise trace is the output from the piezo-accelerometer, which was attached to the side of the cell until it burst. Yellow trace illustrates the response of the direct view photodiode to the debris ignition, and red trace the output from the photodiodes with UV scintillators. There is some cross-talk between the four channels because of amplifier overload. The over-exposed video camera recording of the bright explosion flash was viewed through a 12 mm thick shatterproof polycarbonate window; see Fig. 9 for mechanical layout details. The photodiodes, shown with wires attached mounted in the centre of the polycarbonate window, view through a hole but are protected from flying debris by a stainless steel mesh. Picture width corresponds to 200 mm $\times$ 120 mm high.

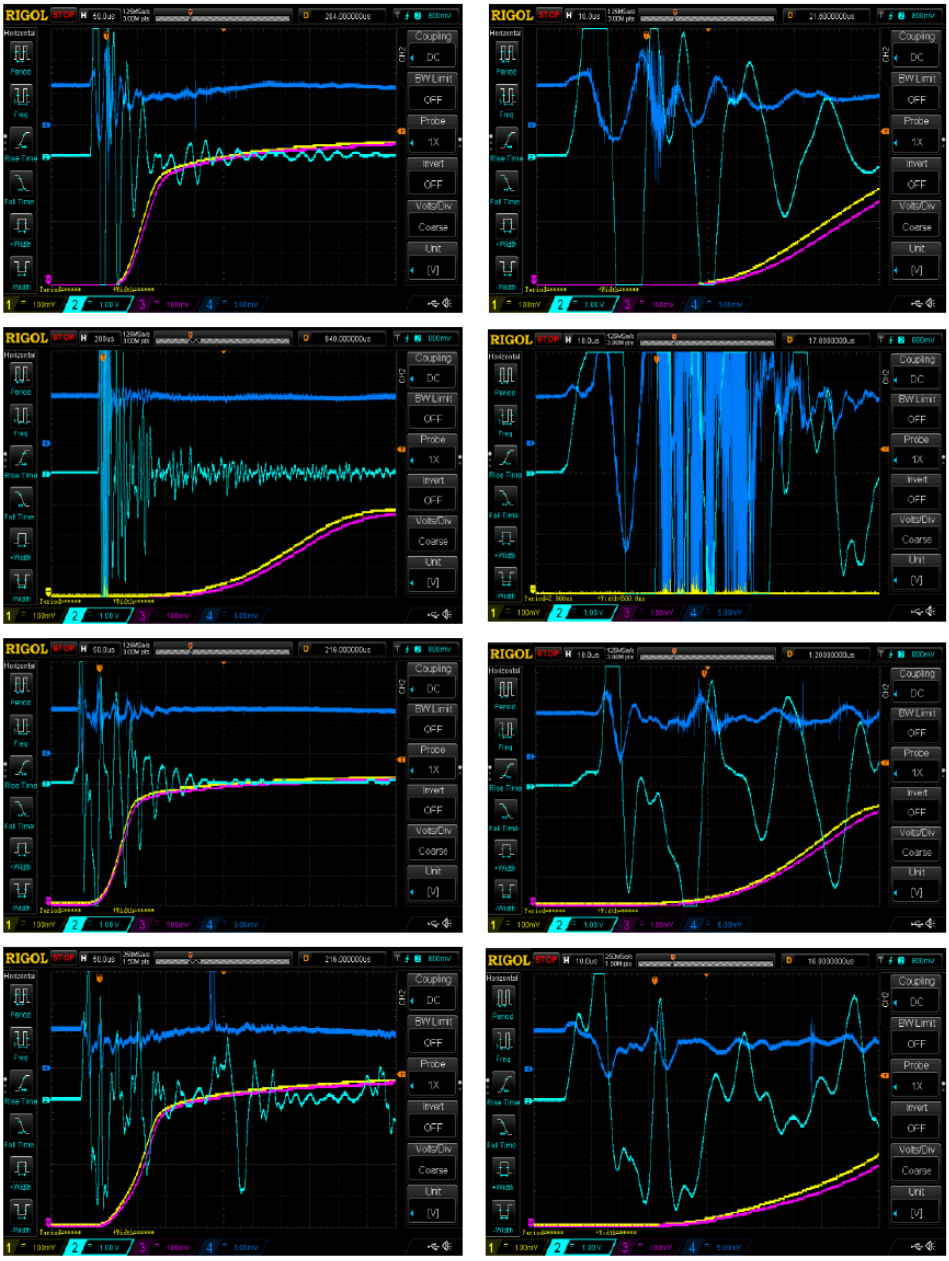

Figure 5. Four examples of explosions at medium (*left*) and high (*right*, 10 μs/division) resolution showing random variability in their characteristics. Experiments Nos. 244, 246, 248 and 273.

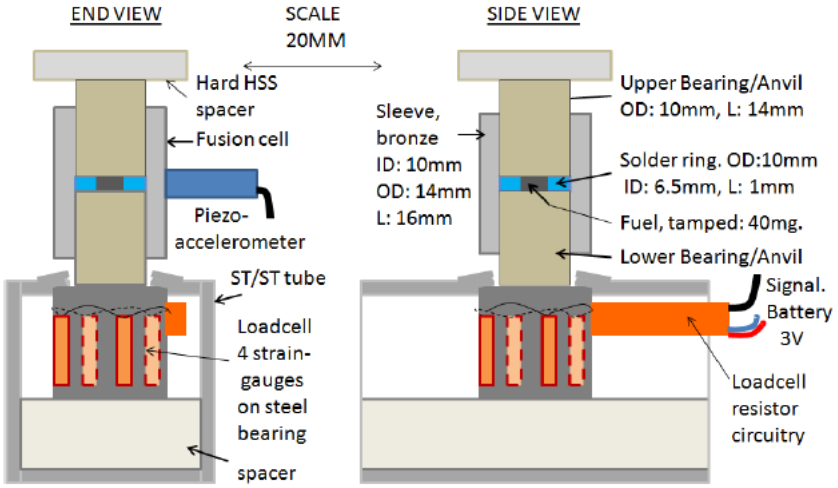

Figure 6. Fusion cell on canister load-cell assembly

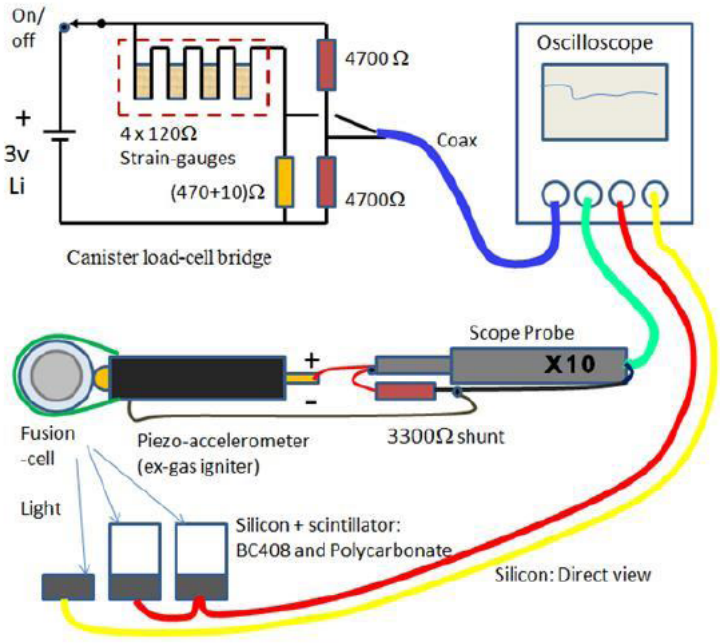

Figure 7. Circuit diagram for Canister load-cell bridge, Piezo-accelerometer (ex-gas igniter), and Silicon detectors (one direct view, two with scintillators).

Figure 8. *Left*: photograph of bottle-jack press assembly. *Right*: close-up view of fusion cell standing on load-cell assembly (Fig. 6), which is securely clamped to the movable work plate (Fig. 9).

2.2. Early experiments

In the first experiments, about 200 mg of the primary fuel powder was put in a compression cell which consisted of two EN31 chrome steel roller bearings (12 mm × 12 mm) as anvils in a mild steel sleeve, sealed with a lead/tin solder

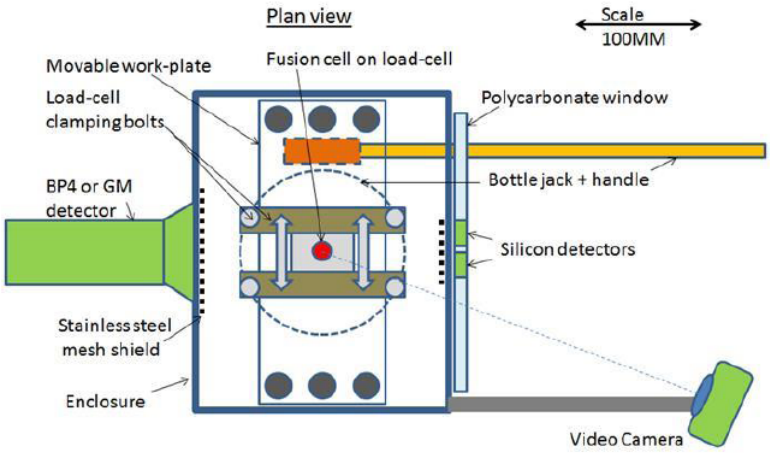

Figure 9. General assembly.

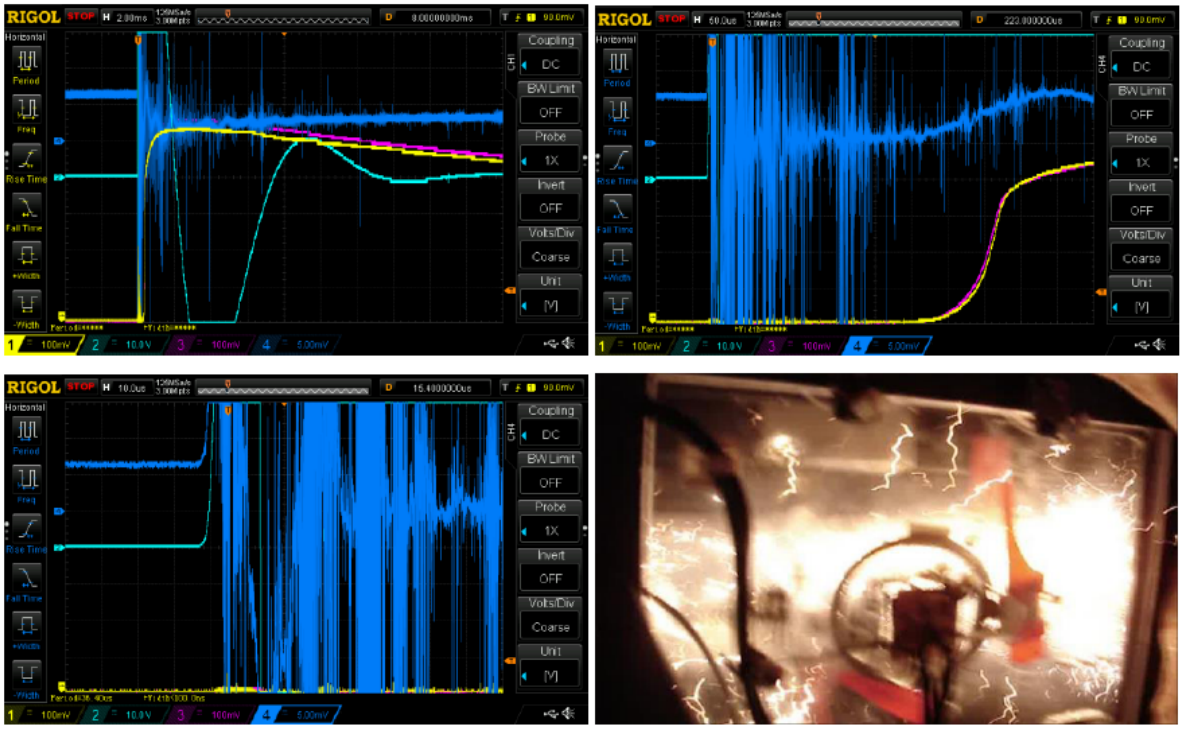

Figure 10. Calcium hydride in place of calcium deuteride: Oscilloscope traces for one strong explosion at low (2 ms/division), medium (50 μs/division), and high (10 μs/division) temporal resolution. Blue trace is the load-cell output showing how the applied load at 20 tons increases rapidly to more than 40 tons during the explosion, which lasts only for 10 μs, followed by load fall-off and mechanical ringing as the cell disintegrates. Turquoise is the output from the piezo-accelerometer attached to the side of the cell until it burst. The blast propagates for 200 μs before the hot ejected debris can ignite in the air, as detected by the photodiodes: yellow trace illustrates the direct view photodiode output, and red the photodiodes with UV scintillators. The video snapshot includes burning tracers which reveal shaking of the assembly. The photodiode detector assembly with wires attached is mounted in the centre of the polycarbonate window as usual, see Fig. 9. Experiment No.196.

ring to contain generated gases, see Fig. 2. When this cell was subjected to a vertical force of 30 tons in a press, the powder was formed into a hard solid disc, but no ignition occurred. The force was then removed so that a thin steel wedge could be placed underneath, before re-applying the force gradually. As a high force level was approached this time, it appeared that some shear occurred within the fuel pellet such that localised hot-spots [5–7] in the shear-plane ignited a chemical exothermic reaction which enabled the fusion process within the enclosed pressurised environment, causing an explosion in the cell.

Figure 3 illustrates two examples wherein the generated gas pressure (ionised deuterium and phosphorus) was great enough over a 1 mm $\times$ 4 mm surface area to create a cutting wedge of steel which immediately cleaved the roller bearing anvil into pieces. As soon as the bearings were cracked enough within the cell, the process ceased because the gases were able to escape through the cracks. This means that the process is not susceptible to run-away in this configuration.

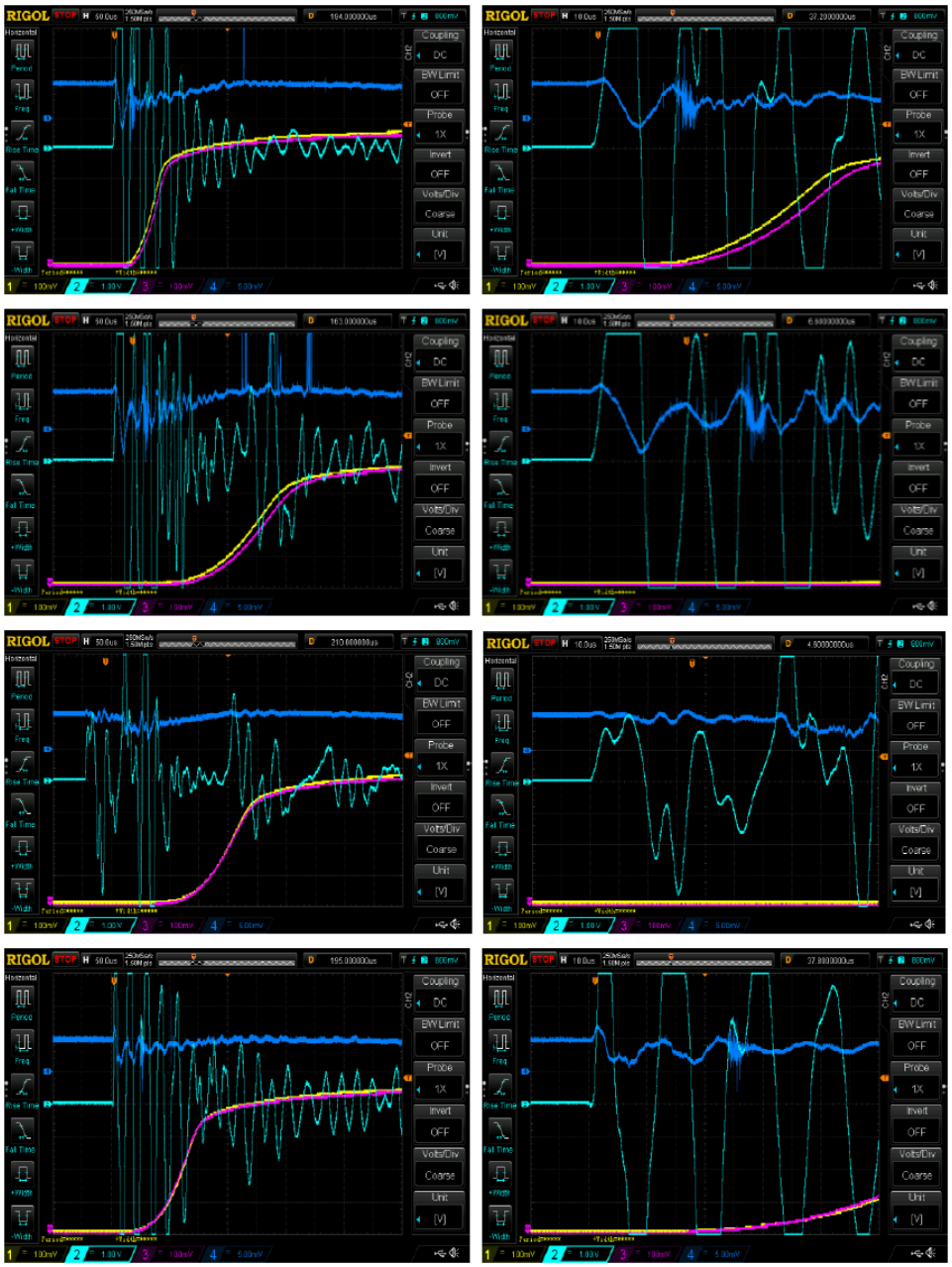

Figure 11. Four more experiments with weaker explosions, using calcium hydride in place of calcium deuteride. Oscilloscope traces shown on the left at 50 μs/division and on the right at 10 μs/division temporal resolution. Experiments Nos.282, 284, 285 and 288.

Figure 12. Debris from four strong explosions using calcium deuteride and calcium hydride, which shattered the anvil bearings in three cases and the upper HSS spacer in two cases.

2.3. Current experiments

The latest experiments have employed smaller roller bearings as anvils within a bronze sleeve such that near axial compression is adequate without the tilting wedge, see Section 2.5 and Fig. 6. Typically, 40 mg of fuel is now used per cell. The compression and explosion reaction force have also been monitored by means of a canister load-cell placed beneath the fusion cell and a piezo-accelerometer clipped to the side. When the reaction is great enough, the local pressure may dent and fracture or cleave the bearing surface. Sometimes the bearings are noisily shattered by the shock-wave. Extracted bearings show blast marks radiating from the hot-spot position. One good example given in Fig. 4 shows these forces and also the explosion flash monitored by UV-enhanced silicon photodiodes (Centronic OSD35-7XCQ). The actual fusion may only last for 8 μs before it breaks the anvils or cell wall enough for gases to escape. The relatively long interval of 400 μs before the flash begins indicates that the flash is due to combustion of hot expelled fuel debris (phosphorus, deuterium) in atmospheric oxygen, after the blast wave has subsided. That is, the fuel debris does not by itself burn exothermically. This delay interval is found to be shorter when the cell sleeve and corresponding blast are less strong. Thus the actual ignition of fusion, lasting only 8μs, is not detected by the

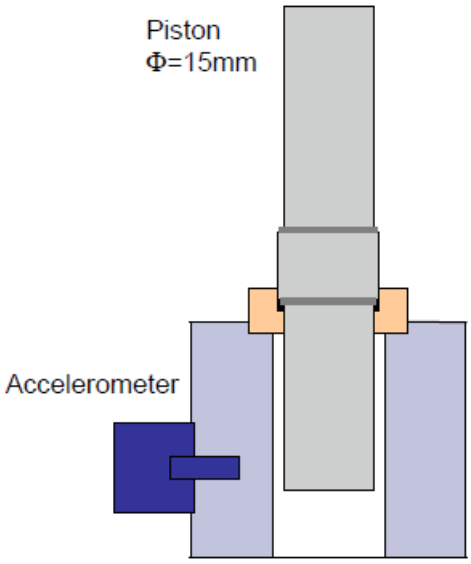

Figure 13. Long shear cell consisting of a case-hardened steel piston with shoulder in a shaped steel sleeve to contain the fuel powder.

photodiodes. An over-exposed video camera snapshot of the very bright flash is shown. When a sleeve is able to resist bursting, there may be no flash at all because the expelled debris is cooled by the inner surface of the sleeve as it squeezes past.

Four more experimental results are presented in Fig. 5 showing that the strength of explosion is variable, although it tends to increase with applied force. In each case, the explosions occur at pressures greater than 15 tons/cm^2 but unpredictably as the pressure is further increased towards 30 tons/cm^2. The hotspot parameters must govern this process. Sometimes there is no immediate explosion, and then the applied force is held at 30 tons for 2 min before releasing and re-applying.

Figure 14. Enlarged view of two typical results of fusion ignition wherein the explosion gas pressure has broken pieces off the piston shoulders, in order to escape upwards.

2.4. Search for nuclear debris

An extensive effort has been put into the search for any nuclear particles emitted by the explosion, but none has been found for sure. Detectors with stainless steel mesh screening were located at 10 cm from the fusion cell and repeatedly subjected to the blast which ultimately ruined a BP4 beta-probe, a ZP1401 GM tube and a ZP1610 proportional counter. In addition, neutron activation was sought many times using indium, lithium, copper, niobium, titanium, aluminium, and vanadium. These materials were placed inside the cell with the fuel then collected with the debris and tested for radioactivity, but none was detected.

2.5. Detailed design features

For other investigators to confirm this work, some detailed practical design information is included in Figs. 6–9. Many configurations have been tried but currently the fusion-cell shown in Fig. 6 is good for ignition under near axial compression up to 30 tons force. The cell consists of two hardened (60–67 Rockwell Scale) chromium AISI 52100 steel roller bearing anvils inside a sintered bronze sleeve. The bearing ends are pre-roughened with coarse sandpaper in order to grip the fuel powder to cause shear within the bulk fuel. It is understood that during initial compression, the malleable solder ring (pre-formed from 1.6 mm diameter solder wire) is squeezed inwards so as to compress the fuel powder. Then as the compression force is increased, the sleeve bulges due to outward pressure from the solder, while the fuel is crushed generating internal shear friction hot-spots wherein the fusion occurs. The cell lower anvil sits upon a canister load-cell (a 16 mm $\times$ 16 mm steel roller bearing with 4 strain-gauges wired in series) to measure the applied axial compression and explosion reaction force. This load-cell is held in place by the pre-formed square stainless steel tube housing. Figure 7 shows circuitry for the strain-gauges, the piezo-accelerometer, and silicon diodes, coupled directly to the oscilloscope. A general side view photograph of the press with its bottle-jack and strong location clamps for the fusion-cell assembly is shown in Figs. 8(a,b). The corresponding plan view schematic, with overall safety enclosure and detectors is shown in Fig. 9.

3. Experiments with Calcium Hydride

Experiments have also been done using calcium hydride in place of calcium deuteride, and unexpectedly found to produce good explosions, see Figs. 10 and 11. Can it be possible that the Coulomb force between the freed hydrogen protons is screened within the hot-spots, leading to deuterium production and energy release?

For both hydride and deuteride, many experiments have emitted weak ignition reports as the applied load is increased above 15 tons, but the strong explosions occur over 25 tons such that the anvil bearings are dented, cracked or well shattered. Sometimes a small wedge is found in the debris, which was the root cause of an anvil splitting in half directly under the source of ignition. Figure 12 illustrates four extreme cases of explosion debris in which the anvil bearings and/or HSS spacer happened to shatter. On average, a 32 ton bottle-jack only survives for 15 experiments because the fast explosion shock-wave damages its input valve before the internal overload valve can operate.

4. Other Cell Designs

Another type of cell design which easily produced the required shearing action is shown in Fig. 13. The fuel powder was put around a case-hardened steel piston rod with a shoulder that compressed the powder as it was pushed through a shaped mild steel sleeve. Upon applying several tons of force, shear in the powder produced hot-spots wherein ignition of fusion broke many pieces off the rod shoulder, see Fig. 14. This allowed the local gas pressure to subside and prevented the fusion from progressing. Clearly, extreme pressure pulses must have been generated to do this amount of damage on hardened steel. Inspection of the steel sleeve adjacent to the hot-spots revealed a melted appearance.

Other methods of inducing fusion with this fuel have been tried, and need further experimentation. For example, externally heating the pressurised cell sleeve caused it to split open and show the burnt interior as a sign of fusion. Therefore, heating the fuel in a container pressurised with deuterium may be one way of producing controlled fusion for energy generation.

5. Proposed Chemical Processes

First of all, phosphorus, calcium and manganese compounds have catalytic properties [8–10]. For example, some primary fusion fuel ($CaD_{1.75}$+ P + Mn) was heated in a test tube and found to decompose readily yielding deuterium gas.

It is hypothesized that chemical and nuclear processes occur within the compressed fuel shear-plane hot-spots [5–7], which are high pressure plasma regions up to 1000 K. Here, ionised manganese and phosphorus may combine exothermically, yielding 104 kJ/mol of MnP [11]. Nearby calcium deuteride, bound by 180 kJ/mol during its production [12], may now be dissociated by energetic phosphorus ions. Deuterium is thereby freed and calcium phosphide formed exothermically at 543 kJ/mol [12], adding further energy to the hot pressurised plasma. Under pressure, freed deuterium atoms will occupy interstitial positions between surface atoms of manganese grains [13] where they are dynamically constrained while being bombarded by energetic deuterons in the plasma. At the same time, bombardment by energetic free electrons adds to the environment of manganese conduction/valence electrons and results in enough screening of the Coulomb force to enable fusion of the free and constrained deuterons.

To support this theory, the transition metal powders listed earlier in Section 2.1 were found to behave like manganese in producing explosions; and deuterides other than calcium were also successful. However, no activity could be induced when pre-formed manganese phosphide was substituted for the elemental manganese and red phosphorus powders. As might be expected, there was no activity in control experiments employing a (Ca + P + Mn) mixture, or dry $Ca(OH)_2$ powder.

This has proved to be a self-restricting technique and there is a residue of unconsumed fuel around the cell after the explosion because the fuel confined alone does not burn easily. A sharp smell of impure phosphine is always apparent.

6. Further Developments

The experiments described above are clearly limited to fusion demonstration only, to prove it is possible in the solid state. For commercial energy generation we need a continuous high energy process, as already tried by various groups [14]. A pellet of fusion fuel would be compressed and heated by powerful laser beams, or heavy-ion beams, or electron beams, or a Z-pinch cell. An alternative process for continuous energy generation may be to heat the source compound in a controlled manner.

When trying these different techniques, the fuel compound could be varied by substituting other chemical elements in part, to get a controllable reaction. For example, calcium hydride has already been substituted for the deuteride and produced explosions.

7. Conclusion

A large number of experiments have been conducted with powdered material comprising a deuteride and catalyst. The technique is understood in terms of pressurised shearing hot-spots within which exothermic chemical reactions facilitate enough Coulombic screening for nuclear fusion of deuterons. Even a mixture of hydride and catalyst produces explosions, so this is a noteworthy phenomenon. In a separate paper, theoretical models will propose how soft X-rays are generated and convert to heat in the material. From an engineering point of view, this discovery may be developed immediately using inertial confinement or other techniques [15].

Safety shielding has been necessary in all experiments with pressurised solid state compounds. The manual compression technique used here is slow enough to allow time for the fusion gases to escape. Impact techniques might strongly confine the gases, resulting in a dangerous fusion avalanche [5].

Acknowledgements

I would like to thank Imperial College Libraries and H. Bowtell for typing.

References

[1] www.LENR-CANR.org.
[2] The international society for condensed matter nuclear science, www.iscmns.org.
[3] C.G. Beaudette, *Excess Heat,* 2nd Edn., Oak Grove Press, 2000.
[4] S.B. Krivit and N. Winocur, *The Rebirth of Cold Fusion*, Pacific Oaks Press, 2004.
[5] S.M. Walley et al. The use of glass anvils in drop-weight studies of energetic materials, *Propellants Explos Pyrotech.* **40** (2015) 351.
[6] Y. Fialko and Y. Khazan, Fusion by earthquake fault friction: Stick or slip? *J. Geophys. Res*. **110** (2005) 1, http://sioviz.ucsd.edu/∼fialko/Assets/PDF/fialkoJGR05a.pdf.
[7] T.E. Tullis and D.L. Goldsby, Flash melting of crustal rocks at almost seismic slip rates, *Am. Geophys. Union* (Fall 2003), http://adsabs.harvard.edu/abs/2003AGUFM.S51B..05T.
[8] E.C. Alyea and D.W. Meek, *Catalytic Aspects of Metal Phosphine Complexes*, American Chemical Society, 1982.
[9] D.J.P. Kornfilt, Calcium Compounds in Catalysis, 2011, http://denmark.academicwebpages.com/wp-content/uploads/gp/2011/gm-2011-3-15.pdf.
[10] J. Brinksma, Manganese catalysts in homogeneous oxidation reactions, https://www.rug.nl/research/portal/files/3048250/titlecon.pdf.
[11] C.E. Myers, E.D. Jung and E.L. Patterson, Vaporization behaviour of MnP(s) and the thermodynamics of the manganese-phosphorus system, *Inorganic Chem.* **19** (1980) 532.
[12] *CRC Handbook of Chemistry and Physics*, CRC Press, 2006.
[13] Gerhard Ertl, Chemical processes on solid surfaces, http://www.nobelprize.org/nobel_prizes/chemistry/laureates/2007/advanced-chemistryprize2007.pdf.
[14] M.M. Basko, Summary talk, *Nucl. Fusion* **45** (2005) S38–S47, http://www-naweb.iaea.org/napc/physics/fec/fec2004/papers/s_1-4.pdf.
[15] R.C. Wayte, International Patent Application No: PCT/GB2014/051386, Publication No: WO2014181097, 13 November 2014.

J. Condensed Matter Nucl. Sci. 18 (2016) 50–75

Research Article

Arguments for the Anomalous Solutions of the Dirac Equations

Jean-Luc Paillet*
Aix-Marseille University, France

Andrew Meulenberg†
Science for Humanity Trust Inc., USA

Abstract

In this paper, we look into the difficult question of electron deep levels in the hydrogen atom. An introduction shows some general considerations on these orbits as "anomalous" (and usually rejected) solutions of relativistic quantum equations. The first part of our study is devoted to a discussion of the arguments against the deep orbits and for them, as exemplified in published solutions. We examine each of the principal negative arguments found in the literature and show how it is possible to resolve the questions raised. In fact, most of the problems are related to the singularity of the Coulomb potential when considering the nucleus as a point charge, and so they can be easily resolved when considering a more realistic potential with finite value inside the nucleus. In the second part, we consider specific works on deep orbits as solutions of the relativistic Schrödinger and of the Dirac equations, named Dirac Deep Levels (DDLs). The latter presents the most complete solution and development for spin $1/2$ particles, and includes an infinite family of DDL solutions. We examine particularities of these DDL solutions and more generally of the anomalous solutions. We next analyze the methods for, and the properties of, the solutions that include a corrected potential inside the nucleus, and we examine the questions raised by this new element. Finally, we indicate, in the conclusion, open questions such as the physical meaning of the relation between quantum numbers determining the deep levels and the fact that the angular momentum seems two orders-of-magnitude lower than the values associated with the Planck constant. As a prerequisite to a deep comprehension of the resolution methods, we recall in the appendices some essential elements of the Dirac theory.
 ISSN 2227-3123

Keywords: Deep electron levels, Dirac equation, LENR, Relativistic quantum physics, Singular solutions

1. Introduction

For many decades, the question of the existence of electron deep orbits (EDLs) for the hydrogen atom led to numerous works and debates. Why once more a study on this subject? For several reasons:

*Corresponding author. E-mail: jean-luc.paillet@club-internet.fr
†E-mail: mules333@gmail.com

 ISSN 2227-3123

- the arguments in favor of the deep orbits have become progressively more mature by the use of relativistic quantum tools for a full three-dimensional description of the system;
- by accepting the reality of a non-singular central potential within a nuclear region, many mathematical arguments against anomalous solutions of the relativistic equations no longer pertain;
- numerical evaluation of the relativistic equations are now detailed and available for interpretation of the models, their implications, and their predictions;
- and, above all, recognition of these levels opens up a whole new realm of atomic, nuclear, and subatomic-particle physics as well as nuclear chemistry.

There are various theoretical ways to define a state of the hydrogen atom with electron deep level (EDL) or deep Dirac level (DDL) orbits. In the following, we denote $H^{\#}$ as any state of hydrogen atom with EDL orbits. Some authors use the term *hydrino* for denoting the $H^{\#}$states owing to the work of [1] on the hypothetical existence of H atoms with orbit levels under the Bohr ground level and where the values of orbit radii are fractional values of the Bohr radius. Here we do not use this term, a physical concept specifically attached to the cited work, because it is not deduced from quantum equations, while we essentially consider the states $H^{\#}$ obtained by the methods of relativistic quantum physics.

With the quantum equations habitually used in the literature for computing the bound states of the H atom, we can note that there is in general a crossroad with a choice of value or a choice of sign for a square root in a parameter. According to which path is chosen, the resolution process leads either to the usual solution or to one called "anomalous" solution, rejected in the Quantum Mechanics textbooks.

In our present study, we note that a $H^{\#}$ solution is always an anomalous solution but *every anomalous solution is not a $H^{\#}$solution.* For example, the anomalous solution also contains the regular energy levels of *anti-hydrogen*. We will see below that it is easy to recognize $H^{\#}$ solutions, if we have an expression of the anomalous solutions obtained by an analytic method. A solution provides the eigenvalues of the Hamiltonian, representing the total energy of the electron, in the form of a family of quantized energy levels depending on quantum numbers. We consider only relativistic equations because, in the deep level orbits considered here, the electrons are relativistic. Indeed, we can make a quick computation:

> In [2], the authors plot the curve of the normalized electron density of the deep orbit wave function corresponding to the ground-state DDL orbit (−2s), and this curve has a peak for a radius equal to ∼1.3 fm. By using the formula of the Coulomb energy potential $\mathrm{CP} = -\alpha c\hbar/r$, we can deduce $|\mathrm{CP}| \sim 1.09$ MeV for this deep orbit. On the other hand, we can deduce from the fundamental dynamics principle in the relativistic framework, that an electron on this deep orbit has a potential energy equal, in absolute value, to $\gamma m v^2 = |\mathrm{CP}| \sim 1.09$ MeV, where v is the electron velocity. The relativistic coefficient γ is equal to $(1 - v^2/c^2)^{-1/2}$. By simple algebraic transformations, we can deduce a quadratic equation on an unknown parameter $V = v^2$. From the positive root of this equation, we obtain $v = 2.75 \times 10^8$ m/s, $\beta \sim 0.91$ and $\gamma \sim 2.5$. These results confirm that the electron is actually relativistic.

Of course, it is possible to obtain anomalous solutions by means of a non-relativistic equation, such as the Schrödinger equation. But in this case the energy levels are the same as the regular ones even if the wave functions are different from the regular solutions. This corresponds to a class of solutions we name "pseudo-regular", obtained also by relativistic equations. This class of solutions is described in Section 3.3.2.

The total energy E corresponding to a regular solution in a non-relativistic form for a bound state electron is expressed in negative value and $|E| \ll mc^2$. In relativistic form, the rest mass of the electron is included and, for atomic electrons, $E \sim mc^2(1 - \varepsilon)$, where $\varepsilon \ll 1$ and depends on the coupling constant α and on quantum numbers. For a $H^{\#}$ solution, the relativistic total energy is of the form $E \sim mc^2\varepsilon$

As the movement of the electron is in a central field, its eigen state equation is usually written in spherical coordinates and it can be decomposed into a part depending on angular parameters θ, φ, and another part, the radial equation. The equation on angular parameters has for solutions the spherical harmonics $Y(\theta, \varphi)$ and the wavefunctions $\psi(r, \theta, \varphi)$ verify $\psi(r, \theta, \varphi) = R(r)Y(\theta, \varphi)$, where $R(r)$ is the solution of the radial equation (here we omitted the quantum numbers indexes). The wavefunction can take a more complex form, for example when using the Dirac equation, but in any case only the radial part can raise questions. Thus, we consider the reasoning on the radial equations and wavefunctions.

2. Discussion on the Arguments Against the H$^{\#}$ States

Here we classify our reflections according to the arguments found in the literature against the existence of these special states of the hydrogen atom and we discuss these arguments.

2.1. The wave function can have a singular point at the origin

This argument is rising in all known cases of H$^{\#}$ states with a $1/r$ Coulomb potential. The spatial part of the solutions of the radial equation, in the most general form, has several factors:

- one factor is a decreasing exponential $\exp(r)$ such that $\exp(r) \to 0$, when $r \to +\infty$,
- another one is $\propto 1/r^s$ with s a real number, due to the form of the Coulomb potential, and
- there can be a further one in polynomial form.

In the case of the "anomalous" solutions, the exponent s of the factor in $1/r^s$ is $s > 0$, then the radial function $R(r) \to \infty$ when $r \to 0$ and the wavefunction $\psi(r, \theta, \varphi)$ does not obey a boundary condition. This problem comes from the expression of the Coulomb potential in $1/r$.

Some authors of H$^{\#}$ solutions remove this trouble by saying that the classical expression of the central potential is a good approximation for the bound state of a single electron atom, but considering the nucleus as a mathematical point is an unphysical abstraction. In fact, the Coulomb approximation in $1/r$ of the central potential generated by the nucleus is suitable if the electron is not too near the nucleus.

At this point, many authors do not consider a non-singular potential and stop without further development of the anomalous solution; but others work on this subject in expressing corrected potentials in the close vicinity of the nucleus.

That is an actual enhancement of the theory, but it unfortunately entails extra difficulties. Indeed, there are no serious difficulties for defining the weakening of the electrical potential near the charge radius of the proton and inside it, by approximating the nucleus as a uniformly charged sphere. But problems rise when wanting to find solutions of the equations by taking into account the chosen potential for the neighborhood of the nucleus. Let *Pn* be this potential, then there are two possible procedures to use *Pn* :

(1) To solve (analytically if possible) the equation with the Coulomb potential and to find a first solution S1, then to solve the equation with *Pn* and find a second solution S2 near and inside the nucleus, and finally connect S1 and S2 in suitable way, i.e. by taking in account continuity conditions and even conditions on derivatives of both solutions at the interface of both potentials. Moreover, we note it would be preferable to beforehand connect carefully the potentials themselves. This procedure of connection has been used in several works, as, e.g., in [2].
(2) In the case where the solution S1 implies the bound electron is almost at the contact of the proton or deeper, i.e. beyond the chosen radius for the potential interface, then we can think S1 is rather erroneous. In this case, the best procedure would be to solve the equation with the whole rectified potential from 0 to the infinity. Of course such a solution would use numerical tools. Note in the case of a complex equation as the Dirac one,

the potential is taken into account only when arriving at the couple of differential equations on the component functions classically denoted as f and g. Nevertheless, at this point, there was not yet a choice between the regular and the anomalous solutions.

2.2. The wave function can be 'not square integrable'

In this case, the wave function cannot be normalized in the entire space and it does not obey a boundary condition for the bound states. This case results essentially from the behavior of the wavefunction ψ at the origin and not for $r \to \infty$

To be normalized, the wavefunction must satisfy $||\psi(r, \theta, \varphi)|| < +\infty$. As the Jacobian of the transformation from Cartesian to spherical coordinates is $J = r^2 \sin\theta$ we have $||\psi(r,\theta,\varphi)|| = \int|\psi|^2 \sin\theta\ r^2 \mathrm{d}\theta\ \mathrm{d}\varphi\ \mathrm{d}r = \int |Y(\theta,\ \varphi)|^2 \mathrm{d}\Omega$ $\int |R(r)|^2 r^2\ \mathrm{d}r$, where Ω is the solid angle. Since the spherical harmonics are normalized, we have only to verify $\int |R(r)|^2 r^2 \mathrm{d}r < +\infty$. In fact the behavior of $|R(r)|^2 r^2$at infinity does not make any difficulty, because the leading factor which induces ψ to vanish is a decreasing exponential factor. Thus, only the behavior of $|R(r)|^2 r^2$at the origin can be a problem.

Here we can cite the work of Jan Naudts [3], where a $H^{\#}$ state is found by using the Klein–Gordon (K–G) equation and the corresponding solution is square integrable. The author derives in one step the K–G equation for the bound electron of the hydrogen atom from the time-dependent Schrödinger equation by introducing the relativistic formulation of the energy. We recall this process in a more explicit way in order to more clearly see what are the implications of the K–G equation and what are its limitations.

- The relativistic total energy of a free particle of mass m is given by the following equation:

$$E^2 = \mathbf{p}^2 c^2 + m^2 c^4.$$

- If we consider an electron of charge e, submitted to an exterior electromagnetic field defined by a scalar electric potential φ and a vector potential $\mathbf{A}$ in covariant form, then the momentum vector $\mathbf{p}$ becomes $\mathbf{p}$ - $e\mathbf{A}$ and the energy E becomes E - $e\varphi$. By substituting in the previous energy equation we obtain $(E - e\varphi)^2 = (\mathbf{p} - e\mathbf{A})^2 c^2 + m^2 c^4$. But, if the electron is in a central Coulomb potential generated by a proton, we have $\mathbf{A}$ =0 and $e\varphi$ is equal to $V = -e^2/r = -\alpha c\hbar/r$, where α is the coupling constant.
- Finally, by expressing E and $\mathbf{p}$ by differential operators, i.e. $E \to i\hbar\partial_t$ $\mathbf{p} \to -i\hbar\nabla$, the energy equation becomes the K–G equation for the electron in the hydrogen atom, as written in the cited paper:

$$(i\hbar\partial_t - V)^2 \psi(r,t) + \hbar^2 c^2 \Delta\psi(r,t) = m^2 c^4 \psi(r,t),$$

  where $\psi(r, t)$ is a time-dependent radial wavefunction and m the rest mass of the electron. Historically this equation was called the *relativistic Schrödinger equation*.
- Then the author tries an ansatz with a function

$$\psi(t,r) = \mathrm{e}^{\frac{i}{\hbar}Et} r^{-l} \mathrm{e}^{-r/r_0}$$

  with the hypothesis $l < 3/2$ and $r_0 > 0$ (do not confuse l with the usual notation for the angular moment). The condition on the exponent l guarantees the behavior of $|\psi(r, t)|^2 r^2$ at the origin and $r_0 > 0$ its behavior at the infinity. So the wavefunction solution is *square integrable*. The resolution by leads to an equation to be satisfied by the parameter l: $l^2 - l - \alpha^2 = 0$, with solutions $l = \frac{1}{2}\left(1 \pm \sqrt{1 - 4\alpha^2}\right)$.

  We can see a possible choice of sign $\pm$. In both cases, the constraint on l is satisfied: $l < 3/2$. The choice of the negative sign leads to a regular solution that corresponds to the ground energy level associated with the

usual quantum number $n = 1$. Indeed the value of the total energy is $E \sim mc^2\left(1 - \frac{\alpha^2}{2}\right)$, thus the binding energy is equal to $BE \sim -mc^2\frac{\alpha^2}{2} = -13.6\,\text{eV}$ and the orbit radius r_0 is equal to 53 pm.

If the positive sign is chosen, the obtained solution is a $H^{\#}$ state, with total energy very low, $E \sim mc^2 \sim 3.73\,\text{keV}$. That means a high value for the binding energy, since $BE \sim mc^2(\alpha - 1) = -507.3\,\text{keV}$.

Naudts calculates excited states by using an analogous ansatz, but they correspond to regular states. The only $H^{\#}$ state obtained is the above one, as he considers only spherically symmetric states, i.e. the zero angular moment states. As the exponent $l > 0$, the origin is a singular point for the wavefunction. Naudts argues against this singularity by saying that the nucleus is not a point, but its charge is "smeared" over a distance of about 1fm. Solving the equation with a smeared out Coulomb potential would produce a solution not diverging at the origin, but with certain minor changes on the $H^{\#}$ state.

Some criticism can be raised about the application of the K–G equation for a question concerning the bound electron of the hydrogen atom.

- The most classical criticism concerns the fact that the electron is a fermion, spin $\pm 1/2$, whereas this equation does not take into account the spin and there is no way to introduce the Pauli spin matrices without destroying the Lorentz invariance. On one hand, this trouble is slight in comparison with the benefit of finding a square integrable $H^{\#}$ solution. On the other hand, it's the same problem for the classical Schrödinger equation and its use is well accepted for finding the energy levels for the light atoms. Moreover, it is not yet time to worry about fine structure for the $H^{\#}$ states.
- A more subtle criticism concerns the conservation equation $\partial_t \rho + \nabla \cdot \mathbf{J} = 0$, where

$$\mathbf{J} = \frac{\hbar}{2im}(\psi^* \nabla\psi - \psi \nabla\psi^*).$$

For the Schrödinger equation, $\rho = |\psi|^2$, it represents a probability density and satisfies the conservation equation. So its space-integral is time-independent and $\mathbf{J}$ represents a probability current density. But from the solutions of the K–G equation, the only possibility is that ρ be proportional to $\frac{\hbar}{2imc^2}(\psi^* \partial_t \psi - \psi \partial_t \psi^*)$. The occurrences of time derivatives are due to the presence of a second time-derivative in the K–G equation. This expression can be reduced to $\rho = |\psi|^2$ in the non-relativistic limit. But the previous expressions including time derivatives, is not necessarily positive and it cannot be considered as a probability density. In fact, it can be interpreted as a charge density in inserting $e\varphi$ (and $e\mathbf{A}$ for $\mathbf{J}$) as indicated in [4,5], because a charge can be positive or negative. Note that this problem does not exist for the Dirac equation, because it contains only first time-derivatives. Regardless, this question does not remove the interest in the $H^{\#}$ solution found by [3].

Finally we note that, if the singular point at the origin can be suppressed (e.g. by means of a corrected potential near the origin), the wavefunction is automatically square integrable.

2.3. The orthogonality criterion can be not satisfied

The Hamiltonian, which represents the total energy, has to be a Hermitian operator in the standard quantum mechanics in order for its eigenvalues to have real values. This leads to the following needed condition: eigenfunctions corresponding to distinct values have to be orthogonal. In [6], de Castro examines the asymptotical behavior of the solutions of the non-relativistic Schrödinger, of the Klein-Gordon and of the Dirac equations by using the Frobenius series method and by considering the variations of this behavior as a function of formal variations of the coupling constant α. Then from the orthogonality condition, he indicates deduced conditions under two different forms for the radial solutions, according to which equation is used:

For the case of the Schrödinger/Klein–Gordon equation,

$$\left(u_k^* \frac{\mathrm{d}u_{k1}}{\mathrm{d}r} - \frac{\mathrm{d}u_k^*}{\mathrm{d}r} u_{k1}\right) \to 0, \quad \text{when } r \to 0, \text{ where } u_k(r) = rR(r),$$

where u_k and u_{k1} are two different eigenfunctions, and the same thing for f_k, f_{k1} and g_k, g_{k1}.

For the case of the Dirac equation, we have a condition on the upper and lower components denoted f, g in usual notation [4]:

$$\left(f_k^* g_{k1} - f_{k1} g_k^*\right) \to 0, \quad \text{when } r \to 0,$$

where u_k and u_{k1} are two different eigenfunctions, and the same thing for $f_k \neq f_{k1}$ and $g_k \neq g_{k1}$.

Next he indicates that for the Klein–Gordon case, only the solution such that u is "less singular" than $\sqrt{r}$ can satisfy the orthogonality criterion. That implies $R(r) \propto r^{-l}$ with $l < 1/2$. And, for the Dirac solution, he finds that only the regular solutions for the components f, g can satisfy the orthogonality, because the condition is $R(r) \propto r^{-l}$ with $l < 1$. So, the problem of the orthogonality is closely related to the behavior of the radial function at the origin, itself related to the singularity of the Coulomb potential at $r = 0$. Therefore, this problem can be resolved by a corrected potential, without singular point at $r = 0$, that corresponds in fact to the physical reality.

We also note several works [7,8] on self-adjoint extension of operators for potentials with singularity. In particular, Nadareishvili and Khelashvili [7] explicitly show that, *in the case of the Klein–Gordon equation with a Coulomb potential, the "singular" (anomalous) solutions satisfy the orthogonality condition and satisfy also directly the boundary condition*, i.e. when $r > 0$, $\lim u(r) = u(0) = 0$.

For the Dirac equation with a Coulomb field, it is more complex. In [9], Thaller uses the notion of essentially self-adjoint operator ([10], p. 256) for potentials with singularity: an operator is essentially self-adjoint if it has an unique extension to a larger domain, where it is self-adjoint. But to satisfy the orthogonality condition and the boundary condition, it is necessary to consider a corrected potential near the nucleus. This point is addressed in Section 3.4.2.

2.4. The strength of the binding seems to increase when the coupling strength decreases

It can seem absurd to make changes of a physical constant whose value is in principle given by 'Dame Nature'. But, it can be very instructive to make this "thought experiment": to imagine variations of the coupling constant α and to examine the consequence of such variations on the energy parameters of the hydrogen atom.

In [11], Dombey points to a very strange phenomenon concerning the $H^{\#}$ solutions of the relativistic equations: when α decreases and tends towards 0, the binding energy of the electron increases and tends towards its maximum. The author solves the Klein–Gordon equation in an analytic way leading to a Whittaker's (second-order differential) equation [12] on the radial function and the solution is classically achieved by transformation into a Kummer's equation [13]. So the radial function has the general form with three factors as we noted in Section 2, where polynomials are obtained by fixing some parameters of the confluent hypergeometric series solution of the Kummer's equation. As in the analytic resolution of the Schrödinger equation, there is a choice of sign for a parameter occurring in the expression of the energy levels. One choice leads to the regular energy levels, while the other sign leads to anomalous ones, E_N, where N is a positive quantum number. Here is the expression of total energy at the level N:

$$E_N = mc^2 \left[1 + \frac{\alpha^2}{\left[N + \frac{1}{2} - \sqrt{\left(\frac{1}{4} - \alpha^2\right)}\right]^2}\right]^{-1/2}. \tag{1}$$

The only difference between the anomalous and the regular solution is the presence of a minus sign before the square root in the denominator of the fraction $\ldots \frac{1}{2} - \sqrt{\ } \ldots$ instead of a plus sign. For the anomalous ground level E_0, the author obtains the same expression as the $H^{\#}$ state energy found by Naudts [3], i.e. $E_0 \sim mc^2\alpha = 3.73$ keV. Now we can trivially see the total energy E_0 of the electron decreases when α decreases, which means its binding energy $|BE|$ increases in absolute value. And finally $|BE| \to mc^2$, the *whole rest mass energy*, when $\alpha \to 0$.

This very strange phenomenon seems to concern only the ground state E_0 because, for $N \neq 0$, we have

$$E_N \approx mc^2 \left(1 - \frac{\alpha^2}{2N^2}\right) \quad \text{for } \alpha \ll 1,$$

thus E_N increases when α decreases, i.e. the usual behavior. Of course, we have the same result as the ones obtained in [3], but now we have an algebraic expression resulting from an analytic process, so we can see at least a mathematical reason for discriminating the $H^{\#}$ solution among the set of the anomalous solutions. Indeed, the explanation lies in the expression Δ in the denominator, $\Delta = N + \frac{1}{2} - \left(\frac{1}{4} - \alpha^2\right)^{1/2}$: if $N = 0$, Δ can be reduced to α^2 for $\alpha \ll 1$, leading to the expression for E_0 above. Nevertheless, we see in some cases there is an infinite family of $H^{\#}$ states and all these states have the strange behavior w.r.t. the coupling constant. It is the case for example in [14], where the relativistic Schrödinger/Klein–Gordon equation is solved by using a more direct method as in [4] providing an infinity of $H^{\#}$ states. An analogous result is obtained by means of the Dirac equation.

Note in the paper cited above [11] the author examines the solutions given by the Dirac equation in two-space-dimensions and finds the same strange behavior of the ground state, which is a $H^{\#}$ state, with respect to the coupling constant.

In fact, we think this result is obtained in a context of an ill-defined system, uniquely on a pure mathematical basis. From a physical point of view, we can see the coupling constant α is actually entangled with several fundamental constants, in particular the Planck constant, the velocity of the light and the elementary electric charge. So, modifying α without much precaution can certainly lead to paradoxical physical results.

Another example, extracted from [9], of this kind of problem concerning a physical constant, in a case where the constraints are simpler: the non-relativistic limit of a relativistic theory can be obtained if one lets c tend to infinity, and thus the relativistic coefficient γ becomes 1 for any speed v. But if doing this on the Dirac operator in an electromagnetic field, one has to proceed carefully because of terms as such as mc^2 which would tend to infinity, and as the term $(e/c)\mathbf{A}$ that would turn off the vector potential $\mathbf{A}$ if c tends to infinity. Then the author is led to develop specific techniques and to define some concepts needed on account of the nature of the so-called *c-dependence* of the Dirac operators.

3. DDL (Deep Dirac Levels). The Deep Orbits Obtained as Solutions of the Relativistic Quantum Equations

In [14], Maly and Va'vra publish their first article where they define the concept of Deep Dirac Levels (DDL) for the electronic orbits of the Hydrogen-like atoms. Here we consider only hydrogen atoms.

In fact, they use two methods for obtaining these deep orbit levels: the former by means of the relativistic Schrödinger equation, and the latter by the Dirac equation. For both equations, they follow the solution method indicated in [4]. We give a quick outline of the solution process, explicitly handled in the appendices, and we discuss the solutions. We emphasize the use of the Dirac equation.

3.1. Solutions obtained by [14] with the relativistic Schrödinger equation

This equation has been written in Section 2.2. After separation of the radial equation, one introduces an ansatz $R(\rho) = \rho^s \mathrm{e}^{-\rho/2} L(\rho)$ into the radial equation, where R represents the radial wavefunction, $L(\rho)$ is a series of powers

of ρ; s is a real parameter and ρ is a real numerical parameter, without physical dimension but proportional to the radius r in spherical coordinates. As usual, new parameters are defined by combining the initial physical parameters of the radial equation, in order to obtain a pure numerical second order differential equation in $L(\rho)$.

One shows that the eigenvalue energy$E$ of the Hamiltonian is defined by the following expression: $E = mc^2\left[1 + (\gamma^2/\lambda^2)\right]^{-1/2}$ where λ is a numerical parameter of the equation and $\gamma = Z\alpha$, α being the coupling constant. It is in fact the Sommerfeld relation. From the differential equation in ρ, we have two conditions to satisfy:

(1) $s(s+1) + \gamma^2 - l(l+1) = 0$, when introducing $\rho = 0$ in the equation, where l is the angular moment quantum number,
(2) $\lambda = n' + s + 1$, to obtain the convergence of the series $L(\rho)$, where $n'$is an integer ≥ 0.

The first condition, a quadratic equation, has two roots:

$$s = -\frac{1}{2} \pm \left[\left(l + \frac{1}{2}\right)^2 - \gamma^2\right]^{1/2}.$$

It is the "crossroad" condition indicated at the beginning of this paper. Indeed, when taking the positive sign in the expression of s, we obtain the usual solution for the electronic energy levels. This choice is taken because with the negative sign we have $s < 0$ for any $l > 0$ and thus the radial wavefunction R tends to infinity when ρ tends to 0 because of the exponential term ρ^s. Note that for $l = 0$, we also have $s < 0$, even when taking the positive sign. But in this case, for small Z and as $\gamma \simeq Z/137$, $\gamma^2 \ll 1$ and s is close to zero. Moreover, considering that the nucleus has a size $a \neq 0$, the potential has no singular point near 0 and is finite everywhere. Then, one can show [4] that the solution R is finite at $r = \rho = 0$ and approaches that solution with a singular-point-Coulomb potential when a tends to 0.

Nevertheless, as noted in [14] for heavy atoms, the value of γ^2 becomes great enough that s (< 0) has a non-negligible absolute value for $l = 0$. For example, in the Cs atom, $Z = 55$ and then $s \approx -0.2$. One can observe that for a higher-Z hydrogen-like atom, i.e. Fr with $Z = 87$, we have s with an imaginary part; but this fact goes beyond the subject of our paper. As we consider only the H atom, it is sufficient to let $Z = 1$. Anyway, at this point we can consider there is no serious reason for systematically eliminating the so-called "anomalous" solutions obtained with a negative sign in the root s. The argument concerning the physical reality of the finite ($\neq 0$) size of the nucleus can be applied in this case too.

The energy levels corresponding to the "anomalous" solutions are provided by the following expression:

$$E = mc^2\left[1 + \frac{\alpha^2}{\left(n' + 1/2 - \left[(l+1/2)^2 - \alpha^2\right]^{1/2}\right)^2}\right]^{-1/2}, \tag{2}$$

where n' is the radial quantum number and l is the angular momentum quantum number. For hydrogen-like atoms, α^2 is simply replaced by $Z^2\alpha^2$. As for the usual solutions, the authors define the total quantum number $n = n' + l + 1$. Then they compute the new energy levels E (by using the formula in γ and λ) for all the possible combinations of the quantum numbers $n = 1, 2, \ldots$; $n' = 0, \ldots, n-1$; and $l = n - n' - 1$. Of course, the values represented by E are the total energy of the electronic orbitals.

The corresponding binding energies, i.e. the values $BE = E - mc^2$ are quoted in several tables (Table 1), together with the energies of the regular solutions (positive sign in the expression of s) and with the non-relativistic Schrödinger levels for comparison. The results for $Z = 1$ are reproduced in Appendix A.8.

Each table is built-up for a different hydrogen-like atom of the class of the alkali metals. In fact, *every anomalous solution is not a deep* orbit: such a deep orbit appears only for $n' = l$, as emphasized by the authors and as we can see in Tables 1 and 2 (where $n = N, n' = M, l = L$).

As we have an analytic expression of E, it is possible to find the "secret" of this discrimination.
For doing this, we start from the formula

$$E = mc^2\left[1+\left(\frac{\gamma^2}{\lambda^2}\right)\right]^{-1/2}, \quad \text{where } \lambda = n' + s + 1 \text{ and } s = -\frac{1}{2} - \left[\left(l+\frac{1}{2}\right)^2 - \alpha^2\right]^{1/2}.$$

For small Z (here $Z = 1$), we can first show that $\lambda \sim n' - l + \alpha^2/(2l+1)$. Then we can see that the condition $n' = l$ drastically reduces the expression of λ: $\lambda \sim \alpha^2/(2l+1)$, and so $\lambda \ll 1$. Carrying this into the expression of E, we can next show that the total energy $E \sim mc^2\alpha/(2l+1)$. As the fraction $\alpha/(2l+1) \ll 1$, the binding energy $|BE|$ is very high and that means the orbit is very deep. So for every l, $|BE| > 507$ keV, which gives an orbit radius of order fm. There is an infinite series of these very deep energy levels.

Concerning the energy levels corresponding to other combinations of the quantum numbers, the tables gives two kinds of results: values similar to the usual energy levels, and values annotated by the authors as "negative energy states, not observable", appearing for $n' > l$. Finally, we can note that for $n' = l = 0$, for the relativistic Schrodinger case, the binding energy $BE = -507$ keV, in agreement with the result found in [3] for the energy of the anomalous solution. Moreover the necessary condition, $n' = l$ for the EDL orbits, explains the negative result of the same author concerning the "excited" states, because he considered only the case of null angular momentum.

3.2. Solutions obtained by means of the Dirac equation

3.2.1. *Determining the DDL solutions*

The authors refer to and use the method developed in [4] that we indicate in Appendix A.6. Here is the expression of the anomalous solutions obtained from the regular solutions by changing the sign "plus" by a sign "minus" between n' and the square root, at the denominator of the internal fraction:

$$E = mc^2\left[1+\frac{\alpha^2}{\left(n' - \sqrt{(k^2-\alpha^2)}\right)^2}\right]^{-1/2}, \tag{3}$$

E depends on two quantum numbers n' and k. The radial quantum number n' can take any positive values 0, 1, 2 … and k is related to the total angular momentum (now including the electron spin). It can take values $\pm1, \pm2, \ldots$ but not the value 0. Indeed, from the relation $\hbar^2K^2 = \mathbf{J}^2 + \frac{1}{4}\hbar^2$ given in Appendix A.4, we can see that k cannot be null, but we can give also a more "physical" argument to understand this fact. In the radial equation, Appendix A.6, the term in k/r plays the role of a repulsive angular momentum barrier that prevents the "fall to the center." It is like the "effective potential" $l(l+1)/r^2$ appearing in the well-known non-relativistic radial Schrödinger equation. One also defines the main quantum number to be $n = n' + |k|$.

As was done for the relativistic Schrödinger equation, the authors built tables of the binding energies for combinations of the specific Dirac quantum numbers n' and k appearing in the expression of E, plus the main (or total) quantum number n and the orbital quantum number l. This latter is connected to k by the relation $l = k - 1$, if $k > 0$, else $l = -k$. This Table 2 also concerns the hydrogen-like atoms of the alkali class. Here we consider only the hydrogen tables and $k > 0$. $\left[n = N, n' = M, k = K, \text{ and } l = L2 = -k \text{ (used with } k < 0) \text{ for the Dirac levels}\right]$.

Here again, every energy level is not a DDL, but *only those computed* for $n'(= M) = k$. The mathematical explanation is similar as the case of the Schrödinger equation: we can show that the energy values E_D of the DDL orbit satisfy $E_D \sim mc^2\alpha/2k$. So, we can see that there is an infinite series of DDL solutions. Now we consider the

expression $E_S \sim mc^2\alpha/(2l+1)$ obtained in the Schrödinger case. Here, the indices D and S refer to the Dirac equation and Schrödinger equation, respectively. While comparing the expressions of E_D and E_S, we can verify the slight shift between the values of E_D and E_S, i.e. $E_D > E_S$ and thus $|BE_D| < |BE_S|$, for the equivalent levels determined by n' and thus by $k = l$. For example, for $n' = 1$, the tables displays $BE_S - 509.8$ keV while $BE_D - 509.1$ keV. Note that the first deep orbit energy $BE_S \sim -507$ keV, for $n' = 0$, has no equivalent in the "Dirac table" of the same atom, because the Dirac number k cannot be null.

It is quite normal to have differences between these values, because the Dirac Hamiltonian includes the additional corrective term of *spin-orbit* energy (Appendix A. 5), associated with the spin precession, and corresponds, for the regular solutions, to a smaller total spread in energy of fine structure levels [4] than for the Schrödinger solutions. In fact this corresponds to a slightly bigger $|TE|$ and thus implies a slightly smaller $|BE|$. Moreover we think this energy shift is much more appreciable at the deep level.

3.2.2. *Some particularities of the DDL solutions*

In considering the approximate expression, $E_D \sim mc^2\alpha/2|k|$ for the total DDL energy deduced from the special condition $n' = k$, we can see that E_D decreases when k increases. Since the total quantum number is defined by $n = n' + |k|$, and $k > 0$, we can write $E_D \sim mc^2\alpha/n$. Thus when n increases, the binding energy $mc^2[1 - \alpha/n]$ increases. So, the variation of the binding energy as a function of the principal quantum number n is the *inverse* of the case for the regular solutions. This fact raises a question: what is the variation of the mean orbit radius as a function of the quantum number n (or k)? It seems this question has never been mentioned, much less addressed. We think the most logical answer, based on the results of [14], should be the following: when n increases, the binding energy increases. That is possible only if the electron moves nearer to the nucleus, so the mean orbit radius decreases. A coarse computation seems to lead to the same hypothesis and a remark in ([2], p.61), the next paper of the authors cited here, corroborates this hypothesis. Under these conditions, we assume that the mean radius corresponds to a charge-accumulation area in orbitals close-about the charge volume of the nucleus. Of course, only a computation based on the variations of the quantum electron density could determine the correct result. This can be the object of a further paper.

Another question leading to further study is: how to physically interpret the fact that DDL orbits appear only when the quantum number n' and k are equal?

3.3. The other energy values provided by the algebraic Expression E

Now we look at the energy values that do not define DDL orbits. To simplify, we consider $k > 0$.

3.3.1. *Negative energies and masses*

Maly and Va'vra [14] indicate that some results in the tables (see also Appendix A. 8) cannot be observed as energy levels in atoms with electrons, because they correspond to "negative energy" states. This situation happens with $k > n'$ for the Dirac case, and for $l > n'$ for the Schrödinger case. We can easily deduce this condition from the expression of E.

Consider only the Dirac case and the process used to obtain the energy expression, as indicated in Appendix A.7. By the end of the process, we have the relation (A.21):

$$2\beta(s + n') = \gamma(\beta_1 - \beta_2) = \frac{2E\gamma}{\hbar c}, \quad \text{where } \beta > 0 \text{ and } s = -\sqrt{k^2 - \gamma^2} = -\sqrt{k^2 - \alpha^2},$$

since here (H atom) we have $Z = 1$. Therefore

$$\sqrt{(k^2-\alpha^2)} = k\sqrt{\left(1-\frac{\alpha^2}{k^2}\right)} \text{ and as } \alpha^2 \ll 1, \quad k\sqrt{\left(1-\frac{\alpha^2}{k^2}\right)} \sim k\left(1-\frac{\alpha^2}{2k^2}\right), \text{ thus } s+n' \sim n'-k+\left(\frac{\alpha^2}{2k}\right).$$

From (A.21), we can see that E has the sign of the expression $s + n'$. If $k > n'$, then $s + n' \leq -1 + (\alpha^2/2k)$, and as the additive term at right is $\ll 1$, we have effectively $E < 0$. There is a similar verification for the similar relativistic-Schrödinger case.

3.3.2. *Pseudo-regular energy levels*

Here again, we consider only the Dirac case, the Schrödinger case being similar. We can show that, for any couple (n', k) such that $k \leq n'$ and $n' \neq k$, E is not a DDL energy. E is almost equal to the energy of a *regular level* corresponding to the principal quantum number $N = n' - k$. Moreover, for any N given, there is only a very slight value shift that depends on the chosen couple (n', k) verifying $n' - k = N$. This can be observed on the values displayed on the tables of [14]. More precisely, we consider the denominator D of the fraction inside the expression $E(n', k)$. By using the same approximation as above in Section 3.3.1, we can write

$$D = \left[n' - \sqrt{(k^2-\alpha^2)}\right]^2 \sim \left[n' - k + \left(\frac{\alpha^2}{2k}\right)\right]^2.$$

If we consider the expression $E_{\mathrm{R}}(n'_{\mathrm{R}}, k_{\mathrm{R}})$ *of a "regular" solution, its inside denominator* D_{R} *is very similar to D, with only a changing of sign, i.e.*

$$D_{\mathrm{R}} = \left[n'_{\mathrm{R}} + \sqrt{(k_{\mathrm{R}}^2-\alpha^2)}\right]^2 \sim \left[n'_{\mathrm{R}} + k_{\mathrm{R}} - \left(\frac{\alpha^2}{2k_{\mathrm{R}}}\right)\right]^2.$$

Now we can see that the value of the energy level $E(n', k)$ is very near any regular level with principal quantum number $N = n'_{\mathrm{R}} + k_{\mathrm{R}} = n' - k$.

Moreover, on account of the term $\alpha^2/2k$ inside D, we can see that for the same value of $N = n' - k$, when k increases then $|E(n', k)|$ decreases and thus the corresponding binding energy $|BE'(N, k)|$ increases. But the variation of E as function of the principal quantum number $N = n' - k$ follows the classical behavior of the regular solutions, i.e. when N increases, then the total energy $E(N, k)$ increases and the shifts induced by k are very small in comparison with the "principal" variation with N. Under these conditions, we can think the mean orbit radius increases with N, as for the "standard" regular solutions. Nevertheless, a question remains: the wavefunctions of the solutions $E(n', k)$ being determined from a parameter s of negative sign, are not the same as the ones of the "normal" regular solutions, especially near the origin. So, we have yet to physically interpret the existence of these *pseudo-regular* solutions of the Dirac equation. This question could be another object of further study.

3.4. The deep orbits obtained by considering a corrected potential near the nucleus

3.4.1. *DDL orbits with a finite potential inside the nucleus*

After their work [14], where the authors defined the DDLs, they continued their study with a second paper [2] where, in particular, they estimate the size of the DDL atoms. For doing this, they start with another method ([15],Vol. II, p.195) for the Dirac equation solution. This method, using similar ansätze, transforms the system of coupled first order differential equations on the radial functions into a second order differential equation, a Kummer's equation. The general solutions of this equation take the form of confluent hyper-geometrical series, requiring suitable convergence

conditions. Of course, there is always the same "crossroad" parameter s that determines the DDL solutions when $s < 0$. In order to make accurate calculations of the size of the DDL atoms, the authors consider that the nucleus has finite dimension, taking into account a finite specific potential inside the nucleus, and they look for the wavefunctions inside the nucleus. For doing this, they choose a potential derived (by adding a constant) from the Smith–Johnson potential, corresponding to a uniformly distributed spherical charge:

$$V(r) = -\left[\frac{3}{2} - \frac{1}{2}\left(\frac{r^2}{R_0^2}\right)\right]\frac{Ze^2}{R_0}. \tag{4}$$

The radial equations with this potential are solved with a couple of functions g_i and f_i in the following form: $g_i = Ar^{\mathrm{Si}-1}G_2(r)$, $f_i = iBr^{\mathrm{Si}-1}F_2(r)$, where $F_2(r)$ and $G_2(r)$ have the form of power series

$$G_2 = a_1 r + a_2 r^2 + \cdots \qquad \text{and} \qquad F_2 = b_1 r + b_2 r^2 + \cdots$$

Recurrent formulas lead to some coefficients. For example, for $k > 0$, k being the Dirac angular quantum number, one has $b_1 \neq 0$, $Si = k - 1 \geq 0$, $a_l = 0$. Only the terms of degrees $n \leq 5$ are kept in G_2 and F_2. Then they show that it is possible to numerically normalize and to "connect" both solutions (outside and inside the nucleus) at a conventional value R_0 of the nucleus, not indicated in the paper.

Now, if we considerer a solution (g_i, f_i) "inside the nucleus", the term of minimal degree of the polynomial g_i is k and the one of f_i is $k-1$. So, in the formula used to verify the *orthogonality criterion* (Section 2.3), $\left(f_k^* g_{k1} - f_{k1} g_k^*\right) \to 0$ when $r \to 0$, the expression to be considered is a polynomial P having a term of minimal degree $2k - 1$ and thus, for any $k > 0$, P does not contain a constant term. We can deduce that *the corresponding global solution satisfies the orthogonality condition*. Next, if we look at the boundary condition, expressed by $g_i \to 0$ and $f_i \to 0$ when $r \to 0$, we can see this property is verified for any $k > 1$.

From the couple of radial functions f and g found outside the nucleus, Maly and Va'vra [2] compute the electron density (*Eld*) outside the nucleus by the formula $Eld = 4\pi r^2\left(|f|^2 + |g|^2\right)$ and they deduce the mean orbit radius

$$\langle r \rangle = A_0 \int_0^{+\infty} r\, Eld \, \mathrm{d}r,$$

where A_0 is a normalization constant. They plot curves of *Eld* for various atoms, for regular and for DDL orbits. In particular, in their reference to ([2], p.63, Fig. 2), they give the curves of *Eld* for DDL orbits corresponding to the quantum number $k = +1$ for H and Li (as hydrogen-like) atoms.

For H, the energy level is ~ -509.1 keV, while for Li (with one electron on DDL) it is ~ -505.4 keV. The authors say that the peak of *Eld* corresponds to the radius of the nucleus, that seems rather logical. By looking at the curve, we can see that the peak occurs for $r \sim 1.3$ fm. After this, the authors propose mechanisms of atomic transitions to the DDLs and they suggest chemical behaviors of the DDL atoms that, in fact, could behave almost as neutral particles. This would explain the difficulty in detecting them. Finally they report experimental results such as calorimetry and radiation detection. This is beyond of the scope of our present paper.

3.4.2. *Techniques used when considering a finite potential inside the nucleus and criticism*

When considering a finite potential inside the nucleus, there are three stages for finding the solution. First the solution is computed outside the nucleus, i.e. for the Coulomb potential, but with considering the radius $r > R_0$, where R_0 is near the "charge radius" of the nucleus. For example, if we consider only the hydrogen atom, the charge radius is ~ 0.87 fm, and in [16] R_0 is computed for a nucleus of mass number A by means of the empirical formula $R_0 = r_0 A^{1/3}$ where $r_0 = 1.2$ fm.

Next, the solution is computed inside the nucleus, with a chosen potential what is an approximation physically suitable for the problem. For example, one can use, as in [16,2], the Smith–Johnson potential, or simply a constant potential, or more complex ones.

Finally, let $g_i(r)$ be the inside solution and $g_o(r)$ be the outside one, both have to be correctly "connected" at $r = R_0$. More precisely, if the initial equation(s) is (are) of differential order 2 as the Schrödinger equation, we have to satisfy the continuity condition for the functions $g_i(R_0) = g_o(R_0)$, and also for their first order derivative, i.e. $g'_i(R_0) = g'_o(R_0)$. In fact both conditions can be combined into a "matching" equation of the form $g'_i(R_0)/g_i(R_0) = g'_o(R_0)/g_o(R_0)$. But for a first-order differential equation such as the Dirac equation that leads to a combined system of two first order equations on two radial functions $f(r)$ and $g(r)$, we have only to satisfy the continuity condition. However, this involves four functions, i.e. $g_i(R_0) = g_o(R_0)$ and $f_i(R_0) = f_o(R_0)$ that can be combined into a simple matching condition $g_i(R_0)/f_i(R_0) = g_o(R_0)/f_o(R_0)$. Of course, the normalization of the whole wavefunctions defined for $r \in [0, +\infty)$ has to be carried out after matching.

Some purist criticisms concern the fact that, for some chosen nuclear potential inside, the whole potential $V(r)$ as a function on $[0, +\infty)$ cannot have a defined derivative at $r = R_0$ but has different left- and right-derivatives. That could entail a problem for the wavefunction at $r= R_0$. Nevertheless, we can suppose that the wavefunction is in fact defined with an infinitesimal smoothing centered at R_0. This introduces a negligible perturbation, but restores the derivative at R_0.

An interesting criticism is found in [16] where the Dirac "anomalous" solution is not rejected, but is in a way combined with the regular one in a linear combination with coefficients to be computed to satisfy the continuity conditions at the matching radius. It seems from the result, that the anomalous solution is involved with a very small ratio, as a little perturbation. We observe that the authors use a solution method based on transforming the coupled Dirac radial equations into a Whittaker's differential equation. This method and the similar one using Kummer's equation (see Refs. cited in Appendix A.7), although rather technical, are often used since they correspond to a "standard" process leading to the solutions. These are confluent hypergeometric series (Appendix A.7) as factors of the same exponential functions corresponding to the ansätze taken in the solution indicated in Appendix A.7, in particular the function ρ^s. Of course, with the finite size of the nucleus, there is no longer any divergence at $\rho = 0$ for this exponential. Nevertheless, if considering both the regular and the anomalous solutions at the same time, a complication appears for the convergence of the series when $\rho \to +\infty$: the convergence condition depends on the sign of the crossroad parameter s. To resolve this difficulty, the authors have to combine both kinds of series in order for the divergences be exactly balanced, when using asymptotic forms of the series. We have to note that the computed coefficients contain the energy parameter E, because of the initial dimensionless transformation of the Dirac radial equations. With these conditions, the authors have to unify the parameter E when they verify the continuity conditions at $r = R_0$. This leads [19, p.2180] to an equation with a single unknown E (in fact they use a dimensionless unknown $E' = E/mc^2$). Here we can see that, if using the solution method proposed in [4] or in [21], then the convergence of the series involved by the ansätze is independent of the crossroad parameter s and that greatly simplifies the problem.

The criticism of the authors [16], about the method used in [2], concerns the lack of dependence on the potential inside the nucleus and on the boundary conditions at the nuclear radius. We can understand this criticism insofar as the method of the authors has for a goal to increase the precision of the atomic electron energy levels values. In fact, matching in a simple way the wavefunction outside the nucleus with a solution inside the nucleus is an approximation that only allows removal of the singularity of the wavefunction at the origin. We think that the form of the nuclear potential can have a significant effect on the energy levels, particularly for deep orbits near the nucleus. So, in order to improve the precision of the DDL levels, we suggest the following method: to start from a corrected global potential built by connecting in a smooth way the Coulomb potential outside the nucleus with a chosen nuclear potential [17], then to numerically solve the radial equations with this global potential and to compute the corresponding DDL energies. This could be the object of further work.

Note finally a method indicated in [9,18], which allows one to "regularize" the Coulomb potential without the arbitrariness of the cut-off near the nucleus (in particular with the choice of a radius R_0). This method consists of taking into account the "anomalous" magnetic moment of the electron in the unmodified Coulomb potential, and it can be generalized to other potentials with singularity at the origin. The author shows that, doing this, the modified radial Dirac operator written in matrix form has an additional term not diagonal $\mu_a \frac{\alpha}{r^2}$ in natural units, where $\mu_a = 0.00058$ determines the anomalous magnetic moment of the electron. This matrix of the modified radial Dirac operator is the following:

$$D_r = \begin{pmatrix} mc^2 + V(r) & \hbar c \left(-\frac{\mathrm{d}}{\mathrm{d}r} + \frac{k}{r}\right) - \mu_a V'(r) \\ \hbar c \left(\frac{\mathrm{d}}{\mathrm{d}r} + \frac{k}{r}\right) - \mu_a V'(r) & -mc^2 + V(r) \end{pmatrix}. \tag{5}$$

We cite the author: " this term acts as a repulsive interaction that forces the wavefunction away from the singularity ". In fact, the factor is extremely small, but it becomes dominant against the attractive diagonal Coulomb term α/r for an electron near the origin. Here, the term "regularize" means that the modified Dirac operator has all the "good" properties for providing counter arguments to the criticism analyzed in Sections 2.1–2.3 and also to the criticism of [16].

4. Conclusion, Open Questions, and Future Work

In the first part of this paper, we discussed the principal arguments against the deep orbits (DDL) for H atom and we showed how it is possible to resolve the questions raised. Next we analyzed the computational results of [2,14] that produced an infinite set of the anomalous solutions, usually rejected, of the relativistic Schrödinger equation and the Dirac equations. We observed that only a subset of these solutions, but an infinite one, corresponds to deep orbits: the ones satisfying the equality between the quantum numbers that determine the values of energy levels, i.e. the radial number n' and the angular number (l for the Schrödinger equation and k for the Dirac equation). We saw that the electron binding energy on these DDL orbits, of order 509–511 keV, increases when the angular quantum number (or the radial number, since it has the same value) increases. This result seems to indicate that the mean radius of the DDL orbits decreases when n' increases. Though it is not explicitly said by the authors, some remarks in their second paper clearly corroborates this hypothesis, and it seems there is an accumulation zone of the orbits in the neighborhood of the nucleus, near a radius of order 1 fm. Of course only a precise quantum computation of the mean radius as function of n' could confirm this hypothesis.

We also noted that another infinite subset of solutions, what we call "pseudo-regular" energy levels, give energy values very near the regular atomic-electron levels, while the corresponding wavefunctions are not the ones of the regular solutions. This result and the previous one about the quantum numbers, raise questions about their possible physical interpretation. Moreover, we think that the situation of the DDL orbits in an extreme field implies a big strengthening of the several "special" known effects that affect the regular orbits, such as the spin-orbit and spin-spin interactions, the zitterbewegung, and the Lamb shift. For example, the spin-spin interaction, responsible for the hyperfine structure, and the corresponding quantum number associated could play an important role in the determination of energy shifts. However, the deep levels are also predicted by the relativistic-Schrödinger (Klein–Gordon) equation, which does not include spin effects; therefore, this contribution must be limited to the Dirac equations. While the relativistic-Schrödinger equation does not include spin effects and the predicted 'angular momentum' quantum numbers are for quantities that are two orders-of-magnitude lower than the values associated with the Planck constant, we might suggest that there is a 'hidden' variable within quantum mechanics that may be associated with relativity. Perhaps there are possible new quantum numbers associated with known physical effects, such as relativistic and field-induced precession and nutation of the electron-spin vector.

Finally, from the analysis of the work [2] on the DDL orbits obtained with a corrected potential near the nucleus and the questions raised about these solutions, we think that a more accurate estimation of the DDL orbit energies and radius should result from a numerical "direct" computation of the radial wavefunction with an improved potential from $r = 0$ to ∞. An alternative to this computation could be to take into account the anomalous magnetic moment of the electron with unmodified Coulomb potential, as mentioned just above. These questions will be the object of further work.

Appendix A. Some Important Points about the Dirac Equation

The Dirac equation is certainly a cornerstone of modern physics: reconciling quantum physics and special relativity with success, accounting for spin of particles, and having the historical source of the concept of anti-particle even before their actual discovery. As it is copiously handled in the literature, we only recall some essential features. We use a minimal formalism, so we do not use tensor notation that would require explanations not useful for the subject of this paper. Likewise we do not call for advanced algebraic knowledge, such as the Clifford Algebra [19] often used in this field. Among the documents that we used, we can cite, in a non-exhaustive way: [4,18,20–24].

A.1. Elements of Genesis of the Dirac Equation

In order to obtain a quantum evolution equation of first order time derivative, and as quantization requires to replace the energy by the time derivative, Dirac first linearized the classical relativistic energy–momentum relation. So, $E^2 = \mathbf{p}^2c^2 + m^2c^4$ was replaced by $E = c\boldsymbol{\alpha} \cdot \mathbf{p} + \beta mc^2$, where $\boldsymbol{\alpha}$ denotes a formal vector constituted from three parameters $\alpha_1, \alpha_2, \alpha_3$ and β is a fourth parameter sometimes denoted by α_0. For the quadratic expression of E be fulfilled, α_i and β must verify algebraic relations, in particular $\{\alpha_\mu,\alpha_\nu\} = \alpha_\mu\alpha_\nu + \alpha_\nu\alpha_\mu = 2\delta_{\mu\nu}$ for $\mu, \nu = 0, 1, 2, 3$. One shows that α_i and β must be at least 4×4 matrices and this dimension is sufficient; but several solutions are possible. In standard representation, the *Dirac matrices*, which are Hermitian operators, are defined by:

$$\alpha_i = \begin{pmatrix} \mathbf{0} & \sigma_i \\ \sigma_i & \mathbf{0} \end{pmatrix} \qquad \text{for } i = 1, 2, 3, \text{ and } \quad \beta = \begin{pmatrix} \mathbf{1} & \mathbf{0} \\ \mathbf{0} & -\mathbf{1} \end{pmatrix},$$

where the four components are 2×2 matrices, the σ_i are the Pauli matrices

$$\sigma_1 = \begin{pmatrix} 0 & 1 \\ 1 & 0 \end{pmatrix}, \qquad \sigma_2 = \begin{pmatrix} 0 & -i \\ i & 0 \end{pmatrix}, \qquad \sigma_3 = \begin{pmatrix} 1 & 0 \\ 0 & -1 \end{pmatrix}.$$

Other representations [18,20] can be used, such as the Majorana or the Weyl (or chiral) matrices.

Next, the linear energy equation was quantized into the "free" Dirac equation in usual way:

$$i\hbar\partial_t \boldsymbol{\psi}(t, \mathbf{x}) = \mathbf{H}_0 \boldsymbol{\psi}(t, \mathbf{x}), \tag{A.1}$$

where the free Hamiltonian $\mathbf{H}_0$, representing the energy of a free particle including the rest-mass energy mc^2 (the right side of the linear energy equation), is the following matrix-valued differential expression:

$$\mathbf{H}_0 = -i\hbar c\, \boldsymbol{\alpha} \cdot \nabla + \beta mc^2. \tag{A.2}$$

So, the Dirac equation can be written in the form of the following wave equation:

$$(i\hbar\partial_t + i\hbar c\, \boldsymbol{\alpha} \cdot \nabla - \beta mc^2)\, \boldsymbol{\psi}(t, \mathbf{x}) = 0. \tag{A.3}$$

By multiplying this equation on the left by $\boldsymbol{\psi}^\dagger$ and its Hermitian adjoint equation on the right by $\boldsymbol{\psi}$, then subtracting, one obtain [4] a conservation equation $\partial_t \rho + \nabla.\mathbf{J} = 0$, where $\rho = \boldsymbol{\psi}^\dagger \boldsymbol{\psi}$ and $\mathbf{J} = c\boldsymbol{\psi}^\dagger \boldsymbol{\alpha} \boldsymbol{\psi}$ are real quantities and ρ, being non-negative, can be interpreted as a position density probability. This is due to the fact that the Dirac equation contains only a first order derivative in time.

In order to match the dimension of the Dirac matrices, the wavefunction $\boldsymbol{\psi}$ has to be a vector-valued function having four complex components. It is called a *spinor* as it can describe the state of a particle with spin $1/2$. One usually regroups the four components of $\boldsymbol{\psi}$ into two 2-vectors: $\boldsymbol{\psi}_a$ with components ψ_1, ψ_2 and $\boldsymbol{\psi}_b$ with components ψ_3, ψ_4.

A.2. Free-particle Solution

Solving the Dirac equation for a free particle highlights very particular features of the solutions, leading to a historical prediction, before the actual discovery, about the existence of "anti-particles". The Dirac equation is equivalent to four simultaneous first-order partial differential equations. They are linear and homogeneous in the components of the spinor $\boldsymbol{\psi}$ formed by the two vectors $\boldsymbol{\psi}_a$ and $\boldsymbol{\psi}_b$. It is natural to try solutions in the forms of plane waves, i.e.

$$\boldsymbol{\psi}_j(r,t) = \mathbf{u}_j \mathrm{e}^{i(\mathbf{k}\cdot\mathbf{r}-\omega t)} \qquad \text{for } \; j = a, b,$$

where the $\mathbf{u}_j$ are two vectors of dimension two. These are eigenfunctions of the energy operator $i\hbar\partial_t$ and of the momentum operator $-i\hbar\nabla$, whose respective eigenvalues are $E = \hbar\omega$ and the vector $\mathbf{p} = \hbar\mathbf{k}$. By developing the Dirac equation, we obtain the following coupled linear equations on the vectors $\mathbf{u}_j$

$$(E - mc^2)\mathbf{u}_a - c(\boldsymbol{\sigma}\cdot\mathbf{p})\mathbf{u}_b = 0,$$

$$(E + mc^2)\mathbf{u}_b - c(\boldsymbol{\sigma}\cdot\mathbf{p})\mathbf{u}_a = 0, \tag{A.4}$$

where $\boldsymbol{\sigma}$ denotes the formal vector of the three Pauli matrices and $\boldsymbol{\sigma}\cdot\mathbf{p} = \sigma_1 p_1 + \sigma_2 p_2 + \sigma_3 p_3$. From the coupled equations, we can deduce the relation

$$\mathbf{u}_a = \frac{c^2\mathbf{p}^2}{E^2 - \left(mc^2\right)^2}\mathbf{u}_a, \tag{A.5}$$

thus the values of the energy E and the momentum $\mathbf{p}$ satisfy the relativistic relation $E^2 = \mathbf{p}^2c^2 + m^2c^4$. But for E,we have the choice between the positive square root E_+ and the negative one E_- .

While solving the system of linear equations for the positive energy, we obtain two linear independent solutions by setting a vector ξ with two possibilities

$$\xi_1 = \begin{pmatrix} 1 \\ 0 \end{pmatrix} \quad \text{and} \quad \xi_2 = \begin{pmatrix} 0 \\ 1 \end{pmatrix} .$$

Then, for each value of **p,** we have two positive energy solutions that are orthogonal and can be normalized:

$$\mathbf{u} = N_+ \begin{pmatrix} \xi \\ \\ \frac{c(\boldsymbol{\sigma}\cdot\mathbf{p})}{E_+ + mc^2}\xi \end{pmatrix}, \tag{A.6}$$

where N_+ is a normalizing factor depending on E_+. We follow the same process for the "negative" energy E_- by taking the previous ansatz with the opposite sign for the exponent, i.e. $i(-\mathbf{k}.\mathbf{r} + \omega t)$, and we can obtain two negative

energy solutions, orthogonal and normalized by a similar factor N_-, obtained by replacing E_+ by E_- in N_+:

$$\mathbf{v} = N_- \begin{pmatrix} \frac{c(\boldsymbol{\sigma}\cdot\mathbf{p})}{E_- - mc^2}\xi \\ \\ \xi \end{pmatrix} \tag{A.7}$$

For both solutions **u**, the upper components dominate in the non-relativistic case, i.e. if $|\mathbf{p}| \ll mc$ so one names these components the "great components." For the solutions **v,** it is the opposite situation, i.e. the lower components dominate.

So, the spectrum of the free Dirac operator $\mathbf{H}_0$ is composed of two infinite intervals separated by a gap: $(-\infty - mc^2] \cup [mc^2 + \infty)$. Now the existence of negative energies has to be interpreted. Paul Dirac suggested a "negative-energy sea" filled with electrons, the "Dirac sea", and it would be possible for high-energy photons to promote electrons out of the sea into positive energies where it would be observable; the "hole" left in the sea would be an observable, as a electron but with a positive charge. So he predicted the existence of the positron, the "anti-particle" of the electron, which was discovered later by Carl Anderson [25]. The concept of Dirac sea is no longer used, particularly in the context of the "single particle" interpretation of the Dirac equation, where it entails some difficulties. Instead and as the relativistic context needs to consider states with unspecified number of particles, QFT [5,20] uses Fock spaces with "2^d quantization", i.e. creation/annihilation operators, particles number operator, etc… But one can see a reminiscence of the Dirac sea in the QED concept of "vacuum polarization."

A.3. Covariance of the Dirac Equation, Spin 1/2

As the Dirac equation was built for being compatible with relativistic effects, it has to be invariant under changes of Lorentz frames. First one can give the Dirac equation a more relativistic form, by multiplying the initial Dirac matrices by the matrix β becoming γ_0, and defining $\gamma_i = \beta\alpha_i$ for $i = 1, 2, 3$. To avoid tensor notation, we use as in [18] the formal notation for bilinear form such as $\langle \gamma, x \rangle := c\gamma_0 t - \gamma \cdot \mathbf{x}$ for any four-vector x in Minkowski space. This form gives a 4×4 matrix and $\gamma.\mathbf{x}$ is the formal scalar product of the spatial vector $\mathbf{x}$ with the vector γ of matrix components γ_i for $i = 1, 2, 3$. Doing this, one can write the Dirac equation in a more symmetric form in space-time variables: $(i\hbar c < \gamma,\ \partial > -mc^2)\boldsymbol{\psi} = 0$, where ∂ denotes the four-dimensional gradient operator, i.e. a four-vector of differential operators $\partial_0 = {}^1\!/_c\partial_t,\ \partial_1 = -\partial_x,\ \partial_2 = -\partial_y,\ \ \partial_3 = -\partial_z$. But beyond the notation, the more important point is that the Dirac equation for a free particle is invariant under the proper orthochronous Poincaré transformations of the space-time coordinates and so it is Lorentz-invariant. Note that the group of general Poincaré transformations is extended to translations in space-time.

We only summarize the relativistic invariance for changes of inertial frames. The corresponding transformations are implemented as unitary operators in the Dirac Hilbert space and they have the following general structure: $\boldsymbol{\psi}(x) \rightarrow \boldsymbol{\phi}(x) = \mathrm{M}\boldsymbol{\psi}(\Lambda^{-1}(x-a))$, where Λ is the well-known matrix associated with Lorentz transformations, and M is a linear operator depending on Λ. Here x is a 4-point in Minkowski space, $x = (ct, \mathbf{x})$ and a is associated with a space-time translation. One can show that, when $\boldsymbol{\psi}(x)$ is a solution of the free Dirac equation, $\boldsymbol{\phi}(x)$ is also a solution.

As $(\mathrm{Det}\ \Lambda)^2 = 1$, we can have $\mathrm{Det}(\Lambda) = \pm 1$. A transformation is *proper* when $\mathrm{Det}(\Lambda) = +1$, i.e. it conserves the direction of the three-space axis of the frame. Moreover the "pure temporal" component $\Lambda^0{}_0$ always satisfies $(\Lambda^0{}_0)^2 \geq 1$, but the transformation is *orthochronous* only for $\Lambda^0{}_0 \geq 1$ and, in this case, it conserves the direction of the time axis. For example, the mirror inversion P is improper, but orthochronous, while the time reversal T is also improper, but it is not orthochronous. One can show any proper orthochronous (p.o.) Lorentz transformation is continuously connected to the Identity transformation (which is of course p.o.). This means it can be formed by consecutive infinitesimal transformations starting from the Identity. Moreover, there are two particular classes of p.o. transformations, *boosts*

and *rotations*, and any Lorentz transformation can be written in a unique way as the composition of a boost and a rotation.

Now we note an interesting result justifying the name "spinor": Consider a rotation of angle φ about e.g. the axis of the coordinate x^3. One can show, from the corresponding Lorentz transformation Λ and the operator-associated M, that such a rotation corresponds to application of the matrix

$$\mathbf{M}[\varphi] = \begin{pmatrix} e^{i\varphi\sigma_{3/2}} & \mathbf{0} \\ \mathbf{0} & e^{i\varphi\sigma_{3/2}} \end{pmatrix}$$

to the spinor $\boldsymbol{\psi}$. As $e^{i\varphi\sigma_{3/2}} = I_2\cos(\varphi/2) + \sigma_3 i\sin(\varphi/2)$, a rotation of angle $\varphi = 2\pi$ gives $M[2\pi] = -I_4$ so $\boldsymbol{\psi}$ is transformed into $-\boldsymbol{\psi}$ and we need a rotation of $\varphi = 4\pi$ to obtain the identity transformation. We recognize that a rotation acts on the *spinor* like it does on a particle of *spin* $^1/_2$. So one can see the explanation of spin as a consequence of the union of special relativity and quantum mechanics.

One can find explicit and concise algebraic computations concerning these questions in [20], where the author starts from the matrices γ in the Weyl representation, uses tensor representations and elements of Clifford Algebra [26]. Here is a very elegant tensor form of the free Dirac equation with the matrices γ**:**

$$(i\gamma^\mu\partial_\mu - m)\boldsymbol{\psi} = 0 \quad \text{where } \left(\gamma^0\right)^2 = 1,\ \left(\gamma^i\right)^2 = -1 \text{ for } i \neq 0 \text{ and } \gamma^\mu\gamma^\upsilon = -\gamma^\upsilon\gamma^\mu \quad \text{if } \mu \neq \upsilon.$$

Finally, concerning discrete transformations, we can note that the *CPT* transformation, a combination of the Charge Conjugation, Parity and Time Reversal transformations has for net effect on a free electron wavefunction to convert it into the positron wavefunction. This *CPT* transformation is of a capital importance in Quantum Field Theory [5] because it reverses the up and down two-component spinors in the Dirac wavefunction in the same way as the matrix $\gamma^5 = i\gamma^0\gamma^1\gamma^2\gamma^3$

A.4. The Dirac Equation for an Electron in a Coulomb Central Field. The Spin-orbit Operator K Associated with Spin Precession

We consider an electron subjected to an external electromagnetic field, in the form of the static Coulomb potential generated by a proton. Then the vector potential **A** can be set to 0, and the scalar potential φ is spherically symmetric. So we have to add the potential energy

$$V = -\frac{e^2}{r} = -\alpha\frac{c\hbar}{r}$$

to the free Hamiltonian $\mathbf{H}_0$, to obtain the "total" Hamiltonian $\mathbf{H} = \mathbf{H}_0 + V\mathbf{I}_4$, where $\mathbf{I}_4$ is the 4D identity matrix.

In principle, the orbital angular momentum $\mathbf{L} = \mathbf{x} \times \mathbf{p}$ commutes with any spherically symmetric function, but it is not a constant of motion in the Coulomb central field as it does not commute with **H**. One has to add the operator $\mathbf{S} = \frac{1}{4}\hbar\alpha \times \alpha$ where "×" is the formal cross product applied, and α the formal 3-vector of the Dirac matrices $\alpha_1, \alpha_2, \alpha_3$. Then the total angular moment $\mathbf{J} = \mathbf{L} + \mathbf{S}$ is a constant of motion. **S** is the *spin operator* of the electron. It is a 3-vector of and its components S_i, for i = 1,2,3, are 4 × 4 matrices. In the standard representation we have

$$\mathbf{S}_i = \frac{1}{2}\hbar\begin{pmatrix} \sigma_i & \mathbf{0}_2 \\ \mathbf{0}_2 & \sigma_i \end{pmatrix}.$$

We can see that **S** is a straightforward extension of the usual spin operator $\mathbf{s} = \frac{1}{2}\hbar\sigma$ of the non-relativistic quantum mechanics.

On account of the spherical symmetry of the Coulomb field, one usually uses spherical coordinates to represent the Dirac operator **H** . So, one can show that the spatial term $\boldsymbol{\alpha}\cdot\mathbf{p}$ of $\mathbf{H}_0$ is transformed into

$$\boldsymbol{\alpha}\cdot\mathbf{p}=\frac{1}{r}(\boldsymbol{\alpha}\cdot\mathbf{x})\left(p_r+\frac{i\hbar}{r}\beta\mathrm{K}\right), \tag{A.8}$$

where p_r is the "radial" momentum given by

$$p_r=\frac{1}{r}(\mathbf{x}.\mathbf{p}-i\hbar)=-i\hbar\left(\partial_r+\frac{1}{r}\right) \tag{A.9}$$

and K is the operator defined by the formula

$$\hbar\mathrm{K}=\beta(\boldsymbol{\sigma}'\cdot\mathbf{L}+\hbar),\quad \text{where}\quad \boldsymbol{\sigma}'=\frac{1}{\hbar}2\mathbf{S}=\begin{pmatrix}\sigma & \mathbf{0}_2\\ \mathbf{0}_2 & \sigma\end{pmatrix}. \tag{A.10}$$

Here **x** represents the vector of the Cartesian coordinates and $r=|\mathbf{x}|$ its norm. The second expression of the radial momentum is its formulation as differential operator in spherical coordinates. Moreover, by substituting the expression of $\boldsymbol{\alpha}\cdot\mathbf{p}$ in **H**, the "spherical" Hamiltonian now reads:

$$\mathbf{H}_{\mathrm{sph}}=\frac{i\hbar}{r}(\boldsymbol{\alpha}\cdot\mathbf{X})\left(\partial_r+\frac{1}{r}-\frac{i\hbar}{r}\beta\mathbf{K}\right)+\beta mc^2+V. \tag{A.11}$$

We can see that K is related to the *spin-orbit* term (see Appendix A.5 the relativistic-correction terms).

Moreover one can show that K commutes with the Hamiltonian and it is related to the total angular momentum **J** by the relation $\hbar^2\mathrm{K}^2=\mathbf{J}^2+\frac{1}{4}\hbar^2$. This expression is obtained by starting from the square of the definition of K. As $\mathbf{J}^2$ has eigenvalues $j(j+1)\hbar^2$, where j can take values $1/2, 3/2, 5/2, \ldots$ the Dirac operator defines a *specific quantum number k* for the eigenvalues of the operator K, taking values $\pm1, \pm2, \ldots$ In fact $k=\mp\left(j\pm\frac{1}{2}\right)$, but it cannot be equal to 0 (see the relation on the square of K). If the quantum number l of **L** is j-$1/2$, then the spin (of magnitude $1/2$) and the orbital angular momentum are parallel, else they are anti-parallel. We can say the quantum number k is associated with the spin-orbit interaction. The physical effect of this interaction is the *precession of the electron spin* ([4, p.433,27]).

A.5. The Relativistic Correction Terms Involved by the Dirac Operator. Fine Structure

It is interesting to see what terms are added by the Dirac equation to a non-relativistic Hamiltonian for the electron in a central potential, such as the classical Schrödinger Hamiltonian. For doing this, one can look for a non-relativistic limit of the Dirac equation and then deduce the relativistic perturbations involved in the Dirac operator. This leads first, for the first order correction in v/c, to the 2-components Pauli equation. Next, various and complex methods can be used, such as the Foldy–Wouthyusen transformation [28], to obtain relativistic corrective terms of higher orders in powers of v/c. Supersymmetry techniques can also be used [9,18]. Then one obtains a Hamiltonian **H'** with corrections at order $(v/c)^2$ having the following form:

$$\mathbf{H}'=mc^2+\frac{\mathbf{p}^2}{2m}+V-\frac{\mathbf{p}^4}{8m^3c^2}+\frac{\hbar}{4m^2c^2}\frac{1}{r}\frac{\mathrm{d}V}{\mathrm{d}r}\boldsymbol{\sigma}\cdot\mathbf{L}\ +\frac{\hbar^2}{8m^2c^2}\Delta V. \tag{A.12}$$

- In this expression, we first recognize the rest mass energy added to the non-relativistic Hamiltonian, i.e. the non-relativistic kinetic energy plus the potential energy.
- The next (second) term corresponds to a relativistic kinetic energy correction. It can be obtained by expanding $E-mc^2$, where E is the relativistic energy defined by $E^2=\mathbf{p}^2c^2+m^2c^4$.

– The third term corresponds to the *spin-orbit* energy, interaction energy between the spin $\boldsymbol{\sigma}$ and the orbital movement $\mathbf{L}$ of the electron. One can physically explain this interaction by the fact that, even in a "pure" electrostatic field, the electron moving in this electric field can also "see" a magnetic field. As the electron has a magnetic moment due to its spin, the magnetic field causes a spin precession (Larmor precession), but this would give twice the spin-orbit term. In fact it is half compensated by an extra relativistic effect on the accelerated frame of the electron, causing an additional spin precession with opposite sign, the *Thomas precession* (for a simple derivation, see [29]). We note that the electron is assumed to be slightly relativistic, so the angular velocity ω_{T} of the Thomas precession is computed by making a first-order approximation to the coefficient $\gamma = \frac{1}{\sqrt{(1-\beta^2)}} \approx 1 + \frac{1}{2}\beta^2$. Then one usually takes for a velocity v, $\omega_{\mathrm{T}} \approx (1/2c^2)\,\dot{\mathbf{V}} \times \mathbf{V}$, while Larmor precession is $\omega_{\mathrm{L}} = -(1/c^2)\,\dot{\mathbf{V}} \times \mathbf{V} = -2\omega_{\mathrm{T}}$.
– Finally the fourth term, called *Darwin term*, is another relativistic correction, but it does not involve angular momentum. This term begins at the non-relativistic limit where the electron is not like a point charge but as a distribution of charge and current in a domain of linear dimension $\hbar/mc$. Physically, it is generally related to the *Zitterbewegung*, a rapid quantum oscillations of the electron blurring the electrostatic interaction with the nucleus and affecting only the s-orbits. Moreover, there is an apparent paradox concerning the spectrum of the standard velocity operator for the position operator, which would consist of $\pm c$. This paradox can be removed by projecting the velocity operator to the particle and the anti-particle sub-spaces of the Hilbert space of the Dirac operator (see e.g. [30]). Quantum Electrodynamics can interpret the Zitterbewegung as quantum fluctuations that allow the creation of particle-antiparticle pairs yielding perturbations of the electric potential [24]. Sometimes one considers it is caused by interference between positive- and negative-energy components [18,31]. Nevertheless, there are also alternative explanations, such as in [32].

Note that the relativistic corrective terms provide an explanation to the physical observation of the fine structure of the Hydrogen and alkali atoms [33]. In fact these effects are not all additive, so the global spin-orbit interaction lowers the effect of the relativistic kinetic energy correction and improves the precision of the corresponding energy w.r.t. measured values. That is an improvement in comparison with the Klein–Gordon equation, which includes also a term of relativistic mass correction and even a Zitterbewegung effect, but no spin-orbit interaction. Nevertheless, the Dirac equation does not account for still subtler spectroscopic observations. It is the case for the hyperfine structure, due to (nucleus) spin-(electron) spin interaction not included in the Dirac Hamiltonian, because the proton is represented only by its Coulomb potential. And also for the Lamb shift, explained in principle by QED effects such as self-energy and vacuum polarization.

Finally, we note that the transformations leading to **H'** are usually done under the hypothesis $E - mc^2 \ll mc^2$ and $|V| \ll mc^2$, what is the case for atomic electrons of hydrogen. However, if the electron is at small distances from the nucleus, therefore in *a very strong electric field* (e.g. for heavy atoms with Z near $1/\alpha$ or for electrons in deep Dirac levels), one should take into account an additional non-linear attractive term of the form $-V^2/2mc^2$ [4,34,35].

A.6. Separation of the Radial Equation

As we consider the case of an electron in a Coulomb central potential, we first use the fact that the potential is time-invariant. So we can separate the time factor from the wavefunction and write $\boldsymbol{\psi}\,[E, \mathbf{x}, t] = \boldsymbol{\psi}\,(E, \mathbf{x})\,\mathrm{e}^{(-iEt/\hbar)}$, where we explicitly indicate that the eigenfunction $\boldsymbol{\psi}$ does depend on an eigenvalue E of the Hamiltonian $\mathbf{H}$. This leads to the stationary equation $\mathbf{H}\boldsymbol{\psi}\,(E, \mathbf{x}) = E\boldsymbol{\psi}\,(E, \mathbf{x})$. Here, $\mathbf{x}$ represents the vector of the Cartesian spatial coordinates.

Next, the stationary equation can be separated in spherical coordinates in a similar, but more complex, manner than in the case of the Schrödinger equation for at least two reasons: in the Dirac theory, the wavefunctions are 4-D, and the

angular momenta are "interlaced" in the four components of the spinors. Here we give only an outline of the required process, which is rather technical and cumbersome. So, in (Appendix A.4) the separation was prepared by defining the radial momentum and the operator K. The following transformed Hamiltonian has been obtained:

$$\mathbf{H}_{\text{sph}} = \frac{i\hbar}{r}(\boldsymbol{\alpha}\cdot\mathbf{x})\left(\partial_r + \frac{1}{r} - \frac{i\hbar}{r}\beta\mathrm{K}\right) + \beta mc^2 + V. \tag{A.13}$$

As in the classical example of the Schrödinger equation, the separation needs two stages:

(a) first, solve the problem of eigenvalues of the angular operators involved in the equation;

(b) next, look for eigenfunction solutions (of the first problem) satisfying the equation.

(a) One may consider the "usual" angular operators J^2, J_z and the new operator K acting only on the angular coordinates, so the eigenvalue problem is independent of r. Moreover, they commute between them. So there is a system of common orthogonal eigenvectors belonging to the Hilbert space $L^2(S^2)^4$ of the square integrable functions on the sphere S^2, for the operators J^2, J_z and K, with respective associated discrete eigenvalues. This allows one to define couples of 2-D spherical spinors $\boldsymbol{\omega}(\theta, \phi)$ similar to the couples of half-spinors defined at the end of (Appendix A.1) and each can be expressed by means of the classical spherical harmonics, which are eigenfunctions of L^2, L_z, considered as functions of the spherical angles θ and φ. The 2-D spinors $\boldsymbol{\omega}(\theta, \varphi)$ provide eigenfunctions of K, the only angular operator occurring in the spherical Hamiltonian $\mathbf{H}_{\text{sph}}$, with associated eigenvalue k.

(b) Now one considers such "angular" eigenfunctions $\boldsymbol{\omega}(\theta,\varphi)$ to form the eigenfunctions $\boldsymbol{\psi}$ common to $\mathbf{H}_{\text{sph}}$ and K.

A wavefunction $\boldsymbol{\psi}$ solution of the Dirac equation can be expressed by a 2-D vector of two 2-D wavefunctions $\boldsymbol{\psi}_1$, $\boldsymbol{\psi}_2$ of the form $\mathrm{X}(r)\,\boldsymbol{\omega}(\theta, \varphi)$, where $\mathrm{X}(r)$ is a scalar function. Here we do not write the quantum numbers in indices (usually k, m or $k, j\pm1/2$). While substituting into the eigenvalue radial equation derived from $\mathbf{H}_{\text{sph}}\boldsymbol{\psi}(E,\mathbf{x}) = E\boldsymbol{\psi}(E,\mathbf{x})$, the operator K is replaced by its eigenvalue represented by k. We note that, while decomposing the Hamiltonian into two halves, some simplifications arise: $\boldsymbol{\alpha}.\mathbf{x}$ applied to the 2-D vector

$$\boldsymbol{\psi} = \begin{pmatrix} \boldsymbol{\psi}_1 \\ \boldsymbol{\psi}_2 \end{pmatrix}$$

is reduced to $\boldsymbol{\sigma}' \cdot \mathbf{x}$ applied to

$$\begin{pmatrix} \boldsymbol{\psi}_2 \\ \boldsymbol{\psi}_1 \end{pmatrix} \quad \text{that gives} \quad \begin{pmatrix} (\boldsymbol{\sigma}\cdot\mathbf{x})\boldsymbol{\psi}_2 \\ (\boldsymbol{\sigma}\cdot\mathbf{x}.)\boldsymbol{\psi}_1 \end{pmatrix}.$$

Next the pseudo-vector nature of $\boldsymbol{\sigma} \cdot \mathbf{x}$ allows us to simplify its application on the spherical spinors, as application of a constant matrix.

A very explicit and detailed process of separation of the radial equation can be found in [21]. From here, and also in the next section (Appendix A.7), we follow the procedure indicated in [4] to obtain and to solve the system of radial equations, because it is technically simple and we can easily see what is done. The radial part $\mathrm{X}(r)$ of the wavefunction $\boldsymbol{\psi}(\mathbf{x})$ solution of the Dirac equation, has two components $F(r)/r$, $G(r)/r$ depending on the radius r and associated with a couple of spherical spinors. Finally, one obtains a system of coupled first order differential equations on the radial functions $F$and G, valid for any electric central potential with spherical symmetry.

$$\left(E - mc^2 - V\right)F + \hbar c\frac{\mathrm{d}G}{\mathrm{d}r} + \frac{\hbar ck}{r}G = 0,$$

$$\left(E + mc^2 - V\right) G - \hbar c \frac{\mathrm{d}F}{\mathrm{d}r} + \frac{\hbar c k}{r} F = 0. \tag{A.14}$$

Because of the definition of $\boldsymbol{\psi}(\mathbf{x})$ in term of the functions F and G, the required normalization condition on $\boldsymbol{\psi}(\mathbf{x})$ is equivalent to the condition

$$\int_{R+} \left(F^2 + G^2\right) \mathrm{d}r = 1.$$

Different processing of the spherical spinors leads to a different, but very similar, system of coupled equations. In fact, one always recognizes all the same terms, such as $(E - mc^2 - V)$, $(E + mc^2 - V)$, the derivatives of the radial functions, kG/r, etc…, but the signs of the coefficients can change.

A.7. Equation Solution

When considering a Coulomb potential and hydrogen-like atoms, the Coulomb potential energy is equal to $V(r) = -Ze^2/r$ and, in this case, analytical solutions can be obtained. As usual, one defines some parameters that allow the introduction of a dimensionless radius variable and pure numerical equations (we use identifiers different from those in [4] to avoid confusion with the matrices α_i and the coupling constant α):

$$\beta_1 = \frac{mc^2 + E}{\hbar c}, \qquad \beta_2 = \frac{mc^2 - E}{\hbar c}, \qquad \beta = \sqrt{\beta_1 \beta_2}, \qquad \rho = \beta r, \quad \gamma = \frac{Ze^2}{\hbar c}. \tag{A.15}$$

An ansatz is defined in two stages:

(1) First one sets $F(\rho) = f(\rho)\mathrm{e}^{-\rho}$, $G(\rho) = g(\rho)\mathrm{e}^{-\rho}$. Then the equations become

$$g' - g + k\frac{g}{\rho} - \left(\frac{\beta_2}{\beta} - \frac{\gamma}{\rho}\right) f = 0, \tag{A.16a}$$

$$f' - f - k\frac{f}{\rho} - \left(\frac{\beta_1}{\beta} + \frac{\gamma}{\rho}\right) g = 0. \tag{A.16b}$$

(2) Next one looks for solutions in the form of power series, where a_n is the coefficient of the term containing ρ^n:

$$f = \rho^s \left(a_0 + a_1\rho + \cdots\right), \qquad g = \rho^s \left(b_0 + b_1\rho + \cdots\right)$$

with a_0 and $b_0 \neq 0$. While substituting f and g into the coupled equations and after equating the coefficients of ρ^{s+n-1}, one obtains two crossed recurrence relations between the coefficients of the series.

$$(s + n + k)\, b_n - b_{n-1} + \gamma a_n - \frac{\beta_2}{\beta} a_{n-1} = 0, \qquad (s + n - k)\, a_n - a_{n-1} - \gamma b_n - \frac{\beta_1}{\beta} b_{n-1} = 0. \tag{A.17}$$

In particular, the relations between a_0 and b_0 are the following, for $n = 0$

$$(s + k)\, b_0 + \gamma a_0 = 0, \qquad (s - k)\, b_0 - \gamma a_0 = 0. \tag{A.18}$$

As the determinant of this linear equation system has to be 0, this gives the following condition on s

$$s = \pm\sqrt{\left(k^2 - \gamma^2\right)}. \tag{A.19}$$

Here the choice of the sign plus determines the "regular" solutions, whereas the minus sign leads to the "anomalous" solutions, which are usually rejected. One can obtain a relation between a_n and b_n for any $n > 0$ by multiplying the first of equations (A.18) by β and the second by β_2

$$b_n \left[\beta\,(s+n+k)+\beta_2\gamma\right] = a_n \left[\beta_2\,(s+n-k)-\beta\gamma\right]. \tag{A.20}$$

One can deduce by simple manipulations from relations (A.18), that both series f and g diverge unless, for some integer n', the coefficients a_n and b_n vanish for all $n > n'$.

In these conditions, both equations of (A.18) give the same relation between $a_{n'}$ and $b_{n'}$, i.e. $\beta_2 a_{n'} = -\beta b_{n'}$. Next, by using relation (A.19) and the definitions of the parameters β, $\beta_1$andβ_2, we obtain the relation

$$2\beta(s+n') = \gamma(\beta_1-\beta_2) = \frac{2E\gamma}{\hbar c}, \tag{A.21}$$

where we can remark that the energy E has the sign of the term $(s+n')$. Thus, for $s = +\sqrt{(k^2-\gamma^2)}$ we have $E > 0$, but if taking $s = -\sqrt{\left(k^2-\gamma^2\right)}$, then $E > 0$ iff $n' > \sqrt{\left(k^2-\gamma^2\right)}$.

From the previous relation, one can obtain the following expression of the energy as functions of the quantum numbers k and n':

$$E = mc^2\left[1+\frac{\alpha^2}{\left(n'\pm\sqrt{\left(k^2-Z^2\alpha^2\right)}\right)^2}\right]^{-1/2}. \tag{A.22}$$

The number n' is the "radial" quantum number and the number $n = n' + |k|$ is the total quantum number. The specific Dirac quantum number k, related to the total angular momentum and corresponding to the physical effect of the spin precession is an important element.

Usually, the regular solutions for the energy level are obtained by taking the positive root for the parameter s in the expression of E, i.e. taking the positive sign between n' and the square root. The choice of $s > 0$ is made for satisfying the boundary conditions at the origin for F and G, $F(0) = G(0) = 0$.

There exist other methods of processing of the initial system of first-order differential equations to obtain the expression of the energy levels E. For example, eliminating one of the two functions of this initial system can lead to a second- order differential equation on the remaining function, such as a Kummer's equation [36]. The solution of this equation is a confluent hypergeometric series ${}_1F_1$, the coefficients of which are determined to obtain their convergence by reducing them to polynomials ([37], p.7). This method is similar to the one used to solve the Schrödinger equation for the H atom. Other methods can lead to a Whittaker's equation [12,38], a modified form of confluent hypergeometric equations [13].

A.8. Evaluated Equation Solution

A computer program was written by Maly and Va'vra [14] that calculates atomic energy levels for Relativistic Schrodinger levels E1S(+), E2S(−) in Table 1, Dirac levels ED1(+) and ED2(−) in Table 2, and the non-relativistic Schrodinger levels $E(N, Z)$ given by a simple Bohr formula. (Tables from [14] are reprinted here with permission. Copyright November 1993 by the American Nuclear Society, La Grange Park, IL.) Note the lack of a 1s level in the deep levels of Table 2.

Table 1. Relativistic Schroedinger levels for H ($Z = 1$) in eV

	$E(N, Z)$	N	N	L	E1S	E2S
1s	−13.605826	1	0	0	−13.606597	−507171.937500
2p	−3.501457	2	0	1	−3.401449	−13.605632
2s	−3.401457	2	1	0	−3.401570	−13.603699
3d	−1.511759	3	0	2	−1.511747	−3.401425
3p	−1.511759	3	1	1	−1.511755	−509755.250000
3s	−1.511759	3	2	0	−1.511790	−3.401207
4f	−1.511764	4	0	3	−0.850357	−1.511744
4d	−0.850364	4	1	2	−0.850358	−13.605434
4p	−0.850364	4	2	1	−0.850361	−13.604666
4s	−0.850364	4	3	0	−0.850376	−1.511683
5g	−0.850364	5	0	4	−0.544228	−0.850356
5f	−0.544233	5	1	3	−0.544228	−3.401415
5d	−0.544233	5	2	2	−0.544229	−510264.468750
5p	−0.544233	5	3	1	−0.544231	−3.401328
5s	−0.544233	5	4	0	−0.544238	−0.850331
6h	−0.544233	6	0	5	−0.377936	−0.544228
6g	−0.377940	6	1	4	−0.377936	−1.511743
6f	−0.377940	6	2	3	−0.377936	−13.605356
6d	−0.377940	6	3	2	−0.377937	−13.604863
6p	−0.377940	6	4	1	−0.377938	−1.511719
6s	−0.377940	6	5	0	−0.377942	−0.544215

Table 2. Dirac levels of hydrogen-like atoms for H ($Z = 1$) in eV.

	$E(N, Z)$	N	M	K	L1	E1D	L2	E2D	
1s	−13.605826	1	0	1	0	−13.605873	1	−13.605873	*
2p	−3.401457	2	0	2	1	−3.401434	2	−3.401434	*
2s	−3.401457	2	1	1	0	−3.401479	1	−509133.375000	
3d	−1.511759	3	0	3	2	−1.511746	3	−1.511746	*
3p	−1.511759	3	1	2	1	−1.511750	2	−13.605512	*
3s	−0.850364	3	2	1	0	−1.711764	1	−13.604422	
4f	−0.850364	4	0	4	3	−0.850356	4	−0.850356	*
4d	−0.850364	4	1	3	2	−0.850357	3	−3.401419	*
4p	−0.850364	4	2	2	1	−0.850359	2	−510064.125000	
4s	−0.850364	4	3	1	0	−0.850365	1	−3.401298	
5g	−0.544233	5	0	5	4	−0.544228	5	−0.544228	*
5f	−0.544233	5	1	4	3	−0.544228	4	−1.511744	*
5d	−0.544233	5	2	3	2	−0.544229	3	−13.605389	*
5p	−0.544233	5	3	2	1	−0.544230	2	−13.604785	
5s	−0.544233	5	4	1	0	−0.544233	1	−1.511710	
6h	−0.377940	6	0	6	5	−0.377936	6	−0.377936	*
6g	−0.377940	6	1	5	4	−0.377936	5	−0.850356	*
6f	−0.377940	6	2	4	3	−0.377936	4	−3.401412	*
6d	−0.377940	6	3	3	2	−0.377937	3	−510381.343750	
6p	−0.377940	6	4	2	1	−0.377937	2	−3.401344	
6s	−0.377940	6	5	1	0	−0.377939	1	−0.850342	

*Negative energy states, not observable.

Acknowledgement

This work is supported in part by HiPi Consulting, New Market, MD, USA; by the Science for Humanity Trust, Bangalore, India; and by the Science for Humanity Trust Inc., Tucker, GA, USA. The authors would like to thank Prof.

Jan Naudts for his useful comments on the manuscript.

Note Added in Review

The authors wish to thank the reviewer for bringing the topic of Nuclear Collapse [34,35] to our attention. While we had not considered the deep-electron *atomic* orbitals of heavy atoms to be part of our deep-electron story, a quick review of the suggested references indicates both experimental evidence and a theoretical basis for confirming the existence of deep-electron orbits beneath those of the atomic orbitals. The references suggest a desired alternative means of populating the deep-Dirac levels (DDLs), since direct population via photo-emission is so highly forbidden. Furthermore, the relativistic DDL electrons provide an alternative to, or basis for, the reference-proposed dense-electron plasma for initiating collapse to super-heavy nuclei. Exploring both fields together certainly appears to be a desirable pursuit.

References

[1] R.L. Mills, *The Grand Unified Theory of Classical Physics*, August 2011 Edition, Black Light Power, Cranbury, 2011.
[2] J. Maly and J. Va'vra, Electron transitions on deep Dirac levels II, *Fusion Technol.* **27** (1995) 50–70.
[3] Jan Naudts, On the hydrino state of the relativistic hydrogen atom, arXiv:physics/0507193v2.
[4] L.I. Schiff, *Quantum Mechanics*, Third edition, Mc-Graw Hill, New York, 1968.
[5] S. Weinberg, *The Quantum Theory of Field*, Vol. 1, Foundations, Cambridge University Press, Cambridge, 1995.
[6] Antonio S.de Castro, Orthogonality criterion for banishing Hydrino states from standard quantum Mechanics, *Phys. Lett.* A **369** (2007) 380–383.
[7] Teimuraz Nadareishvili and Anzor Khelashvili, Some problems of self-adjoint extension in the Schrodinger equation, arxiv.org/pdf/0903.0234.pdf.
[8] Guy Bonneau, Jacques Faraut and Galliano Valent, Self-adjoint extensions of operators and the teaching of quantum mechanics, arXiv:quant-ph/0103153v1.
[9] Bern Thaller, *The Dirac Operator*, in *Relativistic Electronic Structure Theory*, Part 1, Theory (Theoretical and Computational Chemistry # 11), Chapter 2, P. Schwerdtfeger (ed.), Elsevier, Oxford, 2002, pp. 23–105.
[10] M. Reed and B. Simon, *Methods of Modern Mathematical Physics*, Vol. I, *Functional Analysis*, Academic Press, New York, 1980.
[11] Norman Dombey, The hydrino and other unlikely states, arXiv:physics/0608095v1.
[12] E.T. Whittaker and G.N. Watson, *Modern Analysis*, Fourth edition, Chapter XVI, Cambridge University Press, Cambridge, 1940.
[13] http://en.wikipedia.org/wiki/Confluent_hypergeometric_function.
[14] J.A. Maly and J. Vavra, Electron transitions on deep Dirac levels *I, Fusion Technol*. **24** (1993) 307.
[15] S. Fluegge, *Practical Quantum Mechanics*, Vol.2, Springer V. Berlin,1974.
[16] R.T. Deck, Jacques G. Amar and Gustave Fralick, Nuclear size corrections to the energy levels of single- electron and -muon atoms, *J. Phys. B: At. Mol. Opt. Phys.* **38** (2005) 2173—2186.
[17] D. Andrae. Finite nuclear charge density distributions in electronic structure calculations for atoms and molecules, *Phys. Reports* **336** (2000) 413—525.
[18] Bern Thaller, *The Dirac Equation*, Springer, Berlin, 1992.
[19] J. J. Snygg, *Clifford Algebra: A Computational Tool for Physicists,* Oxford University Press, New York, 1997.
[20] David Tong, *Lectures on Quantum Field Theory*, University of Cambridge, UK. http://www.damtp.cam.ac.uk/user/tong/qft.html.
[21] J.J. Sakurai and Jim Napolitano, *Modern Quantum Mechanics*, Second edition, Addison-Wesley, New York, 2011.
[22] W.R. Johnson, K.T. Cheng and M.H. Chen, *Accurate Relativistic Calculations Including QED Contributions for Few-Electron Systems,* in *Relativistic Electronic Structure Theory*, Part 2. Applications (Theoretical and Computational Chemistry #14**),** P. Schwerdtfeger (ed.), Chapter 3, 2004, preprint: http://www3.nd.edu/∼johnson/Publications/markup.pdf

[23] M. Safronova. Lectures in Physics 2-3, 626, University of Delaware. http://www.physics.udel.edu/∼msafrono/626/.
[24] A. Messiah, *Mecanique Quantique*, Vol. II, Dunod, 1960 [In French]. English version: translated from French by J. Potter (Saclay, France), Edit. N-H.
[25] Carl D. Anderson, The positive electron, *Phy. Rev.* **43** (1933) 491–498.
[26] J.E. Gilbert and M.A.M. Murray. *Clifford Algebras and Dirac Operators in Harmonic Analysis*, Cambridge University Press, Cambridge, 1991.
[27] Dr. Bill Pezzaglia, *Lectures Series: The Spin of the Matter, Physics 4250*, Fall 2010, Topic4: Special Relativity and Thomas Precession, CSUEB, Upd. Nov. 2010.
[28] L.L. Foldy and S.A. Wouthuysen, On the Dirac theory of spin-1/2 particles and its nonrelativistic limit, *Phys. Rev.* **18** (1950) 29—36.
[29]] A. Dragan and T. Odrzygo'zd'z, Half-page derivation of the Thomas precession, *Am. J. Phys.* **81** (2013) 631. arXiv:1211.1854v1 [physics.class-ph] 8 Nov 2012.
[30] Jens Bolte and Rainer Glaser, Zitterbewegung and semiclassical observables for the Dirac equation, Ulm-TP, Feb 2004; arXiv:quant-ph/0402154v1.
[31] Zitterbewegung. Wikipedia, the free encyclopedia, August 2014.
[32] Tepper L. Gill, W.W. Zachary and Marcus Alfred, Analytic representation of the Dirac equation, *J. Phys. A: Math. Gen*. **38** (31) (2005) 6955–6976.
[33] Robert Littlejohn, *Lecture Notes Physics 221A Fall 2010*, Notes 23, Fine structure in hydrogen and alkali atoms in http://bohr.physics.berkeley.edu/classes/221/1011/221.html.
[34] S.V. Adamenko and V.I. Vysotskii, Mechanism of synthesis of superheavy nuclei via the process of controlled electron-nuclear collapse, *Foundations Phys. Lett.* **17**(3) (2004) 203–233.
[35] S.V. Adamenko and V.I. Vysotskii, Evolution of annular self-controlled electron-nucleus collapse in condensed targets, *Foundations Phys.* **34**(11) (2004) 1801–1831.
[36] M. Abramowitz and I. Stegun, *Handbook of Mathematical Functions with Formulas, Graphs, and Mathematical Tables,* Nineth edition, Dover, New York, 1970.
[37] John W Pearson, *Computation of Hypergeometric Functions,* School of Mathematics, The University of Edinburgh, 2009/9/4. Link= ox.ac.uk.
[38] G. Arfken and H.Weber, *Mathematical Methods for Physicists*, Sixth edition, Elsevier, New York, 2005.